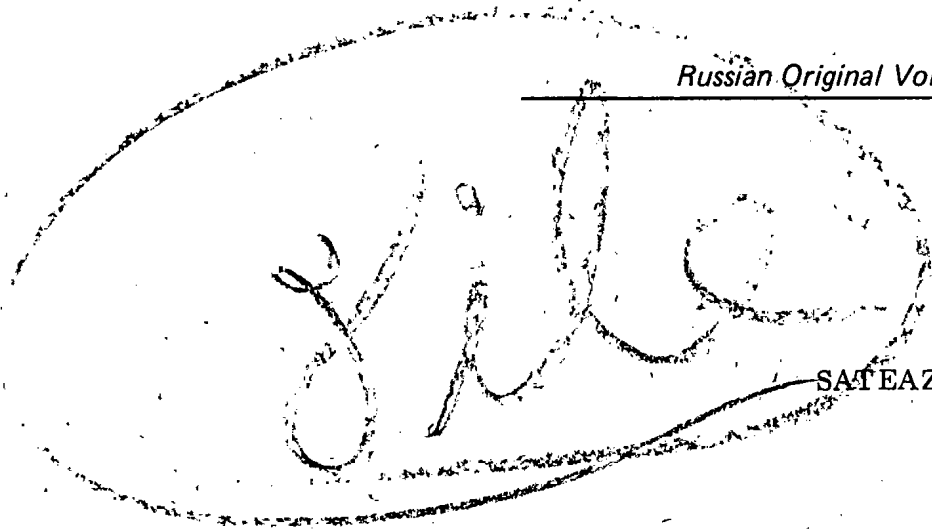


DIY
MC
NS
PS

Russian Original Vol. 37, No. 4, October, 1974

April, 1975

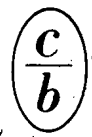


SATEAZ 37(4) 1027-1132 (1974)

SOVIET ATOMIC ENERGY

АТОМНАЯ ЭНЕРГИЯ
(ATOMNAYA ÉNERGIYA)

TRANSLATED FROM RUSSIAN



CONSULTANTS BUREAU, NEW YORK

SOVIET ATOMIC ENERGY

Soviet Atomic Energy is a cover-to-cover translation of *Atomnaya Energiya*, a publication of the Academy of Sciences of the USSR.

An agreement with the Copyright Agency of the USSR (VAAP) makes available both advance copies of the Russian journal and original glossy photographs and artwork. This serves to decrease the necessary time lag between publication of the original and publication of the translation and helps to improve the quality of the latter. The translation began with the first issue of the Russian journal.

Editorial Board of *Atomnaya Energiya*:

Editor: M. D. Millionshchikov

Deputy Director
I. V. Kurchatov Institute of Atomic Energy
Academy of Sciences of the USSR
Moscow, USSR

Associate Editor: N. A. Vlasov

A. A. Bochvar

N. A. Dollezhal'

V. S. Fursov

I. N. Golovin

V. F. Kalinin

A. K. Krasin

A. I. Leipunskii

V. V. Matveev

M. G. Meshcheryakov

P. N. Palei

V. B. Shevchenko

V. I. Smirnov

A. P. Vinogradov

A. P. Zefirov

Copyright © 1975 Plenum Publishing Corporation, 227 West 17th Street, New York, N.Y. 10011. All rights reserved. No article contained herein may be reproduced, stored in a retrieval system, or transmitted, in any form or by any means, electronic, mechanical, photocopying, microfilming, recording or otherwise, without written permission of the publisher.

Consultants Bureau journals appear about six months after the publication of the original Russian issue. For bibliographic accuracy, the English issue published by Consultants Bureau carries the same number and date as the original Russian from which it was translated. For example, a Russian issue published in December will appear in a Consultants Bureau English translation about the following June, but the translation issue will carry the December date. When ordering any volume or particular issue of a Consultants Bureau journal, please specify the date and, where applicable, the volume and issue numbers of the original Russian. The material you will receive will be a translation of that Russian volume or issue.

Subscription
\$87.50 per volume (6 Issues)

Single Issue: \$50
Single Article: \$15

Prices somewhat higher outside the United States.

CONSULTANTS BUREAU, NEW YORK AND LONDON



227 West 17th Street
New York, New York 10011

4a Lower John Street
London W1R 3PD
England

Soviet Atomic Energy is abstracted or indexed in *Applied Mechanics Reviews*, *Chemical Abstracts*, *Engineering Index*, *INSPEC-Physics Abstracts* and *Electrical and Electronics Abstracts*, *Current Contents*, and *Nuclear Science Abstracts*.

Published monthly. Second-class postage paid at Jamaica, New York 11431.

SOVIET ATOMIC ENERGY

A translation of *Atomnaya Énergiya*

April, 1975

Volume 37, Number 4

October, 1974

CONTENTS

	Engl./Russ.
The Seventy-Fifth Birthday of Academician Nikolai Antonovich Dollezhalii	1027 290
ARTICLES	
Basis of the Standard Lifetime of Power Generating Units of Nuclear Power Stations — L. D. Gitel'man, E. F. Ratnikov, and V. V. Khanin	1028 291
Calculation of Hydraulic-Resistance Coefficient and Velocity Profile in Pipes with Regular Roughness — M. Kh. Ibragimov and L. L. Kobzar'	1034 297
The Composition of Uranite from Pegmatite and Uranium—Molybdenum Deposits — V. A. Strel'tsov, V. A. Boronikhin, and A. I. Tishkin.	1043 306
The Mechanical Properties of Single Crystals of Irradiated α -Uranium with Free or Restrained Radiation Growth — Yu. M. Golovchenko, F. P. Butra, V. F. Portnov, V. N. Burmistrov, I. A. Korobeinikov, and O. L. Fufaeva.	1052 316
Comparison of Costs of Purifying Radioactively Contaminated Water by Sorbents of Multiple- and Single-Use — F. V. Rauzen and V. V. Aleshnya	1064 322
Mode Transformation in the Resonator of a Drift-Tube Linear Accelerator — V. A. Bomko, A. P. Klyucharev, and B. I. Rudyak.	1058 326
Longitudinal Instability of a Circulating Beam Interacting with a Passive Resonator — V. I. Balbekov and P. T. Pashkov	1069 332
ABSTRACTS	
Measurement of Ratio of Effective Cross Sections of Capture in ^{238}U and Fission of ^{235}U in a Fast-Thermal Critical Assembly — M. V. Bychkov, A. V. Skobkarev, A. P. Malykhin, I. V. Zhuk, Yu. I. Churkin, and O. I. Yaroshevich.	1073 337
Calculation of Pressure and Temperature within the Casing of a Water—Water Reactor — I. Mishak	1074 338
p Versus T Phase Diagram of the Uranium—Oxygen System — Yu. V. Levinski	1075 339
Can Uranium be Reduced from the Hexafluoride to the Elementary State by Hydrogen? — Yu. N. Tumanov and N. P. Galkin	1076 340
Calculation of Some Diffusion Parameters and Gas Generation of Particles on Heating the Samples after Ionic Bombardment — A. A. Pisarev and V. A. Pisarev.	1077 340
Allowance for Geometry in Activation Analysis Involving Fast Neutrons Generated in a Cyclotron by the Reactions $^9\text{Be}(d, n)^{10}\text{B}$ and $^9\text{Be}(p, n)^9\text{B}$ — V. A. Muminov, B. Akabirov, and N. Abibullaev	1079 342
LETTERS TO THE EDITOR	
Observation of Anomalously Large Pores in Nickel Bombarded by Carbon Ions — V. I. Krotov, S. Ya. Lebedev, and V. N. Bykov.	1080 343
Kinetic Instability of an Intense Beam of Charged Particles in a Storage Ring — N. N. Naugol'nyi	1082 344
Effect of Energy Degradation on the Energy Spectrum of Fast Electrons in Matter — V. S. Remizovich.	1085 346

CONTENTS

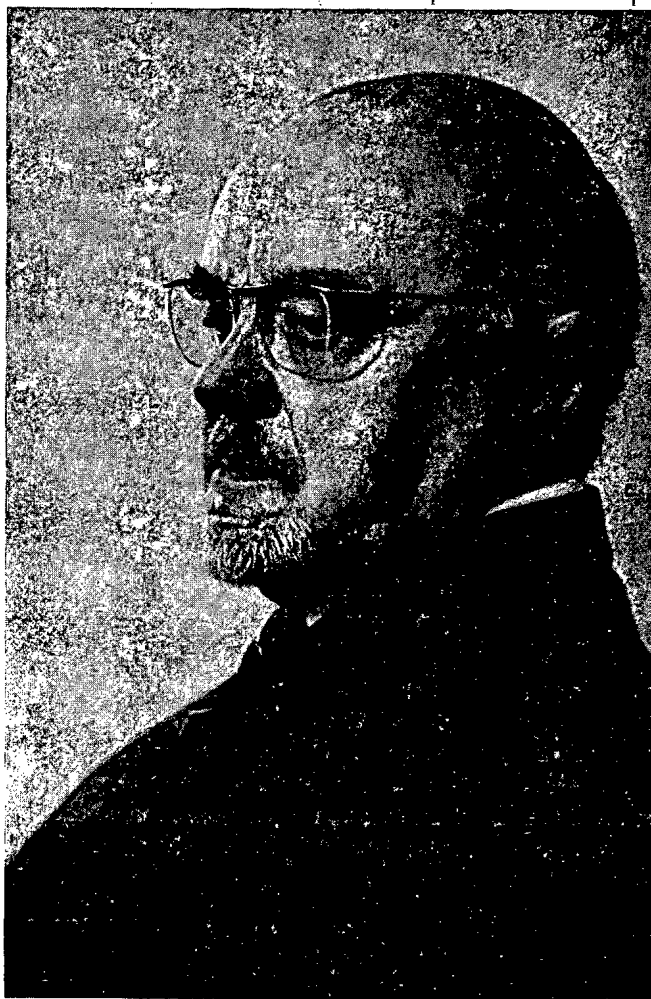
(continued)

Engl./Russ.

Specific Heats of Yttrium and Gadolinium at High Temperatures — I. I. Novikov and I. P. Mardykin.	1088	348
The Method of Recursive Sums and Integrals for Solving Multigroup Neutron Diffusion Equations — V. Yu. Vasil'ev and A. D. Dymnikov	1091	350
Temperature Dependence of Total Cold Neutron Cross Section in Light Water and Benzene — S. B. Stepanov, V. E. Zhitarev, F. M. Zelenyuk, and V. Ya. Krasil'nikov	1094	351
Comparison of Accident Dosimetry Systems at HPRR — I. B. Keirim-Markus, V. A. Knyazev, and S. N. Kraitor	1097	353
Optimal Sample Dimensions for Gamma Activation Analysis — S. P. Kapitsa, Yu. T. Martynov, V. N. Samosyuk, V. V. Sulin, and Yu. M. Tsipenyuk.	1100	356
Determination of ²³⁴ Am Half-Life — V. G. Polyukhov, G. A. Timofeev, P. A. Privalova, V. Ya. Gabeskiriya, and A. P. Chetverikov.	1103	357
COMECON NEWS		
XXVI Session of the Comecon Permanent Commission on the Peaceful Uses of Atomic Energy — V. A. Kiselev.	1106	361
Collaboration Daybook.	1107	361
INFORMATION		
Silver Jubilee of the Soviet of Mutual Economic Aid — A. F. Panasenkov.	1109	363
CONFERENCES AND MEETINGS		
Conference on Physical Aspects of Atmospheric Pollution — B. I. Styro.	1115	367
VIII International Symposium on Thermonuclear Reactor Technology — V. S. Strelkob	1118	368
International Symposium on the Use of Isotope Techniques in Groundwater Hydrology — V. T. Dubinchuk and A. M. Dimaksyan	1120	369
International Conference on Meson Spectroscopy — V. A. Belyakov.	1122	370
Meeting of the Four Nuclear Data Centers — V. N. Manokhin.	1124	371
Meetings of Specialists on Nonneutron Nuclear Data — F. E. Chukreev	1126	372
USSR—Belgium—Holland Seminar on Treatment and Burial of Radioactive Wastes — N. A. Rakov	1127	373
BOOK REVIEWS		
New Books	1129	374

The Russian press date (podpisano k pechati) of this issue was 9/20/1974. Publication therefore did not occur prior to this date, but must be assumed to have taken place reasonably soon thereafter.

THE SEVENTY-FIFTH BIRTHDAY OF ACADEMICIAN
NIKOLAI ANTONOVICH DOLLEZHALI



The editorial staff of "Atomnaya Energiya" cordially congratulate member of the editorial board of the journal Academician Nikolai Antonevich Dollezhal on his 75th birthday and wish him good health, long life and further creative successes.

Translated from Atomnaya Energiya, Vol. 37, No. 4, October, 1974.

© 1975 Plenum Publishing Corporation, 227 West 17th Street, New York, N.Y. 10011. No part of this publication may be reproduced, stored in a retrieval system, or transmitted, in any form or by any means, electronic, mechanical, photocopying, microfilming, recording or otherwise, without written permission of the publisher. A copy of this article is available from the publisher for \$15.00.

ARTICLES

BASIS OF THE STANDARD LIFETIME OF POWER
GENERATING UNITS OF NUCLEAR POWER STATIONSL. D. Gitel'man, E. F. Ratnikov,
and V. V. Khanin

UDC 621.311.25:621.039.003

The standard lifetimes used for nuclear power stations are oriented to the corresponding values for thermal power stations and do not take account of technical—economic characteristics and the rate of scientific—technological progress in nuclear power generation. The experience built up in the planning and operation of commercial nuclear power stations permits, justifiably, an approach to the determination of this index. The solution of this problem nevertheless is related to the preparation of a plan for new standards of amortization in the industry of the USSR.

The timing of plant replacement is determined by the degree of limitation of capital investments in the development of power generation, by the increase of demand for electric power, the production capacity of the power plant design, the overall amount of stock of a theoretically obsolete plant, etc. In order to take account of these limitations, certain authors propose complicated procedures for calculating the long-term lifetimes, the essence of which reduces to the construction of a dynamic model of the extended regeneration of basic resources in this branch [1, 2]. However, the large error in the starting data when forecasting over a long term (20–40 yr) and the idealization of the model, in practice do not justify the complexity of the calculations. It should be kept in mind also that the standard lifetimes are an average quantity established for a number of plants. Therefore, for every actual item, a deviation from the standard lifetime must be assumed.

In the authors' opinion, when establishing the standard lifetimes for plants with a long period of operation, simpler methods can be used which give approximate results but, at the same time, consider the problem as one of iteration.

The lifetime of the power generating plant of a nuclear power station is understood to be the period of time during which the plant maintains its capability of performing production functions within the limits of permissible deviations and in accordance with safety, reliability, production quality and operating efficiency. In special cases, shortening of the plant operation is determined by physical wear, efficiency of maintenance, ethical wear and tear and economic expediency. The standard lifetime of the power generation unit of a nuclear power station is determined by that factor whose effect is manifested earlier than the others. Consequently, in the first stage of the calculations, it is necessary to explain the relation between the lifetimes determined for each one of the factors mentioned.

In this present paper, we discuss the results of investigations carried out by the authors to determine the lifetime of the power generation units of nuclear power stations prior to ethical wear and tear. The methodological prerequisite for determining the lifetime of plants according to ethical wear and tear in long-term calculations is the theorem advanced by Novozhilov [3]. According to this theorem, technology becomes obsolete for use after the costs of the production factory (without renovation) exceeds the lumped costs of a new plant. In order to determine the lifetime of the power generation unit of a nuclear power station prior to total ethical wear and tear, it is necessary to solve the equation

$$S_r^{ST}(t) + S_r^{ST}(t) + S_{pr}^{ST}(t) = S_r^n(t) + S_a^n(t) + S_r^{ST}(t) + S_{pr}^n(t) + E_n[\bar{K}^n(t) - \bar{K}_{OST}^{ST}(t)] + \Delta Z^{SIST}(t), \quad (1)$$

where $S_T^{ST}(t)$ and $S_T^n(t)$ are functions reflecting the change with time t of the fuel component costs of electric power in operative and newly installed power generating units respectively, kopecks/kW·h; $S_r^{ST}(t)$ and $S_r^n(t)$ are functions reflecting the change of maintenance costs of operative and newly installed power

Translated from *Atomnaya Énergiya*, Vol. 37, No. 4, pp. 291–296, October, 1974. Original article submitted August 24, 1973.

© 1975 Plenum Publishing Corporation, 227 West 17th Street, New York, N.Y. 10011. No part of this publication may be reproduced, stored in a retrieval system, or transmitted, in any form or by any means, electronic, mechanical, photocopying, microfilming, recording or otherwise, without written permission of the publisher. A copy of this article is available from the publisher for \$15.00.

generation units, kopecks/kW · h; $S_{pr}^{ST}(t)$ and $S_{pr}^n(t)$ are functions reflecting the change of incidental expenditure on the cost of electric power in operative and newly installed power generation units, kopecks/kW · h; $S_a^n(t)$ is a function reflecting the change in the amortization component cost of electric power in newly installed power generation units, kopecks/kW · h; E_n is the standard coefficient of capital investment efficiency; $K^n(t)$ is a function reflecting the change of specific capital investment in the construction of newly installed power generation units (taking account of the fuel charge), kopecks/kW · h; $K_{OST}^{ST}(t)$ is a function reflecting the change of liquidation costs of the operative power generation unit, kopecks/kW · h; $\Delta Z^{SIST}(t)$ is a function reflecting the change of the lumped costs relative to the power generation system, in consequence of the installation of a new and higher capacity power generation unit (founding of an auxiliary emergency and maintenance reserve), kopecks/kW · h.

We simplify Eq. (1) in the following way. First of all, we neglect the terms $S_{pr}^{ST}(t)$, $S_{pr}^n(t)$ and $K_{OST}^{ST}(t)$ in view of their relatively small value; secondly, the term $S_{pr}^n(t)$ is taken to be equal to a constant quantity, arising from the average costs during the proposed lifetime of the new power generation unit.

It should be mentioned that the determination of the function $\Delta Z^{SIST}(t)$ is very complex. Taking account of this function may influence the result, as with increase of unit capacity of the power generation plant, the incidence of accidents increases. However, as this effect will be to the side of increases of the calculated value of the lifetime, then in the first stage of operation the term $\Delta Z^{SIST}(t)$ need not be taken into account.

We carry out the following substitution:

$$\begin{aligned} S_r^{ST}(t) &= \varphi_{k_1}(t); S_r^{ST}(t) - S_r^n = \varphi_{k_2}(t); \\ S_r^n(t) &= \varphi_{k_3}(t); S_a^n(t) + E_n \bar{K}^n(t) = \varphi_{k_4}(t). \end{aligned}$$

After transformation, we rewrite Eq. (1) in the form:

$$F(t) = \varphi_{k_1}(t) + \varphi_{k_2}(t) - \varphi_{k_3}(t) - \varphi_{k_4}(t) = 0, \quad (2)$$

where k_1 , k_2 , k_3 and k_4 are suffixes assuming values which correspond to a specific variant of the starting data:

$$\varphi_{k_1}(t) = q_{k_1} e^{-s_{k_1} t}; \quad (3)$$

$$\varphi_{k_2}(t) = q_{k_2} + s_{k_2} t; \quad (4)$$

$$\varphi_{k_3}(t) = \begin{cases} q_{k_3} e^{-s_{k_3} t}, & i = 1; \\ q_{k_3} + s_{k_3} t, & 0 \leq t \leq 30, i = 2; \\ b, & t > 30, i = 2; \end{cases} \quad (5)$$

$$\varphi_{k_4}(t) = \begin{cases} \frac{k_{sp}(t) 100}{h_u^t} \left(\frac{1}{T_n} + E_n \right), & i = 1; \\ \frac{a_{ex} k_{sp}(t) 100}{h_{ex}^t} \left(\frac{1}{T_n} + E_n \right), & i = 2; \end{cases} \quad (6)$$

where $i = 1$ corresponds to a function for thermal reactors; $i = 2$ is the same for fast reactors; $k_{sp}(t)$ is a function reflecting the change with time of the specific capital investments in the construction of newly installed power generation units with thermal reactors, roubles/kW; h_u^t and h_u^f are the average number of hours of utilization of installed capacity, h, during the lifetime of a power generating plant with thermal and fast reactors (we assume $h_u^t = 6000$ h and $h_u^f = 7000$ h); T_n is the standard lifetime of the power generation unit of the nuclear power station, yr (we assume $T_n = 30$ yr); a_{ex} is the coefficient which takes into account the increase of the specific capital investments in the construction of the power generation units of nuclear power stations with fast reactors and with MHD generators in comparison with thermal reactors.

The analytic form of Eq. (3) to Eq. (6) is chosen in accordance with the following considerations. The change with time of the fuel component costs of electric power for thermal reactors $\varphi_{k_1}(t)$ and $\varphi_{k_3}(t)$ when $i = 1$, is described most satisfactorily by an exponential function which also was used in the calculations. For future power generation units with fast reactors, a considerable indeterminacy is characteristic in relation to the magnitude and ratio of reduction of the fuel component costs. Therefore, the function $\varphi_{k_3}(t)$ when $i = 2$ over the period of time $0 \leq t \leq 30$ was given in the form of a straight line joining the starting level with the suggested value of the fuel component at the end of this period and beyond its limits this

function was assumed to be equal to a constant quantity b , resulting from the suggestion concerning stabilization of the magnitude of the fuel component costs approximately at this level.

Maintenance costs $\varphi_{k_2}(t)$ have a tendency to increase in proportion with the physical wear and tear of the plant. The analysis carried out by us of the data on maintenance costs over a large number of thermal power stations confirms this conclusion. However, it has not been possible to establish a strict rule for the change of maintenance costs during the period of operation of the power generation plants. Therefore, the simplest linear relation was assumed.

The analytic form of Eq. (6) will be single-valued if $S_2^n(t)$ and $\bar{K}^n(t)$ are expressed in terms of their definitive parameters.

For calculations of the lifetime of the power generation units of nuclear power stations, it is necessary to assume: 1) forecast of a time variation of the running costs (without renovation) of the operative power generation units; 2) forecast of the introduction into commercial operation of prospective types of energy sources and energy converters and forecast of the change with time of their efficiency indices in consequence of structural improvements and of scientific-technological progress in adjacent branches. The uniqueness of the preparation of this data block occurs in that the required data is of a different nature, has a different degree of authenticity and also diversity in form of quantitative presentation. For example, planning data, foreign data, and statistical data concerning the operation of thermal power stations may serve as sources. Moreover, characteristics with a large degree of indeterminacy may be given in the form of discrete level-variants (for example, the magnitude of the fuel component costs for fast breeder reactors will hardly be below 0.03 kopeck/kW·h and not higher than 0.1 kopeck/kW·h).

The question of the specific capital investments is resolved more decisively. The problem is made worse in that the magnitude of this index is determined to a considerable extent by the unit capacity of the power generation plant. Consequently, knowing the law of variation of the specific capital investments on the unit capacity $K_{sp} = f(N_{uc})$ and the increase of unit capacity with time $N_{uc} = \varphi(t)$, the function $K_{sp} = F(t)$ can be constructed.

Analysis of the planning data and published data permits a relationship to be obtained for thermal reactors:

$$K_{sp} = 1447.7 a_T N_{uc}^{-0.3},$$

where a_T is a coefficient which takes account of the cost of the reactor fuel.

Power generation units with a capacity of 1000 MW were chosen as the objective for which the lifetimes were determined. As the range of variation of the starting data was given over wide limits in the long-term and the differences in the technological-economic indices of power generation units with reactors of the VVER and RBMK type are insignificant, the calculations carried out are admissible for both types of reactors.

All the potential "claimants" to the replacement of operative nuclear power stations can be divided into three groups according to their degree of productive utilizability at the instant of the forecast: 1) utilized in the production stages; 2) not having received the final technical exploitation which is expected in the forecast period; 3) not yet studied in a scientific project. From the first group, nuclear power stations with thermal reactors are of the greatest interest with respect to their long-term significance and from the second group, MHD-generators and nuclear power stations with fast reactors; from the third group, the production of power by means of controlled thermonuclear fusion. However, in view of the considerable inertia of the system* it is obvious that they will not all begin commercial operation before 2000 AD. Therefore, sources of the third group have not been taken into account in the forecast. This circumstance, and also the fact that the results obtained have been extrapolated beyond the limits of 2000 AD, have led to the necessity for the introduction of yet another assumption: lifetimes obtained with a value of more than 30 yr are accurate on condition that over the time interval $(2000 + \tau_i)$ † no new source of power, which has not been taken into account in the forecast, will start to be brought into commercial operation. Such an assumption is possible, as the problem being considered is one of iteration. In the next review of standard lifetimes of basic resources (for example, over 10 yr) the possibility emerges of taking account of new trends of scientific-technological progress.

*For example, it is shown in [4] that the period from the start of development of fast power reactors up to the instant of mass utilization amounts to 20 yr approximately.

†Here $\tau_i = t_i - 30$, where t_i is the calculated value of the lifetime in the i -th variant.

For each of the chosen "claimants" the year from which its commercial operation will start on a wide scale was estimated, and the most important parameters were predicted, the change of which to a considerable degree determines the magnitude of the running and capital costs.

The method of expert estimates (the Delphi technique) was used in the investigation; this permits qualitative improvements and rapid changes to be taken into account. The forecasting scheme consists of the following stages: 1) preforecast orientation; 2) formulation of the problem; 3) processing of tables of expert estimates; 4) formation of an expert group; 5) procedure of working with the experts; 6) processing and analysis of expert estimates; 7) verification of forecast; 8) results of forecast.

As a result of the preforecast orientation, a tree of purposes is constructed, representing graphically the objective of the forecast (Fig. 1). This permits its structure to be revealed, significant variables to be distinguished and their hierarchy and interrelationship to be ascertained. Analysis showed that the production efficiency of electric power in nuclear power stations depends to the greatest extent on the increase of the unit capacity of the reactor and the introduction of fast reactors and MHD generators. Accordingly, tables of expert estimates were devised, the increase with time of the unit capacities of thermal neutron, nuclear reactors; the time from which commercial operation of fast neutron reactors will start and the increase with time of their unit capacities; the start of the introduction into commercial operation of MHD-generators. Questionnaires were added to the tables in order to determine the competences of the experts.

An important stage of forecasting by the method of expert estimates is the determination of the representativeness of the expert group. An index of representativeness — the mathematical expectation of competence of the expert group $M(K)$ — has been proposed in the procedure for scientific-technological forecasting according to the complex problems of development of the national economy, developed in [5]. The authors of this procedure assume that the group is representative if the condition $M(K) > 0.67$ is satisfied. For our expert collective body, the mathematical expectation of competence was found to be equal to 0.79. Verification of the representativeness by other methods [6, 7] also confirmed that the group of experts participating in the estimate of the outlook for scientific-technological progress, were highly qualified and adequately representative for considering the conclusions made on the basis of the forecast estimates to be reliable.

In processing the expert estimates by the procedures suggested in [8-10], the following results were obtained:

a) the equations of regression, defining the change with time of the unit capacities of thermal neutron N_{uc}^t and fast neutron reactors N_{uc}^f :

$$N_{uc}^t = 58.4(1972 + t) - 114237, \quad (7)$$

$$N_{uc}^f = 53.2(1972 + t) - 104265, \quad (8)$$

where t is a variable, corresponding to the serial number of the year; 1972 is taken for the start of the reckoning ($0 \leq t \leq 30$);

b) the estimate of the mathematical expectation of the time of introduction into commercial operation of the power generation units of nuclear power stations with fast neutron reactors:

$$M[\tau^f] = 1986;$$

c) the estimate of the mathematical expectation of the starting time for the introduction into commercial operation of MHD generators:

$$M[\tau_{MHDg}] = 1994.$$

An indirect verification showed that the forecast obtained is quite realistic.

The expert estimates obtained comprised part of the data block for solving Eq. (2). Functions reflecting possible variation of running costs of production in nuclear power stations were specified in the form of variants. The values of the coefficients of the functions are given in the table.

TABLE 1. Coefficients of Functions (3)-(6)

Function	Value of coefficients				
	q	s	b	a_p	E_n
φ_{k_1}	0,20	0,01			
	0,20	0,03			
	0,25	0,01			
	0,25	0,03			
	0,20	0			
	0,25	0			
φ_{k_2}	-0,03	0,001			
	-0,03	0,002			
φ_{k_3} for $i=1$	0,20	0,02			
	0,20	0,04			
	0,25	0,02			
φ_{k_3} for $i=2$	0,25	0,04			
	0,1	-0,005	0,03		
φ_{k_4}				1,0	0,08
				1,25	0,12
				1,5	0,15

A series of calculations was also carried out with an additionally introduced condition. The relations $N_{uc}^t = \varphi(t)$ and $N_{uc}^f = \varphi(t)$ were taken not from the equations of regression (7) and (8), but from the equations of the straight lines passing through the boundary (maximum) estimates of the experts in 1980 and 2000 AD:

$$N_{uc}^t = 120(t + 1972) - 236000, \quad (9)$$

$$N_{uc}^f = 100(1972 + t) - 197000. \quad (10)$$

The calculations were carried out according to a specially developed program on a computer. A total of more than 800 variants was evaluated, determined by combinations of different starting parameters.

The following conclusions can be drawn on the basis of the data obtained. In conjunction with the calculations of the most pessimistic estimates relative to the change with time of the technological-economic indices of the power generation of nuclear power stations, brought into operation in the current five-year period, and the most optimistic estimates, the lifetime of future power generation units before total ethical wear and tear amounts to not less than 30 years. Actually, with other combinations of the factors being estimated and with the condition that during this time no new source of power will be brought into use for industrial operation which is significantly more efficient than the existing sources, the lifetimes may prove to be even greater. According to the results of the calculations it may amount to 50-60 years or more.

The result obtained, at first sight, may prove to be unexpected. The lifetime of the power generation units of nuclear power stations exceeds by far this index for thermal power station units. This is due to the considerable qualitative difference in technique and technological processes achieved in nuclear power stations, which permits the fuel cycle of a nuclear reactor to be improved over wide limits and the efficiency of already operating power generation units to be increased constantly. * In connection with this, investigations into the determination of the physical lifetime of the main plant of a nuclear power station acquires importance, as it is the basis for proposing that this period will prove to be less than the lifetime according to ethical wear and tear.

LITERATURE CITED

1. O. T. Bystrova, Planovoe Khozyaistvo, No. 6, 18 (1970).
2. A. G. Zakharin and A. I. Filatov, Élektricheskie Stantsii, No. 2, 2 (1971).
3. V. V. Novozhilov, Measurement of Costs and Results [in Russian], Ékonomika, Moscow (1967).
4. N. A. Dollezhal' et al., Atomnaya Énergiya, 31, No. 3, 187 (1971).
5. V. A. Lisichkin et al., in: Theory and Practice of Forecasting Science and Technology in Member-Countries of the Council for Mutual Economic Aid [in Russian], Ékonomika, Moscow (1971), p. 368.
6. P. N. Zavin, in: Science Management. Forecasting. Information Science [in Russian], Nauka Dumka, Kiev (1970), p. 83.
7. V. D. Patrushev, Some Problems of Selection in Sociological Investigations. Scientific Seminar on the Application of Quantitative Methods in Sociology [in Russian], No. 2, Siberian Division of the Academy of Sciences of the USSR, Novosibirsk (1966), p. 29.
8. Yu. V. Kiselev, Ékonomika i Matematicheskie Metody, 3, No. 3, 57 (1967).
9. L. Smirnov et al., Measurement of Costs and Results [in Russian], Ékonomika, Moscow (1967), p. 243.
10. V. A. Lisichkin, Branching Scientific-Technological Forecasting [in Russian], Ékonomika, Moscow (1971).
11. P. Margen, Atomnaya Tekhnika za Rubezhom, No. 8, 3 (1968).
12. H. Gugenus, Atomwirtschaft, 9, 470 (1969).

*We note that foreign authors estimate the economical lifetimes of nuclear power stations to be greater than 40 years [11, 12].

CALCULATION OF HYDRAULIC-RESISTANCE
COEFFICIENT AND VELOCITY PROFILE IN PIPES
WITH REGULAR ROUGHNESS

M. Kh. Ibragimov and L. L. Kobzar'

UDC 532.542.4

Experiments carried out under the direction of M. D. Millionshchikov on the investigation of the hydrodynamic characteristics of flow in rough pipes and an analysis of the results obtained [1-3] allowed us to develop a method for calculating the velocity fields and the hydraulic-resistance coefficients in pipes having regular roughness. The experiments showed that the hydraulic-resistance coefficient and the velocity profile in a rough pipe are determined by the dimensions, shape, and relative position of the roughness elements. Therefore the calculation method for the hydrodynamic flow characteristics should take account of these parameters.

The treatment of the problem being considered from the point of view of an equivalent roughness is justified for natural roughnesses, when it is impossible to determine the actual surface characteristics. The forms of this roughness are limited in number, and can be classified. For artificial roughness, in view of the large variety of its forms, this method becomes difficult to use. For pipes with regular roughness (roughness formed by identical projections, uniformly distributed over the pipe surface) a more promising approach is that in which the flow past an individual projection is considered as an external flow. Such an approach has been developed in [4, 5]. The methods assumed in these works can be used to calculate the additional resistance caused by the roughness only for the case in which the drag coefficient of an isolated projection and the velocity distribution at the wall are known, and the projections have no effect on each

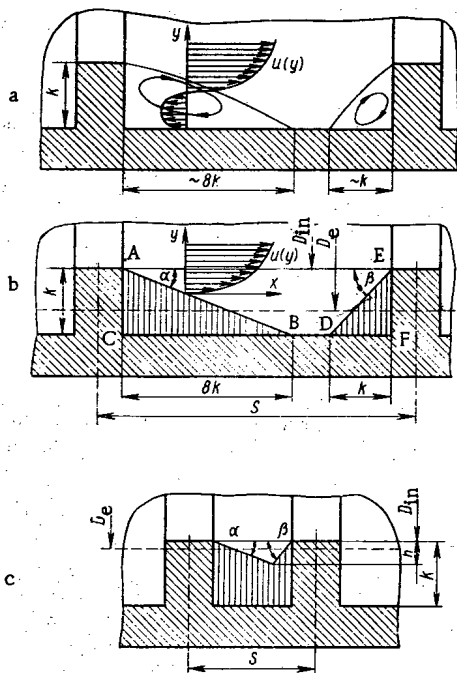


Fig. 1. Pictures of flow past annular projections: a, b) experimental picture and simplified calculation scheme of the flow for large distances between the projections, respectively; c) simplified calculation scheme for flow past projections positioned close to each other.

Translated from *Atomnaya Energiya*, Vol. 37, No. 4, pp. 297-305, October, 1974. Original article submitted September 15, 1973.

© 1975 Plenum Publishing Corporation, 227 West 17th Street, New York, N.Y. 10011. No part of this publication may be reproduced, stored in a retrieval system, or transmitted, in any form or by any means, electronic, mechanical, photocopying, microfilming, recording or otherwise, without written permission of the publisher. A copy of this article is available from the publisher for \$15.00.

other. When the roughness elements are close together, and there is considerable interference, none of the available treatments for calculating the contribution of the pipe roughness to the total resistance are applicable.

In the investigation of the hydraulic resistance of a rough pipe from the point of view of an external flow it is usual to raise the question of the velocity distribution in the immediate proximity of the wall, which depends on the form and magnitude of the roughness. Both for experimental investigation and also for the theoretical description it is difficult to include all the details of the velocity field at a rough wall. Therefore it is usual to consider some mean velocity profile in a fictitious equivalent smooth pipe having the same values of liquid flow rate and pressure losses as the rough pipe. The selection of the equivalent diameter of a rough pipe suffers from a well-known difficulty. As a relatively smooth wall of such a pipe we frequently use a cylindrical surface, having a diameter equal to the reduced diameter:

$$D_{re} = \sqrt{4V/\pi L},$$

where V and L are the inside volume and the length of the pipe, respectively. However, the selection of this diameter is not justified from the physical point of view. If we take into account the presence of vortical zones that arise because of the flow separation behind the projection, where there is no resulting flow in the direction of the main flow, then we can assume that the effective diameter of the rough pipe is less than D_{re} . This is confirmed by the results of the investigations carried out by the authors on the velocity fields in pipes having artificial roughness [2, 3].

To explain the question dealing with the effective diameter of a rough pipe, the actual mass flow rate, known from experiment, was compared with the calculated flow rates determined by integrating the measured velocity profiles [6]. The integration was carried out by two methods: by reading the coordinate y from the reduced diameter D_{re} and from the inside diameter D_{in} . In the investigation we selected variants of roughness with closely spaced annular projections; these variants are characterized by considerable mutual screening of the projections, as a result of which the main flow does not penetrate into the interior of the depressions. A comparison showed that for the pipe variants being considered, the effective diameter should be close to D_{in} .

The selection of the magnitude of the effective diameter of the rough pipe can be substantiated by results of the analysis of the experimental picture of flow past the roughness elements. From the experiments it follows that there is a flow separation at the roughness element, and afterwards the flow rejoins the wall at a distance equal to approximately eight projection heights [7, 8]. At the point of rejoining, a counterflow forms, which moves along the channel wall opposite to the main flow (Fig. 1a). If the flow in front of the projection is completely turbulent, then over a wide range of Reynolds numbers Re and turbulence intensities, no noticeable effect of these parameters on the flow picture and length of the separation zone is detected [7]. In front of the projection there also forms a vortical zone, however, having considerably smaller dimensions than behind the projection [8]; the dimension of this zone in the flow direction can be assumed equal to the projection height (see Fig. 1a).

On the basis of the picture, represented in Fig. 1a, of the flow past the roughness elements, we can draw the following conclusion: since the vortical zones in front of and behind the projection do not participate in the main motion of the liquid, then we do not have to take them into account in the calculation of the effective diameter of a rough pipe.

Figure 1b shows a simplified calculation scheme of the flow past the projections, corresponding to the experimental flow picture in Fig. 1a. The lines AB and DE (see Fig. 1b) — the boundaries of the penetration of the main flow — are assumed to be straight lines. The angles α and β between the boundaries of the main flow and the x axis can be called the angles of penetration of the main flow. The lines AB and DE are considered as boundaries of the unseparated flow, on which the velocity equals zero.

Thus, the effective diameter of a rough pipe can be calculated from the equation

$$D_e = \sqrt{4V_e/\pi L},$$

where V_e is the inside volume of the pipe after deducting the volume of the vortical zones.

When the projections are close together (see Fig. 1c) their flow picture remains the same [8]; the vortical zones overlap. The vertically hatched region in Fig. 1c should not be taken into consideration for determining the effective diameter of the rough pipe.

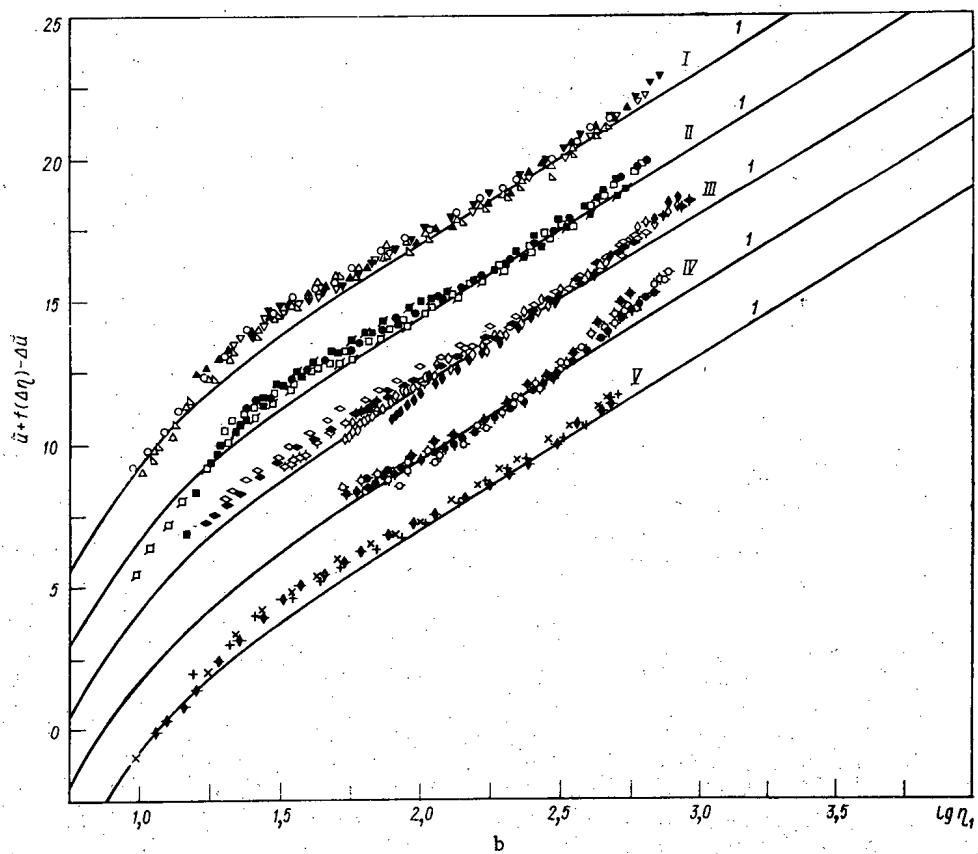
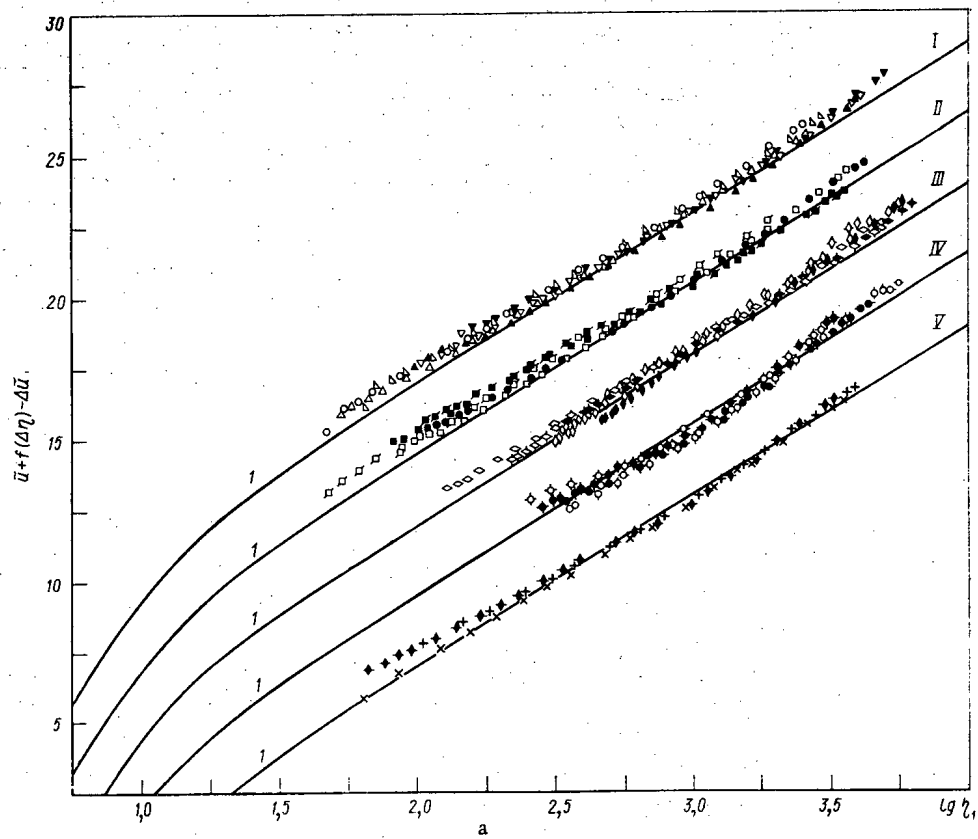


Fig. 2. Experimental velocity profiles in rough pipes: a) $Re = 10^5$; b) $Re = 15 \cdot 10^3$. For the notation for the points, see [2, 3].

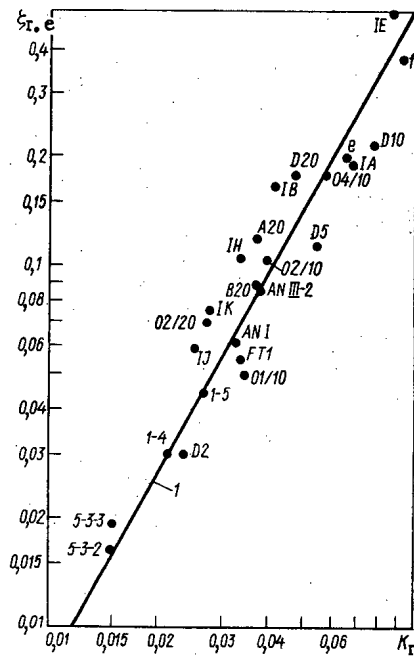


Fig. 3. Dependence of increase in roughness on generalized roughness parameter (the numbers with the points indicate the variants of roughness, taken from [2, 8, 15-18]).

The proposed method for determining the calculated diameter can be applied to roughness of any form (in Fig. 1 the roughness is represented in the form of annuli). For annuli having a smooth surface, the boundaries of the main flow are tangential to the surface of the projection, with the values of the angles α and β not varying ($\alpha = \arctg(1/8)$, $\beta = 45^\circ$). For three-dimensional projections, the angles α and β for each point of the separation line are plotted from the x axis to a plane perpendicular to the separation line at the given point; if the projections have a smooth surface, then we can proceed just as in the case of annuli with a smooth surface.

The picture of the flow past a projection, presented in Fig. 1, is confirmed by experimental data on the hydraulic resistance of pipes with annular insertions. Experiments show that with increasing relative distance between the annuli s/k from 0 to 6-10 (based on the data of different authors) the hydraulic-resistance coefficient increases, and with subsequent increase in s/k , it decreases. This can be explained by the fact that at first ($0 \leq s/k \leq 6-10$) the effective height of a projection h (see Fig. 1c), and, along with it, also the hydraulic-resistance coefficient, increase; then ($s/k \geq 6-10$) the effective projection height remains constant, equal to the geometrical height k , and the hydraulic-resistance coefficient decreases, since the number of projections per unit pipe length decreases.

It was shown in [6] that in measuring the distances y from the effective diameter D_e the experimental velocity profiles in rough pipes are well described by the function

$$\tilde{u} = f(\eta + \Delta\eta) - f(\Delta\eta), \quad (1)$$

where f is the velocity law for a smooth pipe; $\Delta\eta$ is a quantity that characterizes the displacement of the velocity profile for a rough pipe relative to the velocity profile for a smooth pipe. Equation (1) expresses the experimentally established fact that in smooth pipes and rough pipes having the same shearing stress on the wall, the peaks of the velocity profiles coincide.

Figure 2, a and b shows in the generalized coordinates $[\tilde{u} + f(\Delta\eta) - \Delta\tilde{u}] - \log \eta_1$ the experimental velocity profiles constructed by using the effective diameter of the rough pipe; here $\eta_1 = \eta + \Delta\eta$; f is the Millionschikov velocity law for a boundary layer [9]; $\Delta u = 2.5 \ln \{ [1.5(1 + r/R)] / [1 + 2(r/R)^2] \}$ is the Reichardt correction [10], which takes account of the difference between the velocity profile in a circular pipe and that of a boundary layer. The representation in generalized coordinates is essentially the reduction of the velocity profile in a smooth pipe or a rough pipe to the velocity profile for a boundary layer. Since very many points are represented in Fig. 2, for convenience they are divided into five groups (I-V), where the values of the ordinates for group II by a convention are reduced by a factor of 2.5; for group III, by 5; for group IV, by 7.5; and for group V, by 10. The experimental velocity profiles are in satisfactory agreement with the theoretical profile for a boundary layer (see curve 1). The dimensionless displacement $\Delta\eta$ in Eq. (1) is determined from the well-known values of the hydraulic-resistance coefficient and the Re numbers by the method of successive approximations, using the relation

$$\frac{\bar{u}}{u^*} = \sqrt{\frac{8}{\lambda}}$$

Thus, we have established the relation between the hydraulic-resistance coefficient and the velocity profile in smooth pipes and in rough pipes. This relation will be used for calculating the hydraulic-resistance coefficient of a rough pipe.

Hence, a rough pipe can be considered as a smooth pipe with diameter D_e and resistance equal to the resistance of a rough pipe. For a stabilized liquid flow in a rough pipe the equilibrium of the forces applied to an element of liquid bounded by the pipe surface and two cross sections perpendicular to the pipe axis and located at a distance ΔL from each other can be written in the form

$$\Delta p \frac{\pi D_e^2}{4} = \tau_{fr} \pi D_e \Delta L + P_r, \quad (2)$$

where Δp is the drop in static pressure over a pipe section of length ΔL ; τ_{fr} is the tangential stress at the wall, which is assumed constant over a cylindrical surface of diameter D_e ; and P_r is the force of resistance of the roughness projections.

We substitute the following values into Eq. (2):

$$F_e = \frac{\pi D_e^2}{4}, \quad \Delta p = \lambda_e \frac{\Delta L}{D_e} \cdot \frac{\rho \bar{u}_e^2}{2},$$

$$\tau_{fr} = \frac{\lambda_{fr.e} \rho \bar{u}_e^2}{8}$$

(here λ_e and $\lambda_{fr.e}$ are the total resistance coefficient and the frictional-resistance coefficient, respectively), and we obtain

$$\lambda_e = \lambda_{fr.e} + P_r \frac{D_e}{\Delta L F_e \rho \bar{u}_e^2 / 2}. \quad (3)$$

The frictional-resistance coefficient $\lambda_{fr.e}$ can be assumed equal to the frictional-resistance coefficient for a smooth pipe of diameter D_e with given Re ($\lambda_{fr.e} = \lambda_{sm.e}$), and the excess of the total hydraulic-resistance coefficient of a rough pipe over the hydraulic-resistance coefficient of a smooth pipe for given Re can be denoted by $\zeta_{r.e} = P_r [D_e / (\Delta L F_e \rho \bar{u}_e^2 / 2)]$. Then

$$\lambda_e = \lambda_{sm.e} + \zeta_{r.e}. \quad (4)$$

The force of resistance of the roughness projections is related mainly to the resistance of the shape of the individual roughness projections P_{si} . We can assume that

$$\zeta_{r.e} = f(K_r), \quad (5)$$

where the quantity

$$K_r = \sum_i P_{si} \frac{D_e}{\Delta L F_e \rho \bar{u}_e^2 / 2}, \quad (6)$$

which determines the resistance of the shape of the roughness projections, and is related to their geometric dimensions, is called the generalized roughness parameter. The function (5) is determined experimentally.

An analysis of the experimental data on free flow past bodies [11] shows that the resistance of a shape for bluff bodies is a certain function of the angle of attack (the angle between the velocity vector and its projection on the flow surface). For bodies having a constant angle of attack over all their faces (inclined plane, cone) the resistance of the shape for free flow can be represented in the form

$$P_s = cf(\gamma) F \frac{\rho u^2}{2}, \quad (7)$$

where c is the resistance coefficient for a shape with angle of attack equal to 90° ; γ is the angle of attack; $f(\gamma) \leq 1$ is some function of the angle of attack; F is the front face of the body; and u is the free-flow velocity. The coefficient c , which is the resistance coefficient for a body in the shape of a plate located perpendicular to the flow can be assumed constant and independent, within certain limits, of the configuration of the plate (circle, square) and of Re , which is confirmed by experimental data [11].

For free flow past bodies having an angle of attack that is variable over their front face (cylinder, sphere) we can assume that the form of Eq. (7) remains the same, the coefficient c has the same sense, and the function f is determined from the angle of attack, averaged over the front cross section:

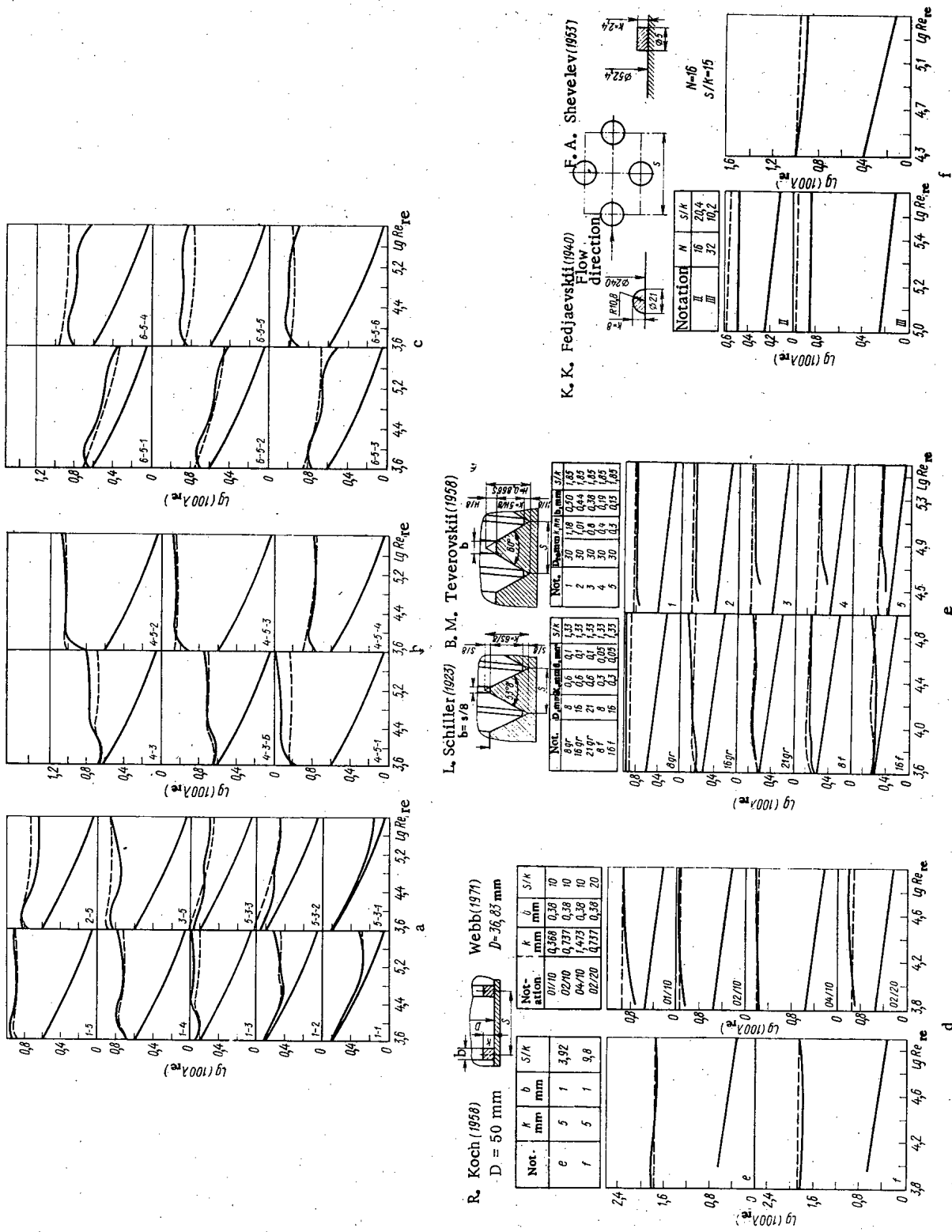


Fig. 4. Comparison of calculated and experimental values of hydraulic-resistance coefficients: a) annular projections [2]; b) multiple screw thread [2]; c) hemispherical projections [2]; d) inserted annuluses [8, 17]; e) triangular screw thread [20, 21]; f) hemispherical [22] and cylindrical [23] projections; - - - calculation; — — — averaging lines of experimental points and theoretical curves for a smooth pipe based on the calculation of Millionshchikov [9] (lower curves).

$$P_s = cf(\bar{\gamma}) F \frac{\rho u^2}{2}. \quad (8)$$

If the velocity field at the flow past the body is inhomogeneous, and the angle of attack is variable over the front face, then the expression for the resistance force of the shape has the form

$$P_s = C \int_F f(\gamma) \frac{\rho u^2}{2} dF, \quad (9)$$

where γ and u are the instantaneous values of the angle of attack and velocity of the liquid, and C is a constant coefficient.

Taking account of (6) and (9), the parameter K_R for regular roughness can be represented in the form

$$K_R = \frac{D_e}{S} N \int_{F_{in}} f(\gamma) \left[\frac{u(\gamma)}{u_e} \right]^2 \frac{dF}{F_e}, \quad (10)$$

where N is the number of roughness projections on the section of pipe of length equal to the longitudinal step S . The instantaneous values of the velocity are calculated from Eq. (1).

For the function $f(\gamma)$ on the basis of the experimental studies [12-14], the following limiting values were determined:

$$\begin{aligned} f(\gamma) &= 1 \quad \text{for } \gamma = 45^\circ - 90^\circ, \\ 0 \leq f(\gamma) &\leq 1 \quad \text{for } 0 \leq \gamma \leq 45^\circ. \end{aligned} \quad (11)$$

The absence of an effect on the resistance of a projection of the angle of attack in the limits of its variation ($45^\circ - 90^\circ$) is in satisfactory agreement with the experimental picture of flow past a roughness element. As was noted above, in front of a steep projection there forms a vortical zone, whose region of action can be approximately marked off by a straight line passing through the leading edge of the projection at a 45° angle to the direction of flow. The boundary of the vortical zone can be interpreted as the effective front face of the projection. With such an assumption, projections with angles of attack from 90° to 45° prove to be equivalent. The limiting values of the function $f(\gamma)$ with variation of the angle of attack from 0° to 45° are satisfied by the function

$$f(\gamma) = \sin^n 2\gamma; \quad (12)$$

the quantity n is determined from experimental data.

The hydraulic-resistance coefficient is calculated from Eqs. (4), (5), and (10), taking into account the interaction of the projections; however, in calculating the quantity K_R the integration is conducted according to the effective frontal cross section F_h , determined by the effective height of the projection h (see Fig. 1c).

The form of the function $\zeta_{r,e} = f(K_R)$ was determined experimentally. Both the characteristic experimental data of the authors of the present work, and also the data of other authors [8, 15-18] were used.

On Fig. 3, along the ordinate axis, we plot the values of $\zeta_{r,e} = \lambda_e - \lambda_{sm,e}$, and along the abscissa axis we plot values of K_R . The numbers with the points in Fig. 3 indicate the notation of the variants corresponding to the notation of the references. We first plotted points for variants of roughness with steep projections, for which $f(\gamma) = 1$. Then we calculated the values of $\zeta_{r,e}$ and K_R for pipes with semicircular annuli; for the exponents in the function $f(\gamma)$ we took the values $0, 1, 2, \dots$. For $n = 2$ the experimental points have optimum agreement with the general law (see Fig. 3). Thus, the function $f(\gamma)$ can be represented as

$$f(\gamma) = \sin^2 2\gamma.$$

The averaging line of all the experimental points in Fig. 3 is approximated by the equation

$$\zeta_{r,e} = 30K_R^{1,8}. \quad (13)$$

For the function $\zeta_{r,e} = f(K_R)$ we fit the experimental points for the roughness with relative height of projections $k/R = 0-0.2$ and relative longitudinal distance between the projections $s/k = 0-20$.

To calculate the hydraulic-resistance coefficient we used the method of successive approximations, which consists of the following. We are given the coefficient $\lambda_e > \lambda_{sm,e}$, based on which for given Re we determined the velocity profile (1), then the parameter K_R , and finally, the calculated values of the resistance coefficient λ_e ; after this, we are given the second approximation for λ_e , etc. To find the velocity

profile (1) it is also necessary to use the method of successive approximations. In [19] a simplified method was proposed for determining the displacement $\Delta\eta$ in Eq. (1) based on the known values of λ_e and Re_e .

The method presented for calculating the coefficient λ_e is used for $\Delta\eta \geq 7.8$. This condition corresponds to the complete appearance of roughness. The function $\zeta_{r,e}(Re_e)$ for $\Delta\eta < 7.8$ (transition from hydraulic smooth regimes to regimes with complete appearance of roughness) is found from an empirical equation, if we know the point on the curve $\lambda_e(Re_e)$ at which $\Delta\eta = 7.8$, i. e., we know $\lambda_{e7.8}$ and $Re_{e7.8}$:

$$\frac{\zeta_{r,e}}{\zeta_{r,e7.8}} = M \left(\frac{1}{\pi} \operatorname{arctg} m \lg \frac{Re_e}{Re_{e7.8}} + 0.5 \right),$$

where M is a normalizing factor:

$$M = \frac{1}{\frac{1}{\pi} \operatorname{arctg} m \lg \frac{Re_{e7.8}}{Re_{e7.8}} + 0.5}.$$

The coefficient determines the slope of the function $(\zeta_{r,e}/\zeta_{r,e7.8})(Re_e)$, and $Re_{e7.8}$ is its position relative to the abscissa axis. The quantity $Re_{e7.8}$ is a criterion that characterizes the measure of the relation of the thickness of the viscous sublayer δ and the effective height of the projection h. For m and $Re_{e7.8}$ we obtain the following empirical equations:

$$m = 95 \sqrt{\frac{h}{Re_e}};$$

$$\lg Re_{e7.8} = 3.3 + \frac{0.00421}{\frac{h}{Re_e} + 0.00132}.$$

The behavior of the function $(\zeta_{r,e}/\zeta_{r,e7.8})(Re_e)$ allowed us to refine the considerations given earlier concerning the nature of the flow past a roughness projection. Thus far, in the calculation method we have assumed that the angle of penetration of the main flow α is constant over the entire region of regimes with increasing roughness, and equals $\operatorname{arctg}(1/8)$. In order to satisfy the experimental data it is necessary to assume that the angle α increases insignificantly with increasing Re_e :

$$\alpha = \operatorname{arctg} \frac{1}{8} [1 + 0.15 (1 - e^{-Re_e/10^6})].$$

The increase in the angle α with increasing Re can be explained by the fact that the structure of the turbulent vortices is destroyed, as a result of which their ability to penetrate into the interior of the depressions increases.

In Fig. 4 a comparison is given of the calculation results based on the assumed method with the experimental data for characteristic variants of roughness. The calculated values of the hydraulic-resistance coefficient and Re are reduced to the diameter D_{re} . The calculations were carried out for two-dimensional and three-dimensional projections of various shapes. In the majority of cases, the calculated values of the hydraulic-resistance coefficients differ from the experimental data by no more than 20%. In individual cases, this difference reaches 25-30%. The coefficient λ for certain variants of rough pipes differs from the coefficient of resistance of a smooth pipe by 1-2 orders of magnitude. For $Re > 4 \cdot 10^5$ in the case of three-dimensional streamlined projections, the calculation error can be greater than 30% owing to the fact that in the calculation, variations in the flow mechanism characteristic for such projections with increasing Re, have not been taken into account.

The agreement between calculation and experiment that has been obtained confirms that we have found the fundamental laws for taking account of the contribution of the roughness of a surface to the hydraulic resistance of a channel.

LITERATURE CITED

1. M. D. Millionshchikov et al., Dokl. Akad. Nauk SSSR, Fizika, 207, 1292 (1972).
2. M. D. Millionshchikov et al., At. Énerg., 34, No. 4, 235 (1973).
3. M. D. Millionshchikov et al., Preprint FÉI-385, Obninsk (1973).
4. L. G. Loitsyanskii, Tr. TsAGI, No. 250 (1936).
5. K. K. Fedyaevskii, Tr. TsAGI, No. 250 (1936).
6. M. D. Millionshchikov et al., Preprint FÉI-417, Obninsk (1973).
7. D. Abbott and S. Kline, Trans. ASME, Ser. D, 84, No. 3, 317 (1962).
8. R. Webb et al., Int. J. Heat and Mass Transfer, 14, 601 (1971).

9. M. D. Millionshchikov, *At. Énerg.*, 28, No. 3, 207 (1970).
10. H. Reichardt, *ZAMM*, 31, 208 (1951).
11. I. E. Idel'chik, *Handbook on Hydraulic Resistances [in Russian]*, Gosénergoizdat, Moscow--Leningrad (1960).
12. K. Fromm, *ZAMM*, 3, 399 (1923).
13. V. Streeter, *Proc. ASCE*, 61, 163 (1935).
14. V. M. Buznik, V. N. Bandura, and G. P. Velichenko, *Izv. VUZ, Énergetika*, No. 3, 114 (1967).
15. H. Mobius, *Phys. Zeitschrift*, 7, 202 (1940).
16. W. Nunner, *VDI--Forschungsheft*, No. 455 (1956).
17. R. Koch, *VDI--Forschungsheft*, No. 469 (1958).
18. J. Gargaud and G. Paumard, *Rapport CEA-R 2464* (1964).
19. L. L. Kobzar', *Preprint FÉI-418*, Obninsk (1973).
20. L. Schiller, *ZAMM*, 3, 2 (1923).
21. B. M. Teverovskii, *Izv. VUZ, Énergetika*, No. 7, 84 (1958).
22. K. K. Fedyaevskii and N. M. Fomina, *Tr. TsAGI*, No. 441 (1940).
23. F. A. Shevelev, *Investigation of Fundamental Hydraulic Laws of Turbulent Flow in Pipes [in Russian]*, Stroiizdat, Moscow (1953).

THE COMPOSITION OF URANINITE FROM PEGMATITE
AND URANIUM—MOLYBDENUM DEPOSITS

V. A. Strel'tsov, V. A. Boronikhin,
and A. I. Tishkin

UDC 549.514.87 + 548.32

Uraninite is a widely occurring mineral of pegmatites and metasomatic high-temperature uranium deposits [1-4]. It is present far less frequently and in smaller amounts in medium-temperature vein deposits, where uranium oxides are represented mainly by pitchblende [5-7]. The theoretical composition of uraninite is often expressed by the formula UO_2 [8, 9], but chemical analysis shows that it always contains not only uranium (IV) but also uranium (VI) and in many cases thorium and rare earths; zirconium and a number of petrogenic elements, particularly calcium, are also sometimes present [8-10]. It has also been established that the content of thorium and rare earths in uraninite from pegmatites is higher than in this mineral from medium-temperature deposits [8-10], and that the lead content is proportional to the age of the mineral. Whereas isomorphic replacement of uranium by thorium and rare earths is an accepted fact, the position of lead in the structure of the mineral and its chemical form are disputed [11-14]. The possibility that calcium is present in the crystal structure of uraninite is admitted only by certain investigations [15], despite the fact that Alberman et al. [16] have given experimental proof of isomorphism in the system UO_2 -CaO. Isomorphism of zirconium with uranium is also postulated [17, 18]. Isomorphism of iron (II) with uranium (IV) is indicated by Heinrich [18], this conclusion being based on the presence of these elements in the composition of davidite. However, the result is purely empirical, because the structure of the mineral has not been interpreted. Most authors assume that the presence in uraninite of calcium, magnesium, ferric and ferrous iron, and other elements, found from time to time and in various different amounts, is due to fine intergrowth of the corresponding minerals with uraninite [9, 10, 19, 20].

The practical use of x-ray spectrometry in mineralogical research opened up new possibilities for investigating the composition of minerals and the distribution pattern of individual elements in them. To perform investigations by this method we selected uraninite crystals from deposits of the pegmatite and uranium-molybdenum types. Such a choice of deposits with markedly different geological conditions of formation enabled us to get a fuller picture of the changes in the mineral's composition.

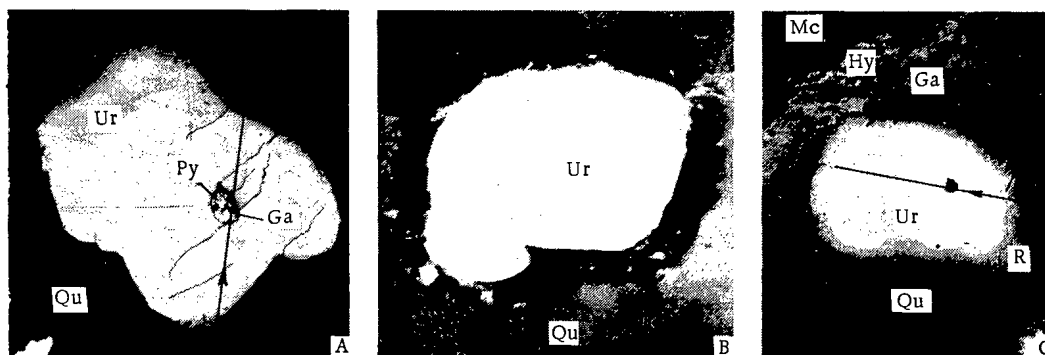


Fig. 1. Optical image of crystals A, B, and C of uraninite (polished section; magnification of A and B 350, magnification of C 165): Ur, uraninite; Ga, galena; Py, pyrite; Qu, quartz; Mc, microcline-perthite; Hy, hypersthene; R, rim of decomposed hypersthene; the lines are the profiles of the concentration curves.

Translated from *Atomnaya Energiya*, Vol. 37, No. 4, pp. 306-315, October, 1974. Original article submitted September 27, 1973.

© 1975 Plenum Publishing Corporation, 227 West 17th Street, New York, N.Y. 10011. No part of this publication may be reproduced, stored in a retrieval system, or transmitted, in any form or by any means, electronic, mechanical, photocopying, microfilming, recording or otherwise, without written permission of the publisher. A copy of this article is available from the publisher for \$15.00.

TABLE 1. Composition of Uraninite from Pegmatites from X-Ray Spectral Analysis Data (wt. %)

Elements	Crystal A		Crystal B		Crystal C	
	edge region	overall field	edge region	overall field	edge region	overall field
U	54,9	52,4	55,4	54,1	54,1	53,0
Th	7,8	7,8	9,0	8,7	7,9	8,2
Pb	21,7	21,9	21,0	21,0	18,9	21,0
Ca	0,2	0,3	0,4	0,3	0,3	0,2
Fe	0,2	0,1	0,2	0,3	0,2	0,1
O (calculated)	11,75	11,37	12,02	11,75	11,45	11,49
Totals	96,55	93,87	98,02	96,15	92,85	93,99

Note. The low analysis totals are due to the absence of quantitative determinations of rare earth elements.

Uraninite was analyzed in a Cameca MS-46 micro-analyzer. We recorded the intensities of the analytical lines UL_{α_1} , PbL_{α_1} , FeK_{α_1} , CaK_{α_1} , ThM_{α_1} , CeL_{α_1} , VL_{α_1} , ZrL_{α_1} , SiK_{α_1} , SK_{α_1} with an accelerating potential of 35, 30, 30, 20, 20, 20, 20, 20, and 20 kV, respectively (probe current 15 nA). The crystal-analyzers were LiF for UL_{α_1} and PbL_{α_1} , quartz (1011) and "PET" for FeK_{α_1} , "PET" for CaK_{α_1} , ThM_{α_1} , CeL_{α_1} , YL_{α_1} , and SK_{α_1} and "KAP" for ZrL_{α_1} and SiK_{α_1} . The sensitivity of the determination of the elements in uraninite was as follows: Pb 0.3%, Fe 0.06%, Ca and S 0.05%, Th 0.04%, Zr 0.07%, and Si 0.07%. The standards were metallic uranium, iron, zirconium, silicon, and ThO_2 of ar grade, and also galena and Iceland spar. Rare earth elements were not analyzed quantitatively owing to the absence of standards. To determine the true concentrations, the relative intensities were corrected by factors derived from a modified Springer program [21], in which we used the μ/ρ ratios from [22], the values of s and σ being taken from [23]. The accuracy of the determination of iron and calcium in uraninite was of the order of ± 20 rel. % and ± 5 rel. %, respectively; that of the other elements was ± 2 rel. %.

In the pegmatite deposit, the age of which is about 1,800,000,000 years, * uraninite was formed in paragenesis with molybdenite in the stage of formation of hypersthene-feldspathic veins imposed on pegmatites [24]. The principal mineral of the next stage is quartz; it contains inclusions of pyrite, pyrrhotite, and chalcopyrite. Uraninite metacrystals are usually located in hypersthene or at its contact with microcline-perthite, less frequently in the latter itself. Replacement of minerals of the hypersthene-feldspathic veins by quartz of the later stage led to the appearance of uraninite and molybdenite (sometimes with relicts of silicates) in it. The usual size of the uraninite crystals is about 0.5 mm, the color in reflected light is gray, the reflectance in the wavelength range 440-740 nm is 18.4-16.0%. The crystals are permeated by microcracks which are occasionally filled with galena, pyrrhotite, and quartz. Furthermore, the uraninite crystals display oval galena inclusions, not more than a few microns in diameter.

For analyses in the x-ray microanalyzer we used uraninite crystals present in hypersthene, microcline-perthite, and quartz. Figure 1 gives the results of an investigation of three crystals (A, B, and C) from the same specimen. Qualitative identifications, performed by electronic and x-ray scanning of cross sections and areas, revealed that (regardless of the associated minerals) uraninite contains not only uranium but also thorium, lead, calcium, iron, cerium and other rare earth elements. Zirconium and silicon are sometimes present. No other elements were detected with the sensitivity range of the method.

Figure 2 shows the distribution pattern of uranium, thorium, lead, iron, sulfur, and calcium in uraninite. In crystal A uranium and thorium are distributed uniformly, but in crystals B and C the edges are slightly enriched with them. The marked increase in the thorium concentration in the bottom right-hand part of crystal C is correlated with the grain of some kind of mineral with no uranium. The distribution pattern of these elements is also seen in the profiles (Fig. 3). The marked decreases in the uranium and thorium concentrations observed on the graphs are due to galena and pyrite inclusions in crystal A and to the presence of a free space in crystal C. This is readily seen both in the photomicrographs obtained by means of an ore microscope (see Fig. 1), and in photographs of scanning in reflected electrons with negative modulation (see Fig. 2, I).

Lead is distributed fairly uniformly; higher concentrations of this element (see Fig. 2, IV) are due to galena inclusions. This is indicated by sectors with sulfur concentrations higher than the background concentration (see Fig. 2, VI), corresponding exactly in position and configuration to the sectors of higher lead concentration.

Iron is also distributed fairly uniformly (see Fig. 2, V). The iron concentration in the crystals always exceeds the background value. The occasional and slight increases in the concentration of this element usually correspond to pyrite inclusions visible under the microscope (see Fig. 1, crystal A). However, the sectors of higher iron concentration do not always coincide with those of higher sulfur concentration; this is seen from a comparison of photographs V and VI (Fig. 2) and the concentration curve of crystal A

* The age was determined by the U/Pb method.

TABLE 2. Composition of Uraninite from Pegmatites, from Chemical Analysis Data (wt. %)

Oxides	1	2	3
Na ₂ O	0,22		
K ₂ O	0,06		
SrO	0,003		
MgO	Traces		
CaO	0,30	0,30	0,32
MnO	0,20		
Fe ₂ O ₃ , FeO	0,62	0,22	0,23
PbO	20,95	19,01	20,09
Al ₂ O ₃	0,59		
∑TR ₂ O ₃	2,85	2,85	3,01
SiO ₂	1,09		
TiO ₂	0,03		
ZrO ₂	0,046		
ThO ₂	5,95	5,95	6,29
UO ₂	37,77	39,77	42,03
UO ₃	25,55	25,55	27,00
MoO ₃	0,20		
P ₂ O ₅	0,065		
S	0,32		
H ₂ O ⁻	Not detected		
H ₂ O ⁺	0,98	0,98	1,03
Totals	99,63	94,63	100,00

Note. 1) Complete chemical analysis of the mineral; 2) the same analysis without elements due to mechanical admixtures of other minerals; 3) preceding data converted to 100 %.

with this element. From Table 1 and the graphs in Fig. 3 we can draw the conclusion that with an overall high lead concentration and only a local increase in the sulfur concentration above the background value, only a small part of the lead in uraninite is combined with sulfur in galena. This confirms the conclusion drawn by Kirkinskii and Makarov [13]. A comparison of the results of x-ray spectral (Table 1) and chemical (Table 2)* analyses shows fairly close agreement of the results of these two analytical methods only in the case of calcium, iron, and lead. The absence of quantitative determinations of the rare earths and the impossibility of separate analysis of U(IV) and U(VI) by the x-ray spectral method did not enable us to calculate the crystallochemical formula of uraninite.

In the uranium-molybdenum deposit, the age of which, according to the K-Ar method, was about 270,000,000 years, uraninite was segregated in the third stage of mineral formation. It was preceded by the stages of beresitization of the country rocks and of formation of quartz veinlets; quartz-carbonate veinlets with sulfides were formed in the final stage. Uraninite metacrystals, hundredths or thousandths of a millimeter in size (sometimes present together with hydromica), form disseminations around pitchblende veinlets in the rock. In reflected light the mineral is gray; the reflectance is 16-17%. Galena inclusions are very rarely seen in the uraninite.

Qualitative analysis, performed by scanning 40 uraninite crystals in reflected electrons and x-rays, revealed that they contained lead, iron, and calcium as well as uranium. Thorium, rare earths, zirconium, silicon, sulfur, and other elements were not detected within the sensitivity range of the method. As we see in the photographs of one of the analyzed crystals (Fig. 4), all the elements detected are distributed uniformly, which is also confirmed by the concentration curves (Fig. 5). The fairly uniform distribution of lead and iron in uraninite at the background content of sulfur, together with the uniform distribution of calcium enable us to assume that these elements are present as isomorphous impurities.

Table 3 lists the results of quantitative analysis of five uraninite crystals identical in qualitative composition to the other crystals. The variations of the element contents are slight, being less than 1.3% even for uranium. The total percentage of the elements in each analysis is also within the norm.

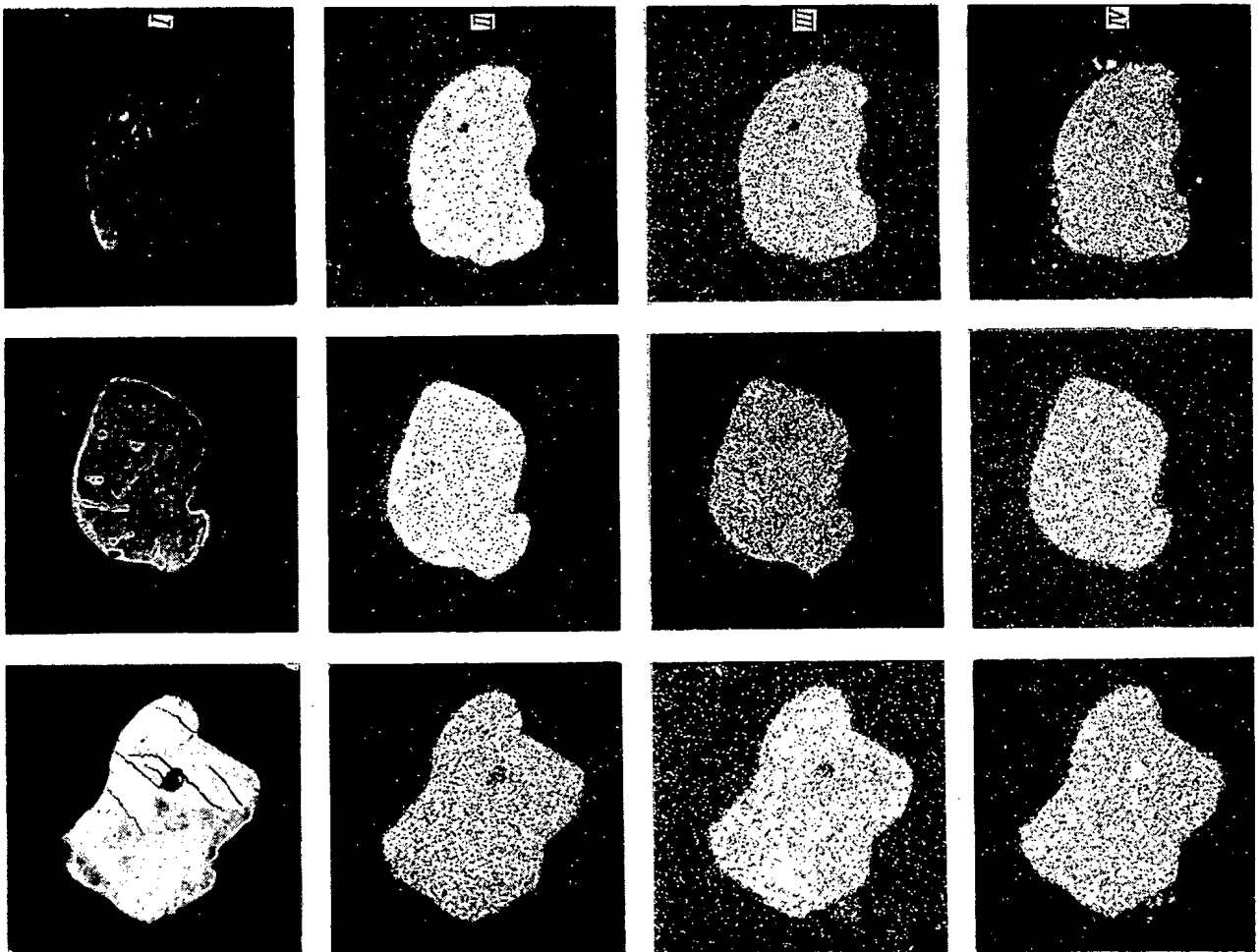
*The analysis was performed in the Central Chemical Laboratory of the Institute of Geology of Ore Deposits, Petrography, Mineralogy, and Geochemistry, Academy of Sciences of the USSR, by D. N. Knyazeva.

(Fig. 3). This indicates that uraninite contains inclusions not only of iron sulfides, but also of iron oxides.

The concentration of calcium, which is uniformly distributed, exceeds the background concentration over the whole area of the uraninite crystals. The marked increase in the calcium concentration (Fig. 2, VII) is correlated either with microcracks and inclusions (crystals A and B) or with an independent mineral (crystal C, lower right-hand side). The cerium and yttrium concentrations in uraninite everywhere exceed the background with uniform distribution of both elements.

The zirconium concentration does not exceed the background value in any of the crystals investigated. The occasional sectors with high concentrations of this element correspond exactly both in shape and size to the sectors with higher silicon concentrations. We can therefore infer that the uraninite crystals contain fine, non-uniformly dispersed zircon crystals, usually not visible under the microscope.

Quantitative determinations of the uranium, thorium, iron and calcium contents of the mineral (Table 1) at points with no inclusions of other minerals revealed slight variations in these contents both in different sectors of the same crystal and in different crystals. It will be seen from Table 1 that at the edges of the crystals the uranium contents are usually higher and the lead contents lower, i. e., the peripheral sectors of the crystals are enriched



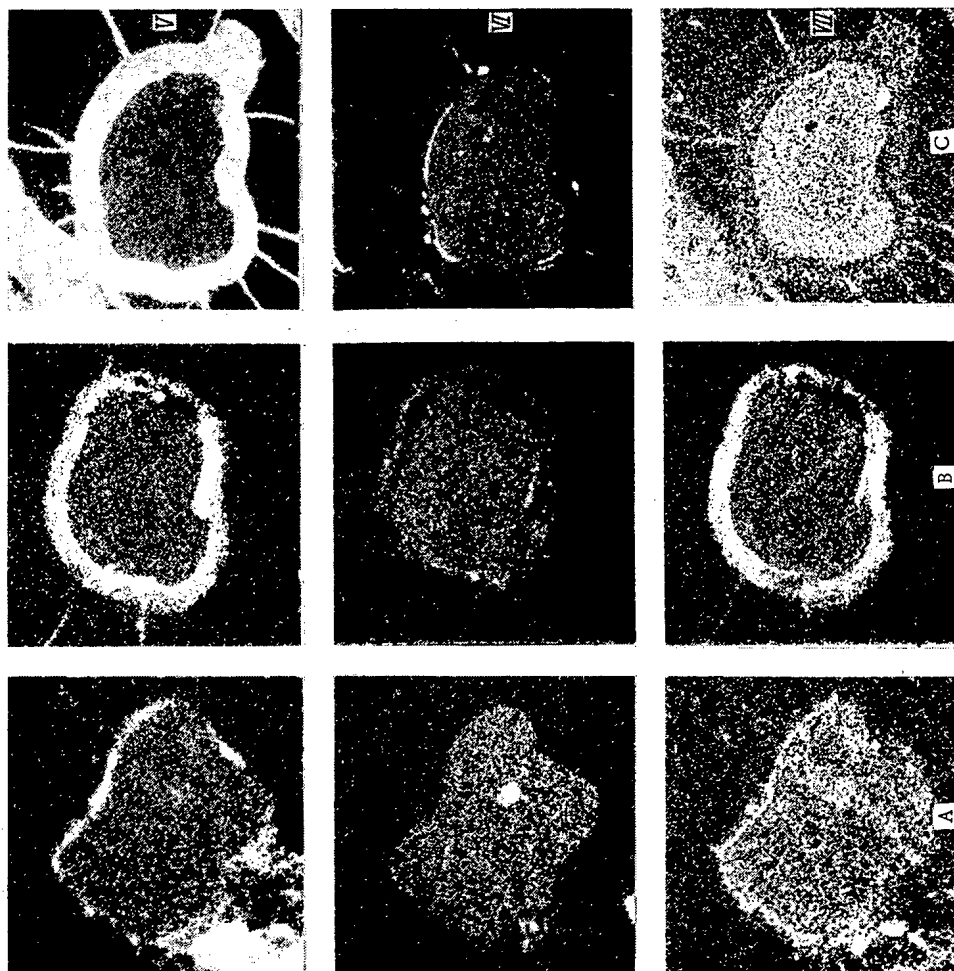


Fig. 2. Distribution pattern of elements in uraninite crystals: I) scanning in absorbed electrons, negative modulation; II-VII) scanning in x-radiation $UL\alpha_1$, $ThM\alpha_1$, $FeK\alpha_1$, $SK\alpha_1$, $CaK\alpha_1$; scanning areas in crystals A and B $250 \times 250 \mu$, in crystal C $300 \times 300 \mu$.

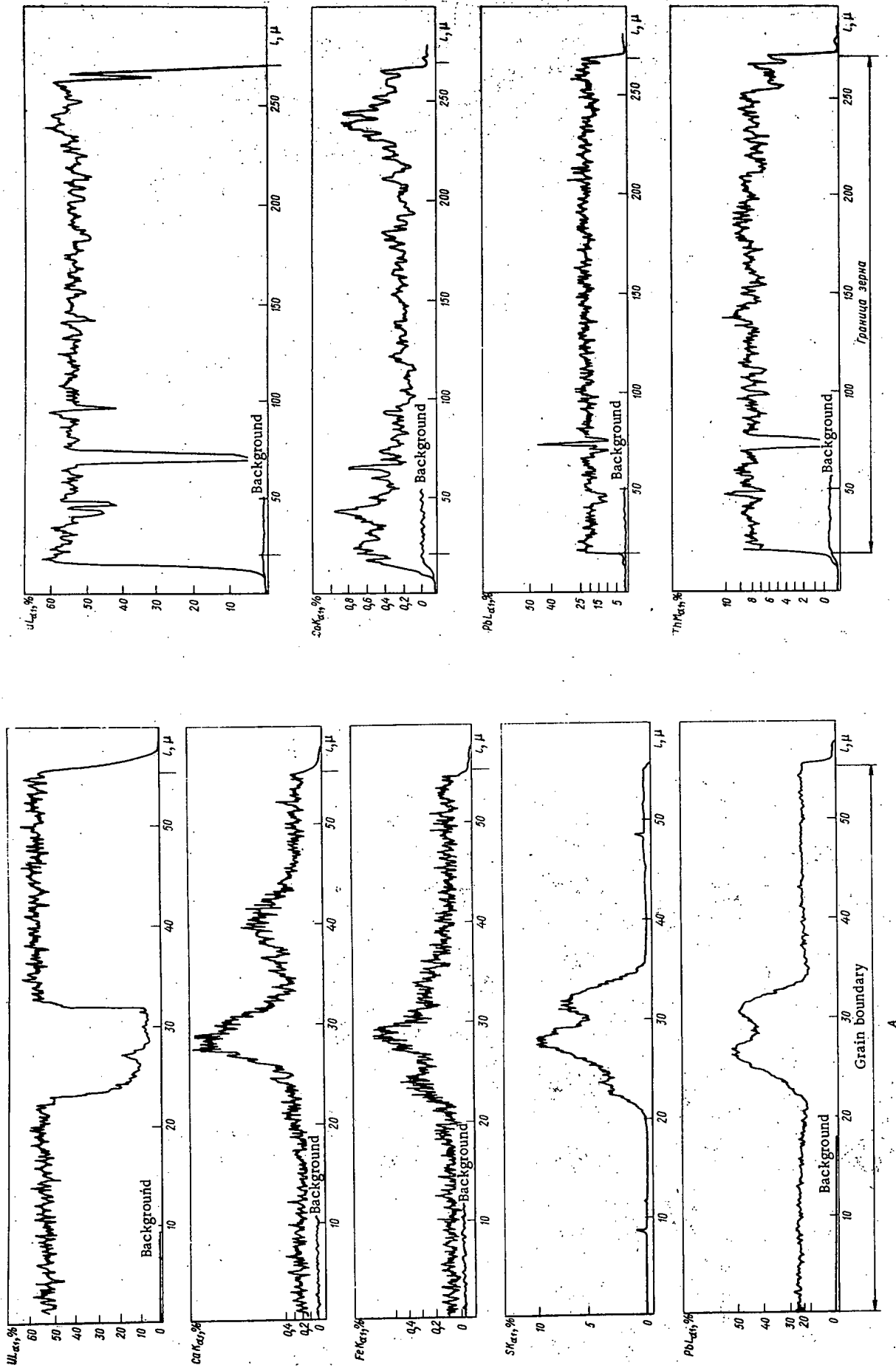


Fig. 3. Distribution pattern of elements from profiles in crystals A and C.

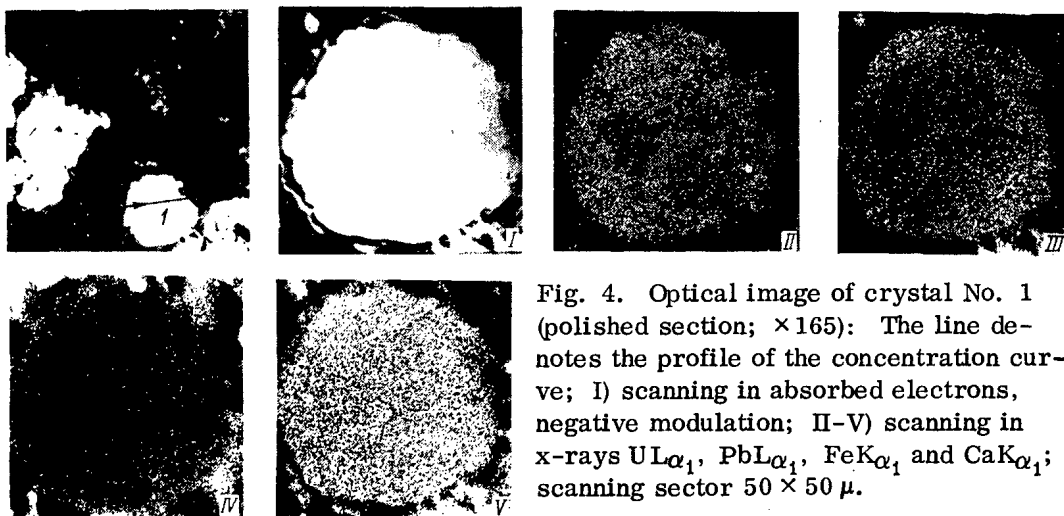


Fig. 4. Optical image of crystal No. 1 (polished section; $\times 165$): The line denotes the profile of the concentration curve; I) scanning in absorbed electrons, negative modulation; II-V) scanning in x-rays UL_{α_1} , PbL_{α_1} , FeK_{α_1} and CaK_{α_1} ; scanning sector $50 \times 50 \mu$.

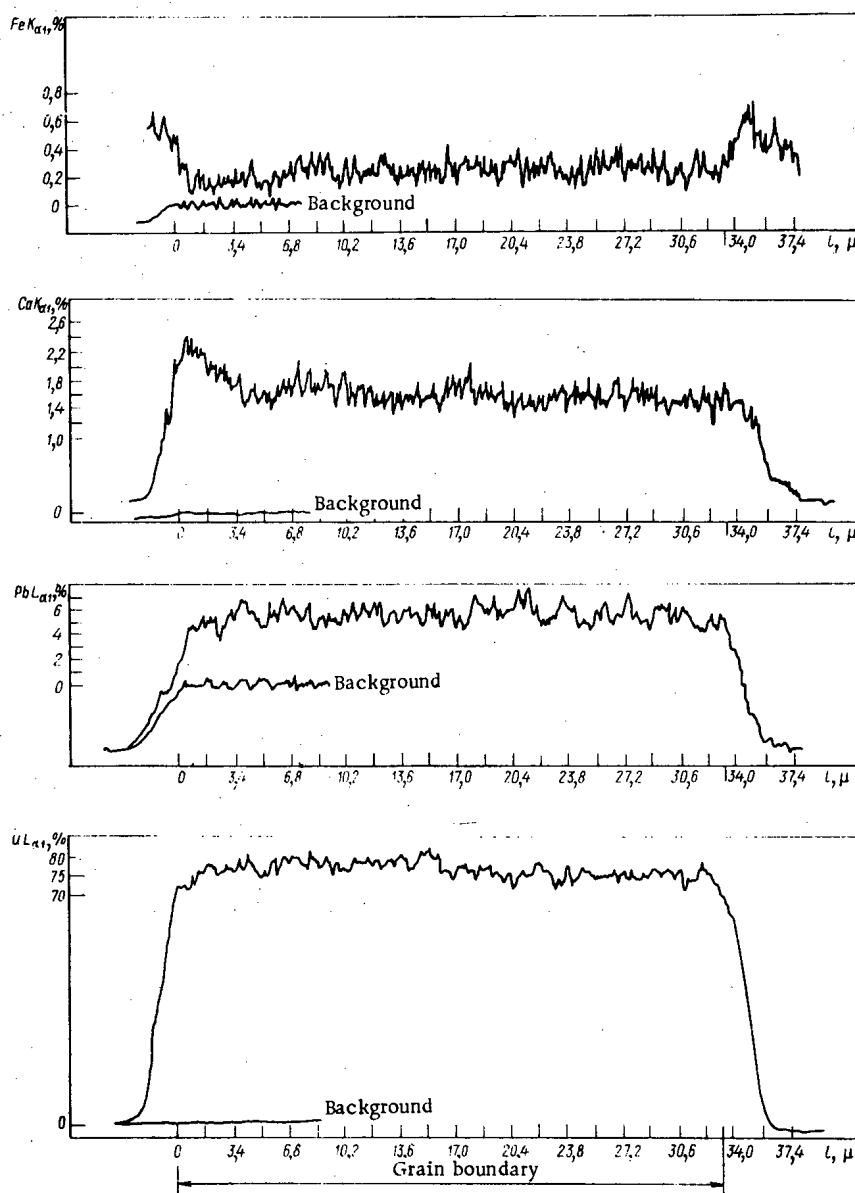


Fig. 5. Distribution pattern of elements over the profile in crystal No. 1.

TABLE 3. Composition of Uraninite from Uranium—Molybdenum Deposit from X-Ray Spectral Analysis Data (wt. %)

Elements	Specimen No. 282		Specimen No. 46		Specimen No. 158
	Crystal No. 1	Crystal No. 5	Crystal No. 12	Crystal No. 23	Crystal No. 16
U	77,4	77,9	77,6	77,8	76,5
Pb	5,34	5,66	5,41	5,30	5,92
Ca	1,54	1,87	1,22	1,24	1,93
Fe	0,19	0,17	0,19	0,23	0,14
O (calculation)	14,61	14,32	14,50	14,56	14,63
Totals	99,38	99,92	98,92	99,13	99,12

The following conclusions can be drawn from our data.

1. The uraninite from both deposits always contains not only lead, but also uniformly distributed calcium and iron, which must be regarded as elements isomorphic with uranium and must be included in the ideal formula of uraninite. Thorium and rare earth elements, which are also distributed uniformly, are characteristic only of high-temperature uraninite. Zirconium, detected by chemical analyses in the mineral from both deposits, is due to zircon inclusions, as previously noted by Zhukova [25]. The absence of isomorphism between uranium and zirconium in uraninite, in contrast to the isomorphism in zircon, may also be characteristic of other uranium deposits (an example of the manifestation of the reverse polarity law [26]).

2. Ancient high-temperature uraninites differ from the later medium-temperature uraninites by the higher lead content and the lower calcium content. Only a very small part of the lead present in uraninite is combined with galena. Whereas the differences in the lead contents are due to the different ages of the mineral, the lower calcium content of high-temperature uraninite does not agree with experimental data on the effect of temperature on the solubility of calcium oxide in uranium dioxide [16]. The observed discrepancy is apparently due to migration of calcium from uraninite when the minerals of uraninite-containing pyroxene-feldspathic veins are replaced by quartz. This assumption is also confirmed by the reduced lead content in the edges of uraninite crystals. All this evidence indicates a change in the composition of uraninite as time passes, not only as a result of nuclear reactions of radioactive elements, but also as a result of the superimposition of more recent hydrothermal processes.

LITERATURE CITED

1. A. E. Fersman, Selected Works, Pegmatites [in Russian], Vol. 6, Izd-vo Akad. Nauk SSSR, Moscow (1960).
2. N. P. Ermolaev and L. S. Tarasov, in: Principal Features of the Geochemistry of Uranium [in Russian] Izd-vo Akad. Nauk SSSR, Moscow (1963), p. 70.
3. A. I. Tugarinov, *ibid*, p. 110.
4. V. S. Kazakov, A. V. Kuz'menko, and I. S. Rutkevich, in: Geology and Problems of the Origin of Endogenous Uranium Deposits [in Russian], Nauka, Moscow (1968), p. 43.
5. A. I. Tishkin et al., in: Proceedings of the Second Geneva Conference [in Russian], Vol. 3, Atomizdat, Moscow (1959), p. 110.
6. Vik. L. Barsukov, G. B. Naumov, and N. T. Sokolova, in: Principal Features of the Geochemistry of Uranium [in Russian], Izd-vo Akad. Nauk SSSR, Moscow (1963), p. 139.
7. A. I. Tishkin, in: Geology of Hydrothermal Uranium Deposits [in Russian], Nauka, Moscow (1966), p. 322.
8. O. I. Shubnikov, Minerals of Rare Earth Elements and Their Diagnostics [in Russian], Izd-vo Akad. Nauk SSSR, Moscow (1952).
9. A. I. Tishkin, Minerals: Uraninite [in Russian], Vol. 2, (2nd edition), Nauka, Moscow (1965), p. 118.
10. V. M. Soboleva and I. A. Pudovkina, Uranium Minerals [in Russian], Gosgeoltekhizdat, Moscow (1957).
11. R. Berman, *Amer. Mineralogist*, 42, No. 11-12, 705 (1957).
12. V. A. Leonova, *Dokl. Akad. Nauk SSSR*, 126, No. 6, 1342 (1959).
13. V. A. Kirkinskii and E. S. Makarov, Problems of Geochemistry [in Russian], Nauka, Moscow (1965).
14. V. I. Lebedev, *Zap. Vses. Mineralog. O-va*, 88, No. 6, 667 (1959).
15. E. S. Makarov et al., *Geokhimiya*, No. 3, 193 (1960).
16. K. Alberman et al., *J. Chem. Soc. Structure Reports*, 15, 1352 (1951).
17. E. S. Makarov, in: Principal Features of the Geochemistry of Uranium [in Russian], Izd-vo Akad. Nauk SSSR, Moscow (1963), p. 27.
18. E. W. Heinrich, in: Mineralogy and Geology of Radioactive Raw Materials [Russian translation], IL, Moscow (1962), p. 13.
19. R. V. Getseva and K. T. Savel'eva, in: Manual for Identification of Uranium Minerals [in Russian], Gosgeoltekhizdat, Moscow (1956), p. 103.

20. V. A. Leonova, *Zap. Vses. Mineralog. O-va*, 88, No. 1, 21 (1959).
21. G. Springer, *Fortschr. Mineral.*, 45, 1 (1967).
22. K. Heinrich, *X-Ray Absorption Uncertainty. The Electron Microscope*, Wiley (1966).
23. P. Duncamb and G. Reed, *Nat. Bur. Standards. Spec. Publ.*, No. 298 (1968).
24. A. I. Tishkin and V. A. Strel'tsov, in: *Outlines of the Geochemistry of Individual Elements [in Russian]*, Nauka, Moscow (1973), p. 148.
25. V. I. Zhukova, *At. Énerg.*, 9, 1, 52 (1960).
26. V. S. Sobolev, *Introduction to the Mineralogy of Silicates [in Russian]*, L'vovsk. Gos. Un-ta, L'vov (1949).

THE MECHANICAL PROPERTIES OF SINGLE CRYSTALS OF IRRADIATED α -URANIUM WITH FREE OR RESTRAINED RADIATION GROWTH

Yu. M. Golovchenko, F. P. Butra,
V. F. Portnov, V. N. Burmistrov,
I. A. Korobeinikov, and O. L. Fufaeva

UDC 669.822:621.039.553.3

A study of the mechanical properties of single crystals of α -uranium irradiated by neutrons with free radiation growth has shown that these crystals have marked residual plasticity in comparison with polycrystalline uranium irradiated in similar conditions of dose and temperature. However, when the dose is increased the single crystals rapidly grow; their relative elongation under tension rapidly falls to zero when the radiation growth reaches 50% under a flux of $2 \cdot 10^{20}$ neutrons/cm² [1].

Radiation growth of uranium is due to the formation of new atomic layers parallel to the (010) plane by aggregation of intermediate atoms created by the irradiation. Thus the marked damage to the lattice resulting from shifting of atoms and formation of stable complexes of defects leads to complete blocking of the plastic deformation systems.

It was supposed that during irradiation of single crystals of uranium under restrained radiation growth, the equilibrium concentration of single radiation defects should be reduced owing to their accelerated annihilation in the stress field, leading to a lower rate of formation of stable complexes of defects, and consequently to an increase in the plastic properties of the crystals over those obtained by irradiation with free radiation growth. This is confirmed by the information in [2]: structural damage is less in neutron-irradiated graphite when growth is restrained than when the specimens grow freely.

There is no information on the quantitative values of the external stresses which restrain changes in

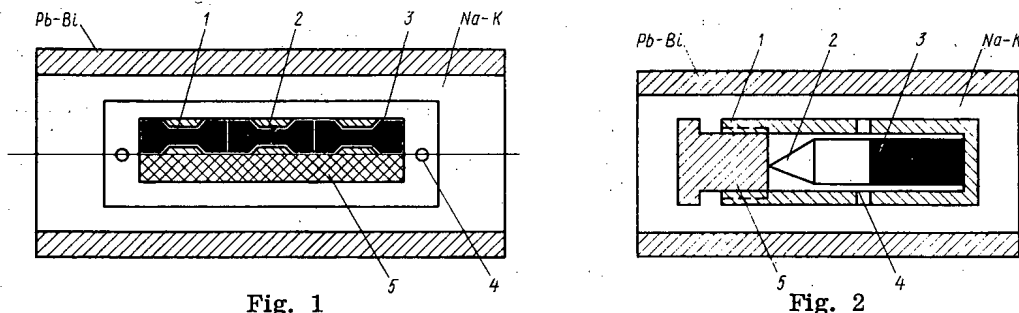


Fig. 1. Box for irradiating single crystals of α -uranium with restrained growth. 1) Monocrystalline specimen; 2) brass insert; 3) projection in box to width of specimen; 4) holes for attachment of lid of box; 5) brass plate equal to thickness of specimen.

Fig. 2. Device for determining stress restraining elongation of single crystal during radiation growth. 1) Cylindrical steel box with internal diameter of 4 mm; 2) aluminum crusher; 3) monocrytalline specimen; 4) hole for passage of Na-K alloy; 5) screw-threaded plug.

Translated from *Atomnaya Energiya*, Vol. 37, No. 4, pp. 316-321, October, 1974. Original article submitted September 27, 1973.

© 1975 Plenum Publishing Corporation, 227 West 17th Street, New York, N.Y. 10011. No part of this publication may be reproduced, stored in a retrieval system, or transmitted, in any form or by any means, electronic, mechanical, photocopying, microfilming, recording or otherwise, without written permission of the publisher. A copy of this article is available from the publisher for \$15.00.

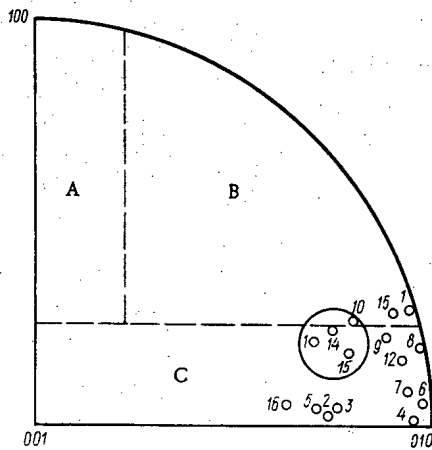


Fig. 3. Orientation of longitudinal axes of flat single crystals and region of orientation of longitudinal axes of cylindrical single crystals.

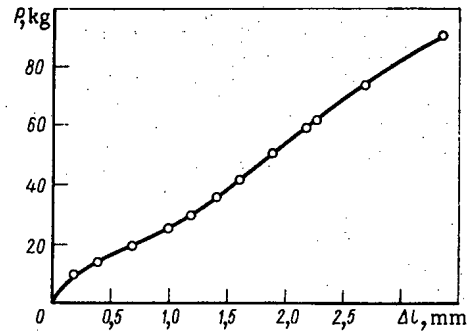


Fig. 4. Calibration curve of compression of crushers.

the dimensions of uranium crystals due to radiation growth. From the work of Buckley [3] it follows that the force which restrains the dimensional changes exceeds 2 kg/mm^2 , and when elongation of a single crystal by radiation growth is limited, it undergoes plastic deformation.

In this connection we have studied the mechanical properties of single crystal of α -uranium irradiated with free or restrained radiation growth, and have determined the force which prevents elongation of a single crystal as a result of radiation growth in a direction close to [010].

Specimens, Growth Conditions, and Experimental Method

Monocrystalline specimens were prepared from electrolytic uranium of high purity (99.99%) by $\alpha \rightarrow \beta$ recrystallization.

To study the mechanical properties we used flat tensile test specimens with working sections 8.5 or 10 mm long and with cross-sectional areas of 0.6–0.82 mm².

The specimens for irradiation with restrained growth were placed in aluminum boxes which limited their growth in all directions (Fig. 1). The stresses which restrained the shape changes of the uranium were determined on cylindrical specimens 3 mm in diameter and 7–11 mm long. The indicators were aluminum crushers. The device for determining the stresses which restrain shape changes is shown in Fig. 2.

Single crystal specimens of both types were chosen so that their longitudinal axes were close to the [010] direction with maximum radiation growth (Fig. 3).

The boxes with the specimens and the device for determining the stresses restraining shape changes were placed in a capsule filled with liquid Na–K alloy. Some of the flat tensile test specimens were suspended freely in the capsules.

The specimens were irradiated in a water channel of an SM-2 reactor to integral fluxes of $2.4 \cdot 10^{20}$ or $6.4 \cdot 10^{20}$ neutrons/cm². The neutron flux intensity at the point of irradiation was $2.2 \cdot 10^{14}$ neutrons/cm² · sec. The temperature of the uranium specimens during irradiation were below 100°C.

Tensile tests on the specimens were performed at room temperature on a remotely-controlled MM-150D machine with automatic recording of the tensile test diagram. The loads and extensions were recorded to within 1%.

After irradiation, the specimens and crushers were measured on an MID-1 remote microscope to within 0.01 mm.

The stresses restraining shape change were determined from the shortening of the crushers with the aid of calibration curves (Fig. 4). During irradiation, the crystals and crushers became curved; therefore the shortening was determined as the mean of the maximum and minimum lengths of the crushers.

TABLE 1. Mechanical Properties of Single Crystals Irradiated with Free and Restrained Growth and Annealed (Tensile Deformation at Room Temperature)

$\Phi = 2.4 \cdot 10^{20}$ neutrons/cm ²						$\Phi = 6.4 \cdot 10^{20}$ neutrons/cm ²					
specimen No.	state	σ_b , kg/mm ²	$\sigma_{0.2}$, kg/mm ²	δ_{rel} %	annealing conditions	specimen No.	state	σ_b , kg/mm ²	$\sigma_{0.2}$, kg/mm ²	δ_{rel} %	annealing conditions
1	Free growth	33,7	—	0		13	Restrained growth	18,2	16,8	1,2	600° C, 2h
2	The same	16,8	—	0		14	The same	21,8	11,0	3,3	
3	" "	29,5	—	0		15	" "	32,0	9,9	1,8	
4	" "	8,5	—	0		16	" "	8,5	7,7	3,4	
5	" "	40,6	26,0	3,5							
6	Restrained growth	34,3	17,9	4,0	600° C, 2 h						
7	The same	28,7	14,3	1,3							
8	" "	43,1	19,6	2,7							
9	" "	38,3	13,0	5,8							
10	" "	33,5	11,5	4,4							
11	" "	32,7	14,1	2,5							
12	" "	19,1	17,1	17,1	600° C, 2h						

To check the results, we tested the crushers under compression after irradiation. The load corresponding to the onset of plastic deformation of the crusher was taken to be equal to that restraining force which could prevent changes in the dimensions of the uranium specimens during radiation growth. The results obtained by the two different methods were in good agreement.

RESULTS

In connection with the anisotropy of the lattice of α -uranium, it is customary to distinguish three groups of single crystals (Fig. 3) with different deformation types — the so-called A, B, and C crystals [4].

Some of the test specimens belonged to group C, in which the main type of deformation under tension is twinning in the (172), (176), and (112) planes, and under compression twinning in the system (130)—[310] followed by slip in the twinned regions. Other specimens belong to a transitional group, since one cannot draw a sharp boundary between group B and C. These crystals deform either by slip in the system (010)—[100] under tension or compression, like the B-crystals, or by twinning followed by slip, like the C crystals. The results of mechanical tests on the irradiated crystals are listed in Table 1.

Investigation of the specimens irradiated with free growth by a flux of $2.4 \cdot 10^{20}$ neutrons/cm² revealed that they break without residual elongation at low stresses.

Increase in the irradiation dose led to such marked changes in the shapes and sizes of the specimens that they were unsuitable for further tests and broke when bent through less than 90°.

Specimens which had been irradiated with restrained growth by a flux of $2.4 \cdot 10^{20}$ neutrons/cm² retained their residual plasticity to the level of 1.3–5.8%. An increase in the integral flux to $6.4 \cdot 10^{20}$ neutrons/cm² somewhat reduced the plasticity ($\delta = 1.2$ –3.3%). Annealing of the specimens irradiated with either free or restrained growth at 620°C for 2 h leads to some restoration of the plasticity.

Table 2 lists the results of a determination of the stresses restraining the dimensional changes in the specimens during radiation growth.

TABLE 2. Stresses Which Prevent Shape Changes in Uranium Crystals due to Radiation Growth

Integral flux, neutrons/cm ²	Restraining stress, kg/mm ²	Integral flux, neutrons/cm ²	Restraining stress, kg/mm ²
$2.4 \cdot 10^{20}$	6,5	$2.4 \cdot 10^{20}$	7,1
$2.4 \cdot 10^{20}$	7,2	$6.4 \cdot 10^{20}$	7,0

The measured value of the stress restraining the changes in uranium during irradiation was 6.5–7.2 kg/mm² and remained constant when the flux was increased. From the results of these experiments we determined the critical shear stress of twinning, σ_s , since the crystals deformed on compression by twinning in the system (130)—[310]. The value of σ_s was calculated from the expression $\sigma_s = \sigma_0 \sin \chi_0 \cos \lambda_0$, where σ_0 is the yield point (in our case, the stress which prevents changes of shape), and $\sin \chi_0 \cos \lambda_0$ is an orientational factor relating the direction of the specimen

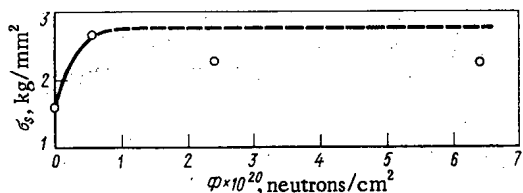


Fig. 5. Critical shear stress vs neutron flux Φ for twinning system (130)–[310].

From our results and the literature data [1, 6] we plotted a graph of the critical shear stress of twinning in the system (130)–[310] vs the degree of irradiation (Fig. 5). We see that the critical shear strength of twinning in this system depends only weakly on the flux and reaches saturation at a flux of less than $5.5 \cdot 10^{19}$ neutrons/cm². The slight discrepancy between our results and those in [1] must be sought in the difference between the methods of measurement.

DISCUSSION OF RESULTS

Single Crystals Irradiated with Free Radiation Growth. From earlier [1, 7] and the present results we can infer that crystals of α -uranium of various orientations, when irradiated with free growth, completely lose their residual plasticity under tension: the B-crystals do so at a dose of $2 \cdot 10^{20}$ neutrons/cm², and the C-crystals at $2.4 \cdot 10^{20}$ neutrons/cm², while A-crystals irradiated with a dose of $5.5 \cdot 10^{19}$ retain their tensile plasticity. There is no information on the behavior of these crystals at high doses. However, the existing indirect data can be used for this purpose.

According to [1, 7], crystals of various orientations, when irradiated, acquire various reductions in the residual elongation, which are as follows: for the A-crystals, 45% (from 130 to 70%); for B-crystals, 75–90% (from 160 to 44–16%); and for the C-crystals 95% (from 120 to 7%). Thus, according to the degree of increase of radiation blocking of various systems of deformation of α -uranium, these systems can be arranged in a series: i) system of deformation by twinning (130)–[310]; ii) system of deformation by slip, (010)–[100]; iii) system of deformation by twinning on large-index planes (172), (176); etc., etc.

In comparing the influence of the test temperature for nonirradiated crystals and the dose of irradiation on the critical shear stress of slip in the system (010)–[100] and twinning in the system (130)–[310], we can make the following observations. Reduction of the test temperature of the nonirradiated specimens [1, 7, 8] and increase of the dose to $2 \cdot 10^{20}$ neutrons/cm² [4] leads to a marked growth in the critical shear stress of slip in the system (010)–[100]. At the same time, neither reduction of the temperature [7, 8] nor increase in the dose to $6.4 \cdot 10^{20}$ neutrons/cm² (see Fig. 5) has any appreciable influence on the critical shear stress of twinning in the system (130)–[310].

This leads us to infer that crystals of α -uranium deformed by twinning in the system (130)–[310] (A-crystals in tension or C-crystals in compression) should retain their residual plasticity at radiation doses of $6.4 \cdot 10^{20}$ neutrons/cm² or more.

The changes in the properties of freely growing crystals when the radiation dose is increased or after annealing can be explained by the observations of Hudson [9, 10], who found that radiation defects in uranium foils are reinforced by increasing the dose or by annealing which reduces the number of these defects and increases their size.

Single Crystals Irradiated with Restrained Radiation Growth. In considering the causes of the retention of plasticity by these crystals, we must note that irradiation causes elastic macrocompressive stresses in them. If the rate of radiation growth exceeds the rate of radiation relaxation, the elastic stresses will increase. On the attainment of some critical value, these stresses will relax as a result of plastic deformation by the most advantageous system of deformation, either twinning (130)–[310] or slip (010)–[100]. In assessing the plastic deformation capability in postreactor tension of specimens which have been restrained during irradiation, we must bear in mind the inhomogeneity of the C-crystals, i. e., the fact that they contain regions with different orientations, namely twinned regions which will have an orientation favorable for slip in the system (010)–[100] and untwinned regions (with the original orientation) which deform under stress by twinning in the planes (172), (176), and (112).

The explanation of the marked residual plasticity of the test specimens must evidently be sought in the different types of strengthening of systems of twinning and the system of slip during irradiation with

axis to the plane and direction of twinning [5].

The values of σ_s thus found are the same for crystals irradiated by fluxes of $2.4 \cdot 10^{20}$ and $6.4 \cdot 10^{20}$ neutrons/cm², and are equal to 2.2 kg/mm².

According to [1, 6], the critical shear stress of twinning in the system (130)–[310] is 1.5 kg/mm² for nonirradiated crystals and 2.6 kg/mm² for crystals irradiated with a flux of $5.5 \cdot 10^{19}$ neutrons/cm².

free and restrained growth. In free crystals both these systems of deformation are completely blocked [1], but in restrained crystals at least one is not completely blocked. This state is realized if we consider that stresses greatly retard recombination of the point defects under tension and promote it under compression of the lattice [6]. The decrease in the concentration of point defects in a compressed crystal must lead to a decrease in the rate of accumulation of stable complexes of defects.

Simultaneously with this we can suppose that the stresses increase the mobility of the vacancies in the compressed regions in the [010] direction. In freely growing crystals in which stresses are absent, diffusion of vacancies in the [010] direction is hindered [11]. Adsorption of vacancies by the additional layers should lead to a decrease in the dimensions and stability, and possibly to partial disappearance of the latter.

Thus irradiation of restrained single crystals leads to a decrease in the rate of accumulation of stable complexes of defects, and consequently to a lower change in properties.

Konobeevskii et al. [1], like the present authors, established a complete loss of plasticity of irradiated B-crystals, in contrast with previous investigations [7] in which these crystals displayed marked residual plasticity. These discrepancies are due to the different conditions of irradiation: Butra et al. [7] studied crystals restrained between two plates, i. e., irradiated with hindered growth.

The rise in plasticity ($\delta = 17\%$) during annealing of single crystals irradiated in the restrained state by a flux of $2.4 \cdot 10^{20}$ neutrons/cm² indicates that the deformation-blocking defects in the restrained specimens are less stable than those formed in freely-expanding crystals, annealing of which gives a total plasticity of 3.5%. To judge by the results of annealing of specimens irradiated in the restrained state by a flux of $6.4 \cdot 10^{20}$ neutrons/cm², we can suppose that the small rise in plasticity ($\delta = 3.5\%$) is due not only to an accumulation of stable complexes when the irradiation dose is increased, but also to an accumulation of foreign atoms of fission fragments, causing stable damage which is not removed by annealing. These changes also cause differences between the properties of restrained crystals irradiated by different fluxes.

Restraint of Shape Change and Radiation Growth. Plastic deformation by twinning in the system (130) — [310] in restrained single crystals occurs during irradiation with stresses which prevent shape change. For specimens of the chosen orientations these stresses are 6.5–7.2 kg/mm² and are independent of the flux. The constancy of the stresses restraining shape change is due to the fact that the critical shear stress of twinning depends only weakly on the flux, reaching saturation at lower degrees of irradiation than in our experiments. For single crystals of other orientations deformed by compression in this system, this stress will be somewhat different. For example, for crystals oriented strictly in the [010] direction, the stress restraining shape change is calculated to be 4.8 kg/mm². The deviation of the restraining stress towards larger values than the experimental ($\delta = 7$ kg/mm²) for crystals of any other orientations will apparently be negligible, because a stress of 4.8 kg/mm² in the [010] direction will be reached before the crystal develops a force in any other direction.

Together with the study of restraint of shape change in uranium, the question arises of the restraint of radiation growth and of the influence of stress on the rate of radiation growth.

In the opinion of Buckley [3], who studied the influence of external stresses on radiation growth in uranium, retardation of this process as a reduction of the efficiency of accumulation of aggregates is possible, but only at stresses not less than the macroscopic yield point. He showed that application of stresses of up to 2 kg/mm² does not affect the rate of growth of a pseudomonocrystal of uranium. This stress was insufficient not only for appreciable retardation of the rate of radiation growth, but also for suppression of shape change. The presence of a state of stress must evidently lead to retardation of radiation growth, because the formation of additional layers by aggregation of point defects involves, first, the work done in overcoming the elastic forces, secondly, a reduced concentration of point defects, and thirdly, a reduction in the anisotropy of diffusion of point defects.

The results of our present work do not directly confirm that there is a reduction in the rate of radiation growth under the influence of stress; however, the data from mechanical tests on single crystals indirectly confirm this assumption.

LITERATURE CITED

1. S. T. Konobeevskii et al., in: *The Radiation Physics of the Solid State and Reactor Materials Science* [in Russian], Atomizdat, Moscow (1970), p. 178.

2. B. Richards and E. Kellet, *J. Nucl. Mater.*, 25, No. 1, 45 (1968).
3. S. Buckley, in: *Uranium and Graphite*, Institute of Metals, London (1962), p. 41.
4. F. P. Butra et al., *Fiz. Met. i Metall.*, 15, 873 (1963).
5. V. M. Klassen-Neklyudova, *Mechanical Twinning of Crystals* [in Russian], Izd-vo Akad. Nauk SSSR, Moscow (1960).
6. S. T. Konobeevskii, *The Action of Irradiation on Materials* [in Russian], Atomizdat, Moscow (1967).
7. F. P. Butra et al., *At. Énerg.*, 19, No. 4, 372 (1965).
8. R. Teeg et al., *J. Nucl. Mater.*, 3, 81 (1961).
9. D. Hudson et al., *Phil. Mag.*, 7, 377 (1962).
10. D. Hudson, *Phil. Mag.*, 10, 949 (1964).
11. S. Seigle and A. Opinsky, *Nucl. Sci. and Engng.*, 2, 38 (1957).

MODE TRANSFORMATION IN THE RESONATOR OF A DRIFT-TUBE LINEAR ACCELERATOR

V. A. Bomko, A. P. Klyucharev,
and B. I. Rudyak

UDC 621.384.6.01:621.384.643

Cavity resonators with drift-tubes are widely used in linear accelerators for energies up to 200 MeV. One of the basic shortcomings of such a device (especially in long resonators) is low stability under transient and steady state conditions of the distribution of amplitude and phase characteristics of the accelerating field with respect to all kinds of frequency perturbations and with respect to the magnitude of the beam current. This is caused by the poor dispersion properties of this kind of resonator for the working wave, so that any perturbation leads to coupling between the fields of the working wave and neighboring wave modes. In recent years methods have been developed for stabilizing the field distribution [1-5] which are based on compensating for the interactions between modes. However, these methods all have the disadvantage of considerable complexity and a tedious alignment procedure. In addition, the use of stabilized devices hinders control of the degree of stabilization of the field distribution. This is due to the method used to control the energy of heavy particle beams in linear accelerators [6, 7].

It was shown in [8-10] that the changes in amplitude and phase of the working field (wave) along the resonator due to loading by the beam or to the appearance of frequency perturbations (of any origin whatever) may be expressed by means of the amplitude and frequency characteristics of higher number modes E_{0l} ($l = 1, 2, 3, \dots$).

The RF energy expended in compensating for losses at the resonator surfaces and in accelerating the beam produces a response in the resonator which leads to excitation of these waves despite the fact that the RF feed works only at a specified frequency. In this case, the nearer the frequencies of the higher order waves are to the frequency of the working wave the larger the amplitude with which they appear in the resulting field [11]. Thus, the main problem with any field stabilization technique is to ensure that the frequencies of the modes adjacent to the fundamental are as high as possible.

The present article describes the results of an experimental study of the processes involved in transformation of wave modes belonging to the lower part of the wave spectrum E_{0l} ($l = 1, 2, 3, \dots$) which are excited in drift-tube resonators when an antipode rod resonator system as shown in Fig. 1 and described in [12, 13], is introduced. These investigations were carried out on the resonator of a linear multiply-charged ion accelerator (LUMZI-10) of length 18 m, with 97 drift-tubes, with accelerator units ranging from 7 to 28 cm in length, and with a working wavelength of 2.13 m.

Interaction of Two Resonant Systems

When many resonant systems interact simultaneously a complex pattern of wave mode transformations is observed. Thus, the experiments were carried out in succession: beginning with simple systems and proceeding to complex multicomponent mode transformation processes. We now consider the simplest case of two interacting resonant systems.

One of the resonant systems is the drift-tube resonator itself. The other is a conducting rod attached radially to the wall of the resonator. The coupling of the natural mode fields of this kind of rod with the fields of E_{0l} waves is largest if the angle between the rod and the drift-tube supports is 180° [12, 13]. Then, as in what follows, the conditions for coupling with the RF feed are such that only E_{0l} modes are excited. Excitation of rod resonator systems is then indirect (due only to resonance interaction with the fields of these modes).

Translated from *Atomnaya Energiya*, Vol. 37, No. 4, pp. 326-331, October, 1974. Original article submitted August 27, 1973; revision submitted January 28, 1974.

© 1975 Plenum Publishing Corporation, 227 West 17th Street, New York, N.Y. 10011. No part of this publication may be reproduced, stored in a retrieval system, or transmitted, in any form or by any means, electronic, mechanical, photocopying, microfilming, recording or otherwise, without written permission of the publisher. A copy of this article is available from the publisher for \$15.00.

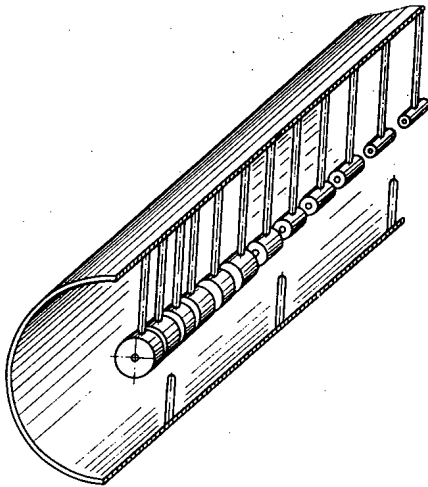


Fig. 1. Accelerator structure with stabilizing devices.

The variation in frequency of the resulting waves as a function of the closeness of the natural frequencies of the resonator and the rod resonant system is shown in Fig. 2. The required frequency difference between the interacting resonant systems was reached by varying the insertion depth, b , of the rod. The natural frequencies of the resonator for E_{01l} modes are denoted by the symbol f_l ($l = 0, 1, 2, 3, \dots$) in the figure. In the case of all these waves a resonance splitting and the appearance of coupling frequencies is observed as their natural frequencies converge with that of the rod. This agrees with the general idea of resonance interactions between two systems [14]. In this case the change in mode frequencies with index l corresponds to their smooth transformation into the coupling frequency as the rod length is increased and subsequently into its natural frequency, combined with the onset of transformation of the rod frequency into the coupling frequency, and finally into the natural frequency of the resonator corresponding to the $E_{01(l-1)}$ wave. This kind of smooth transformation is followed for all modes, so the frequency dependences shown in Fig. 2 appear outwardly to be a smooth transformation of higher modes into lower.

Two families of curves are shown in Fig. 2. They correspond to different positions of the rod on the generatrix of the resonator (solid curves — rod placed at a point equidistant from the end walls of the resonator; dotted curves — rod placed in close proximity to the end wall). In the first case the coupling coefficient is maximal for all odd waves ($l = 1, 3, \dots$) and minimal for even waves. At the point where they coincide an especially small deviation of the coupling frequencies from the partial frequencies is observed for the zeroth mode ($l = 0$), for which there exist only longitudinal components of the electric field in the ideal case. Waves with odd increases have a significantly larger degree of interaction since the rod is placed in one of the modes of the longitudinal (maximum radial) components of the electric field. Thus, the natural frequencies begin to be transformed into the coupling frequencies at a much larger distance from the points of coincidence and they change very smoothly.

A series of curves showing the transformation of the longitudinal field distribution along the axis of the resonator when varying the length of a rod placed in the node of the longitudinal field of the E_{011} wave is given in Fig. 3. The group of curves, A, corresponds to transformation of the field of an E_{010} wave for low coupling frequencies. At first (upper curves) the field grows near the output side of the resonator and decreases near the input side. Then it becomes increasingly more similar to the longitudinal field distribution of the natural mode of the rod (lower curves). Analogously, the group B corresponds to this change for an E_{011} wave. Over some portion of these frequency changes a field distribution is observed which is a combination of the fields of two secondary waves. These are the upper branch of the coupling frequency of

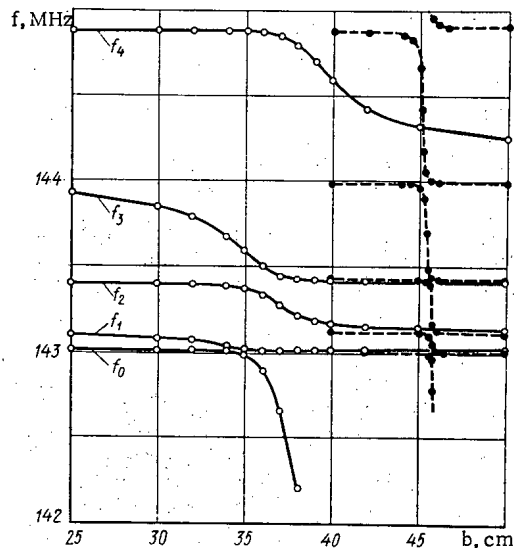


Fig. 2. Frequency properties of the resulting waves as a function of rod length.

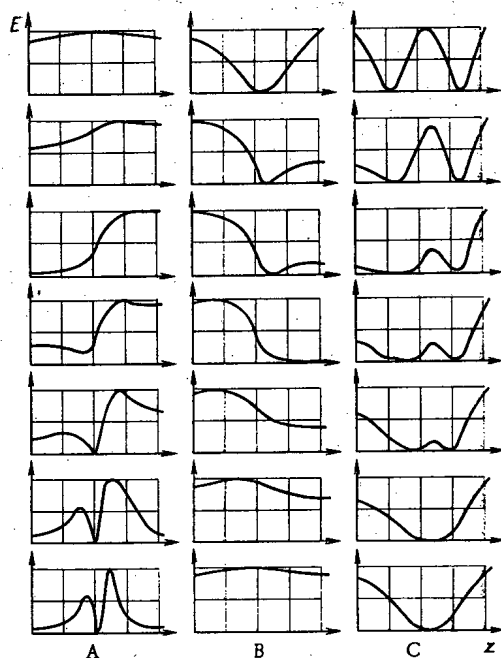


Fig. 3. Change in the field distribution of E_{010} , E_{011} and E_{012} waves due to a resonant rod (top to bottom).

the E_{010} and the rod modes (denoted by E_{010}^+) and the lower branch of the coupling frequency of the E_{011} and the rod modes (denoted by E_{011}^-). As the rod length is increased further there is a gradual development of fields corresponding to a transformation from E_{011}^- into E_{010}^+ and then into the field of a pure E_{010} wave.

An analogous process occurs for wave E_{012} as well. The position of the rod corresponds to the maximum of the longitudinal field in the central half wave. In this case of coincidence of the properties of the secondary waves, E_{012}^- and E_{011}^+ , and later a gradual transition of E_{011}^+ into E_{011} is also observed. A process similar to degeneracy of the central half wave is observed in Fig. 3C. For increasingly higher modes this process of smooth transition of wave fields with changing rod length occurs in an analogous fashion. It may be written in the form of a symbolic chain:

$$E_l \rightarrow E_l^- \rightarrow E_{l-1}^+ \rightarrow E_{l-1}^* \quad (1)$$

Here the asterisk denotes the result at the end of the chain. For simplicity the first two numbers in the mode indices of the waves are left out.

At rod lengths corresponding to coincidence points a significant drop is observed in the field. This is explained by the fact that the interacting resonant systems have different Q-factors. For weak coupling, a low Q for the rod resonance weakens its effect on the field distribution in the cavity. For strong coupling, the Q for the resulting waves is reduced. Experimental studies confirm these conclusions. At the $E_{01l}^- \rightarrow E_{01(l-1)}^+$ transition points a significant reduction of the fields was always observed (in some cases by three orders of magnitude).

Wave Interactions in Multiply-Connected Systems

When two or more rods are placed in a cavity the interactions become more complicated. Increasing the number of rods allows a greater splitting of the resulting mode frequencies from the lower boundary of the E_{01l} band. Thus a greater stabilizing effect on the field distribution of the working wave may be obtained. The general form of the accelerator is shown in Fig. 1. In choosing the locations for the rods along the generator of the cavity we proceed from the fact that the maximum coupling coefficient results when the rods are placed at nodes in the longitudinal field distribution. Thus in the following we have placed them at the nodes of waves whose index l was equal to the number of rods, n .

In the general case, the process of successive interaction of one coupling wave with another, produced as a result of n rod resonances, one after the other, as their lengths increase, may be represented in the form of the (typical) chains:

$$\begin{aligned} E_l \rightarrow E_l^- \rightarrow E_{l-1}^+ \rightarrow E_{l-1}^- \rightarrow E_{l-2}^+ \rightarrow \dots \rightarrow E_{l-n}^* \quad \text{for } l > n; \\ E_l \rightarrow E_l^- \rightarrow E_{l-1}^+ \rightarrow E_{l-1}^- \rightarrow E_{l-2}^+ \rightarrow \dots \rightarrow E_0^+ \rightarrow E_0 \quad \text{for } l = n; \\ E_l \rightarrow E_l^- \rightarrow E_{l-1}^+ \rightarrow E_{l-1}^- \rightarrow E_{l-2}^+ \rightarrow \dots \rightarrow E_0^+ \rightarrow E_0 \rightarrow E_0^- \quad \text{for } l > 5. \end{aligned} \quad (2)$$

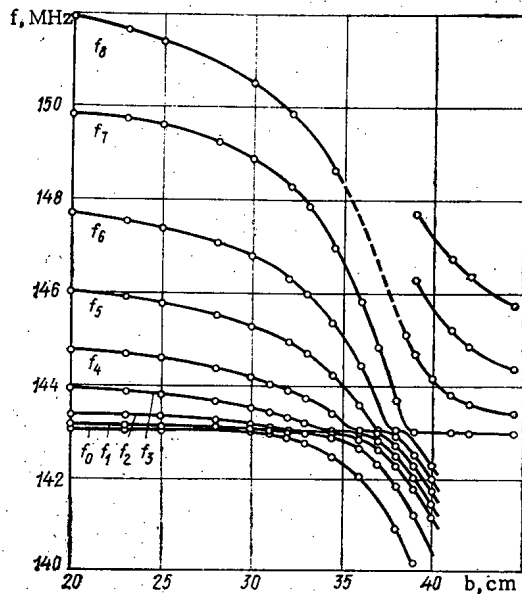


Fig. 4. Frequency characteristics of the resulting waves as a function of the length of the seven rods.

These transformation chains show that a wave with index $l = n$ is converted to a zeroth mode wave as a result of successive resonant intermode interactions. All waves with higher indices become waves of the first, second, etc. modes, respectively. Waves with mode indices lower than the number of rods undergo analogous transformations at the beginning of the chain. However, at the end of the chain they are successively transformed into zeroth mode waves and then degenerate into the lowest secondary wave with a coupling frequency approaching the frequency of a rod mode.

Figure 4 shows the results of an experimental investigation of the frequency transformations in the cavity of LUMZI-10. Seven rods of equal length were placed at the nodes of the E_{017} wave for the cavity. The rods were placed opposite the accelerating structures which had drift-tubes of varying lengths and diameters. The sequence of seven transformations of the E_{010} wave is apparent in the figure. The formation of a new frequency spectrum of E_{01l}^* modes is observed in the right hand side of the figure. In the E_{01l} wave spectrum, the frequencies of all waves with $l > 0$ are the coupling frequencies over a wide range

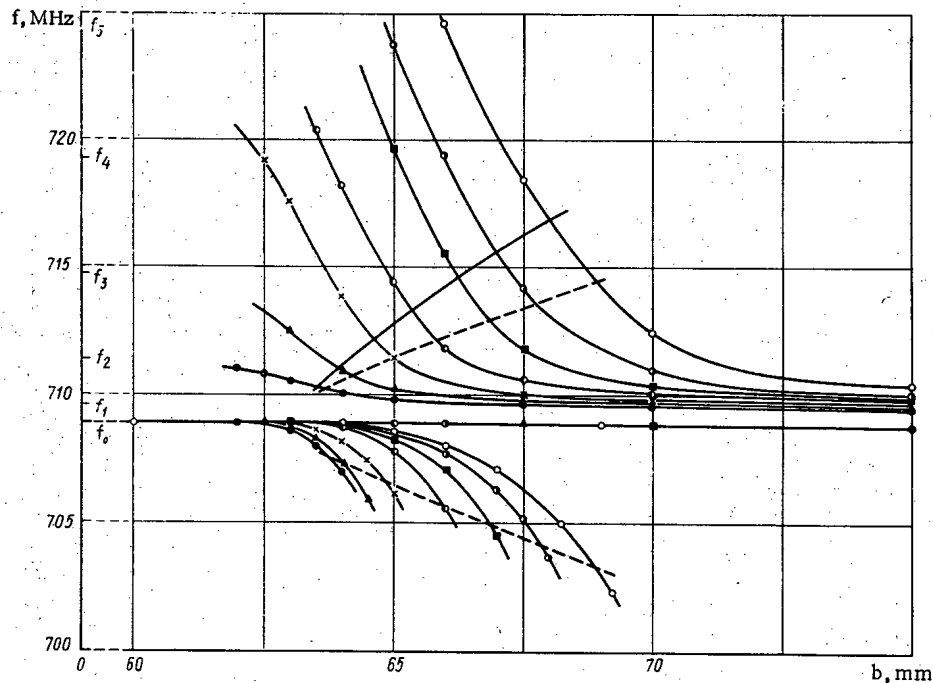


Fig. 5. Frequency characteristics of the resulting coupling waves E_{01l}^* , E_{010} , and E_{010} in the resonator for various numbers of resonance rods: ●) 1; ▲) 3; ×) 5; ○) 7; ■) 9; ●) 12; ○) 16.

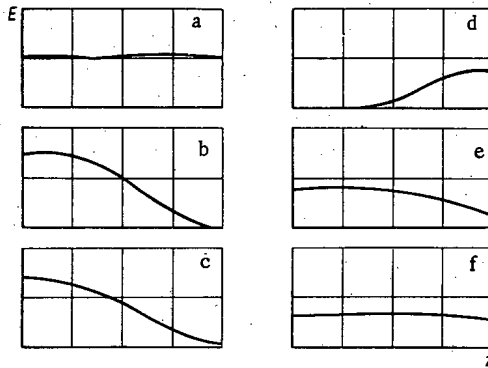


Fig. 6. Variation of the stability of the field distribution in compensated and uncompensated apparatus.

of rod lengths and they approximate the frequencies of the E_{01l} waves very smoothly. This ensures the absence of rigid requirements in the tuning accuracy of the frequencies for other kinds of stabilized systems.

The right hand part of the frequency spectrum of Fig. 4 shows that if the length of the rods is changed in this range then it is possible to regulate the steepness of the dispersion curve within wide limits and thereby to change the degree of stabilization. This is a fact of considerable importance for linear accelerators in which the energy of the accelerated particles is regulated. The creation of segments with a uniform accelerating field distribution whose lengths are less than that of the cavity and the control of the lengths of these segments require a certain weakening of the stabilizing action of the rods.

Compensating for the Effect of Parasitic Waves

The optimal conditions to compensate for the perturbing effect of parasitic waves on the field distribution of the working wave were determined. As is known [1, 3] this is done by constructing a part of the dispersion curve which is symmetrical to the lower boundary of the frequency spectrum of the E_{01l} mode ($l = 0, 1, 2, \dots$). In the case of antipode stabilization the intensity of opposing wave modes was taken into account while studying the compensation effect. Maximum compensation was sought by varying the length of the rods in the frequency range of the secondary coupling waves at the end of the chain of Eqs. (2).

Figure 5 shows the results of an investigation of the frequency transformations obtained in an experimental cavity with drift-tubes and an antipode stabilizer, whose length was the same as the cavity of the LUMZI-10 heavy ion linear accelerator and whose transverse dimensions were 5 times less. The two families of curves are, respectively, the resulting values of the upper and lower coupling frequencies of the E_{01l}^* mode for the case $l-n = 1$ as a function of the length of the rods, b . The parameter is the number of rods, n . The intensity of the lower coupling waves is very small due to the low Q -factor of the rod resonances and the reduced coupling coefficient of these resonances with the natural modes of the resonator. As a consequence of the compensation the effect on the field distribution of the E_{010} waves begins to appear for rod lengths much less than the length needed to ensure an equal distance between frequencies.

The results of an experimental investigation of the degree of stabilization of the E_{010} field distribution for the above mentioned model are shown in Fig. 6. Curves a and b correspond to the case when there are no stabilizing elements present. A uniform field distribution (see curve a) is established in the unperturbed resonator. However, following a perturbation by $\Delta f/f = 2\%$, the frequency of the last unit of the accelerator structure underwent a significant dip (see curve b). The remaining curves were obtained when 12 rods in an antipode system were placed in a cavity at the perturbation frequency. From Fig. 6c and d, it is clear that the length of the rods was not optimal, so that the coupling waves corresponding to the upper or lower resonances have a greater effect. Curve e corresponds to a rod length such that the upper and lower coupling frequencies are equally spaced from f_0 . The resulting dip denotes a larger effect due to the upper coupling modes (E_{01l}^*). The field distribution (see curve f) corresponds to the optimum when the effect due to the upper and lower waves on the field distribution of the working wave for a perturbation in the cavity is compensated for.

The results of this study of the interaction of waves in the cavity of a linear accelerator have great practical significance. They enabled the development of a method for stabilizing the field distribution of the working wave based on the use of a new stabilizing structure. This investigation made it possible to determine the optimum conditions to compensate for the coupling between fields of the working wave and other natural modes of the cavity and to significantly improve the cavity dispersion properties.

LITERATURE CITED

1. S. Giordano and I. Haanwecker, Proc. Linear Accel. conf., Los Alamos, 1966 (1968), p. 88.
2. G. Dome and P. Lapostoll, Proc. Linear Accel. Conf., Brookhaven, 1968 (1968), p. 445.
3. D. Swenson et al., Intern. Conf. High Energy Accel., Cambridge, 1967 (1967), p. 167.
4. B. Epstein, Tran Duc Tien. [2], p. 457.
5. A. Carne et al., V Intern Conf. High Energy Accel., Frascati, 1965; Rome (1966), p. 624.
6. V. A. Bomko, A. P. Klyucharev, and B. I. Rudyak, Atom. Énerg., 31, 123 (1971).
7. V. Bomko et al., Deutsches Patentamt, Offenlegungsschrift 2105781; USA Patent No. 371016, 1973; French Patent No. 2083888, 1972.
8. T. Nishikawa, IEEE Trans. Nucl. Sci., NS-12, No. 3 (1965), p. 630.
9. K. Batchelor, IEEE Trans. Nucl. Sci. NS-14, No. 3 (1967), p. 295.
10. S. Giordano et al., *ibid*, p. 303.
11. L. Alvarez et al., Rev. Scient. Instr., 26 (1955), p. 111.
12. V. Bomko et al., Particle Accelerators, 3 (1972), p. 63
13. V. A. Bomko and B. I. Rudyak, Preprint KhFTI 73-13 [in Russian], Kharkov (1973).
14. V. B. Shteinshleiger, Wave Interaction Phenomena in Electromagnetic Resonators [in Russian], Moscow, Oborongiz (1955).

COMPARISON OF COSTS OF PURIFYING RADIOACTIVELY
CONTAMINATED WATER BY SORBENTS OF MULTIPLE-
AND SINGLE-USE

F. V. Rauzen and V. V. Aleshnya

UDC 621.039.7

Ion exchange is one effective method of separation of radioactive components from solutions. Radioactive isotopes usually present in radioactively contaminated waters are multivalent elements. They can be separated from solutions in the process of sorption without separating other salts from these solutions. The radioactive isotopes of cesium, iodine, and sodium are exceptions. Selective natural and artificial sorbents are used for the sorption of cesium.

The known synthetic ion exchange resins (for example, phenol-carboxyl resin duolite CS-100 [1], and carboxyl resin obtained by condensation of salicylic acid and formaldehyde and crosslinked phenol [2]) permit removal of cesium from more than 1000 columnar volumes of solutions containing up to 3 g/liter sodium salts. After becoming saturated with radioactive isotopes, selectively-acting resins are flushed by nitric acid (for the transfer of the radioactive isotopes into solution) and by sodium hydroxide solution (for regeneration of sorption properties). After desorption and regeneration the solutions are evaporated and the still residues go into storage. The ion exchange resins are used repeatedly.

Research workers in many countries are striving to find cheap single-use sorbents. Installations exist where purification is done by sorption by natural minerals such as vermiculite [3], clinoptilolyte [4], filtrolyte [5], and lignin [6]. Artificial inorganic sorbents are also being used and synthesized for this purpose [7, 8]. Such sorbents are used only once; after use they are buried, sometimes along with the tower in which they were kept.

The object of the present work is a comparison of the economics of the technological schemes of purification of radioactively contaminated water with single- and multiple-use of sorbents.

Basic Data for Economic Comparison

For the comparison of the two variants we shall make the following assumptions.

1. Identical preparatory operations are carried out in both schemes (preparation of the solution and coagulation). Coagulation is necessary not only for the separation of the suspended and colloidal particles from the solutions, but also for the separation of alkali-earth elements (calcium, magnesium). This is necessary for eliminating the effect of the latter on the sorption of cesium ions by both organic and inorganic sorbents.

TABLE 1. Consumption of Reagents in Regeneration of 1 m³ of Sorbent and Their Cost

Reagent	Consumption, kg	Cost 1 ton, ruble
Nitric acid	120	74
Sodium hydroxide	80	120
Industrial water	5000	0,015

2. If the sorbents are used only once, whence their capacity is exhausted, they are removed for burial.

3. The useful life of multiple-use sorbents is 10 years; after this they are buried. Mechanical losses of the sorbent comprise 5% per year. The rate of filtration is equal to three columnar volumes per hour. The consumption of the sorbent is less than 0.008 liter/m² of the purified solution.

Translated from *Atomnaya Energiya*, Vol. 37, No. 4, pp. 322-325, October, 1974. Original article submitted October 25, 1973; revision submitted April 8, 1974.

© 1975 Plenum Publishing Corporation, 227 West 17th Street, New York, N.Y. 10011. No part of this publication may be reproduced, stored in a retrieval system, or transmitted, in any form or by any means, electronic, mechanical, photocopying, microfilming, recording or otherwise, without written permission of the publisher. A copy of this article is available from the publisher for \$15.00.

TABLE 2. Values of D Ensuring $E_c = 0.5$ ruble/m³ of Solution

P_b , ruble/m ³ of wastes	V_m	P_o , ruble/m ³ of sorbent			
		20	100	200	400
200	100	1,5	2,1	2,7	4,2
	200	1,8	2,5	3,4	5,6
	300	2,4	3,3	4,3	6,5
	400	3,3	4,5	6,1	9,1
120	100	1,1	1,7	2,5	4,1
	200	1,4	2,2	3,1	5,1
	300	1,8	2,9	4,2	6,8
	400	2,8	4,4	6,4	10,4
80	100	0,8	1,5	2,3	4,0
	200	1,1	1,9	3,0	5,1
	300	1,5	2,6	4,1	7,1
	400	2,4	4,3	6,7	11,4
40	100	0,5	1,2	2,1	3,9
	200	0,7	1,6	2,8	5,1
	300	1,0	2,3	4,0	7,3
	400	1,8	4,1	7,1	13,0
20	100	0,4	1,1	2,0	3,9
	200	0,5	1,5	2,7	5,1
	300	0,7	2,1	3,9	7,5
	400	1,3	4,0	7,3	14,0

4. After the capacity of the regenerable exchanger is exhausted, it is flushed with two columnar volumes of 6% nitric acid solution, two columnar volumes of 4% sodium hydroxide solution, and one columnar volume of water. The five columnar volumes of solution thus obtained are evaporated. The degree of evaporation is 25 (concentration of salts in the still residue ~800 g/liter).

5. The used sorbents and the still residues from the evaporation of the regenerants represent the waste and are stored with or without solidification.

We shall compare the variants of purifying radioactively contaminated waters with the use of single- and multiple-use sorbents taking into consideration and different items of expenditure in separation. These include expenditures in sorbents and reagents, and also in burial and evaporation.

For the scheme with regenerable sorbents the sum of these expenditures can be determined from the formula

$$C_m = \frac{R_r + V_r P_y + V_{er} P_b}{V_m} + V_s P_m; \quad (1)$$

for the scheme with single-use sorbents

$$C_o = \frac{R_o + R_b}{V_o}. \quad (2)$$

Here C_o and C_m are the nominal expenditures in the treatment of 1 m³ of the solution in single- and multiple-use in ruble/m³ solution; V_m and V_o are the volumes of the solution purified in one cycle and referred to the volume of the sorbent in the tower (the volume can change in the range 100-2000 m³ solution/m³ of sorbent); R_e are the operational costs in evaporating 1 m³ regenerant, ruble/m³ of regenerant; R_r are regenerant costs for regeneration of 1 m³ sorbents after their use, ruble/m³ of sorbent; V_r is the volume of regenerant per 1 m³ of sorbent (equal to 5 m³ of regenerant/m³ of sorbent); R_m and R_o are cost per 1m³ of multiple- and single-use sorbent, ruble/m³ of sorbent; V_s is the consumption of regenerable sorbents in purifying 1 m³ of solution, it is equal to 10⁻⁵ m³ of sorbent/m³ of solution; V_{er} is the volume of regenerant after evaporation (equal to 0.2 m³ regenerant/m³ of sorbent); R_b is the expense for burial of 1 m³ of waste, ruble/m³ of waste.

The expected annual saving from replacing regenerable sorbents by single-use sorbents is given by the formula

$$E_c = [(C_m - C_o) + E(K_m - K_o)] Q. \quad (3)$$

where K_m and K_o are specific capital expenditure in ruble · yr/m³; E is the standard efficiency coefficient equal to 0.12 yr⁻¹ [9]; Q is the annual productivity in m³ solution/yr.

The use of regenerable sorbents is associated with the following complications of the technological scheme being reflected in the amount of capital expenditure: firstly, additional reagent and evaporation plants are necessary; secondly, additional communications, gate valves, and pumps for the supply of the reagents from the reagent plant to the sorption towers are necessary; thirdly, the towers must be made of stainless steel.

The specific capital expenditure is taken equal to the expenditures for the Moscow purification station, where the productivity is 150,000 m³/yr [10]. A departure from this productivity does not imply changes of capital expenditure and leads only to a change in the amount of equipment.

The specific capital investment in the evaporation plant is 1.8 ruble · yr/m³. The specific capital expenditures in the reagent plant together with the installation of additional communications and equipment roughly comprise 0.14 ruble · yr/m³. In replacing the carbon steel towers by stainless steel towers the specific capital expenditure increases by 0.06 ruble · yr/m³.

The specific capital expenditure in the scheme with regenerable sorbent is higher than the corresponding expenditure in the scheme with single-use sorbent by 2 ruble · yr/m³. Formula (3) now becomes

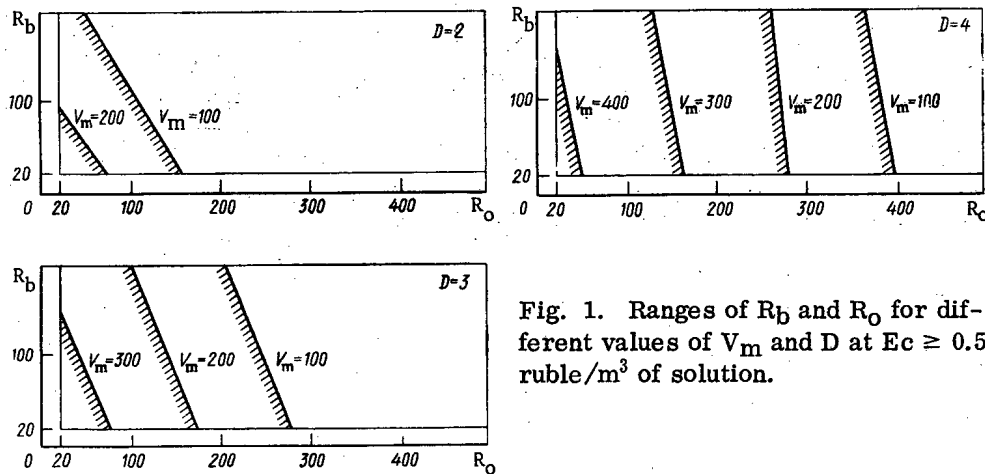


Fig. 1. Ranges of R_b and R_o for different values of V_m and D at $Ec \geq 0.5$ ruble/ m^3 of solution.

$$Ec = (C_m - C_o + 0.24) Q \text{ ruble/yr.} \quad (4)$$

Expenditures in Purification of Radioactively Contaminated

Water

Expenditures on Sorbents R_m and R_o . At present only synthetic resins are known among the regenerable sorbents. Their cost varies in the range 2-5 thousand ruble/ton [11] or 1000 ruble/ m^3 , since 1 m of sorbent occupies a volume of 3-5 m^3 .

Since the consumption of regenerable sorbents is less than 0.008 liter/ m^3 of the purified solution, the expenditures in regenerated sorbents can be neglected. Not having accurate data on the cost of single-use sorbents and taking into consideration the continuing study of their synthesis and selected we estimate the cost of the sorbents to be equal to 20-500 ruble/ m^3 of sorbent.

Burial Expenditure. The cost of treatment and burial of 1 m^3 waste is [10]: burial of liquid concentrates 200 ruble; cementing and storage of blocks 115 ruble; bitumenization and storage of blocks 85 ruble. With an increase of the productivity of bitumenization installation the cost of bitumenization and storage of blocks may be expected to decrease to 60 ruble/ m^3 . We assume that the cost of burial lies in the range 20-300 ruble/ m^3 of wastes, i. e. we include a cost which is several times smaller than that existing now.

Evaporation and Reagent Expenditures R_e and R_r . These expenditure items pertain only to the use of regenerable sorbents. At the Moscow purification station the evaporation cost per 1 m^3 of regenerant is 21.4 ruble/ m^3 [10].

The consumption of reagents in regeneration of 1 m^3 sorbent and their costs are given in Table 1.

The overall cost of reagents in regeneration of 1 m^3 of sorbent and the evaporation of these solutions ($V_r R_e + R_r$) is about 130 ruble.

Saving from Replacement of Regenerable Sorbents by

Single-Use Sorbents

For identical productivity, formula (4) can now be written in the form

$$Ec = [(130 + 0.2R_b + 0.24V_m) D - R_b - R_o] \times \frac{1}{V_m D} \text{ rubles}/m^3, \quad D = V_o/V_m. \quad (5)$$

Thus the economy from the replacement of purification by multiple-use sorbents by purification by single-use sorbents is

$$Ec = f(R_o, R_b, V_m, D). \quad (6)$$

The behavior of (6) as a function of these factors was investigated using a computer. The numerical values $Ec > 0$ were determined in the following range of variations of the parameters: $D = 1-4$; $R_b = 20-200$; $R_o = 20-500$; $V_m = 100-2000$.

It was found that: 1) the value of Ec for the above values of R_b , R_o , D , and V_m varies in the range

TABLE 3. Values of D Ensuring $E_c = 1$ ruble/ m^3 of Solution

R_b , ruble/ m^3 , of wastes	V_m	R_o , rubles/ m^3 of sorbent			
		20	100	200	400
200	100	2,3	3,2	4,2	6,4
120	100	1,8	2,8	4,1	6,7
80	100	1,4	2,6	4,0	6,9
40	100	1,0	2,2	3,7	7,1
20	100	0,7	2,1	3,8	7,2

0-1.47 ruble/ m^3 and does not exceed 1.5 ruble/ m ; 2) E_c decreases with the increase of R_o and R_b ; 3) E_c increases with D; 4) for $E_c > 0.3$ E_c decreases with the increase of V_m , while for $E_c < 0.3$ it increases with V_m . This happens because for extreme values of V_m the values of E_c change in the following way: for $V_m = 100$ from 0 to 1.47, and for $V_m = 2000$ from 0 to 0.30.

For $E_c < 0.5$ the saving in using single-use sorbents instead of regenerable sorbents will be very small. The annual saving is (thousand ruble): less than 16 for daily productivity of 100 m^3 , less than 82 for 500 m^3 , and less than 165 for 1000 m^3 .

The values of D, for which E_c is equal to 0.5 and 1 ruble/ m^3 , are given in Tables 2 and 3. The values of D are very large (> 10) for $V_m > 400$ at $E_c = 0.5$ ruble/ m and for $V_m > 100$ at $E_c = 1$.

The range of values of D, V_m , R_o , and R_b , for which $E_c \geq 0.5$ ruble/ m^3 of solution, are shown in Fig. 1. It follows from this figure that a perceptible saving from the replacement of regenerable sorbents by single-use sorbents can be obtained only in the following conditions.

1. The volume of the solution purified by regenerable sorbents in one cycle is smaller than 500 columnar volumes.
2. In storage of the wastes in liquid form ($R_b = 200$ ruble/ m^3) D must not be less than two to four and R_o no more than 150 ruble/ m^3 .
3. In cementing of the wastes ($R_b = 120$ ruble/ m^3) it is necessary that $D \geq 2-3$ and $R_o \leq 60$ ruble/ m^3 . For $D \geq 3-4$ R_o may reach 150 ruble/ m^3 .
4. In bitumenization of the wastes ($R_b = 80$ ruble/ m^3) and for identical volume of the filter cycle ($D = 1$) $R_o \leq 20$ ruble/ m^3 . If $D = 2$, $R_o \leq 100-150$ ruble/ m^3 is admissible.

CONCLUSIONS

The investigations of the expenditure in the purification of radioactively contaminated water make it possible to plan the paths to be followed in subsequent investigations on the synthesis and selection of sorbents and also on the development of methods of solidifying and burial of wastes.

1. A search for cheap single-use sorbents with isotope separation capacity exceeding the capacity of regenerable sorbents at least by a factor of two.
2. Production of regenerable sorbents with such a capacity that would ensure purification of more than 300-500 m^3 of solution per 1 m^3 of sorbent.
3. Development of cheaper burial processes.

LITERATURE CITED

1. R. Blanco et al., Practices in the Treatment of Low- and Intermediate-Level Radioactivity, IAEA, Vienna (1966), p. 793.
2. F. V. Rauzen and N. P. Trushkov, At. Énerg., 35, 2, 105 (1973).
3. R. Burns et al., Practices in the Treatment of Low- and Intermediate-Level Radioactivity, IAEA, Vienna (1966), p. 793.
4. C. Amberson et al., ibid, p. 419.
5. H. W. Live et al., ibid, p. 355.
6. P. Denjonghe et al., Proc. 2nd Conference on Peaceful Uses of Atomic Energy, 5, 18, New York (1958), p. 68.
7. N. Van de Voorde et al., Management of Low- and Intermediate-Level Radioactive Wastes, IAEA, Vienna (1970), p. 669.
8. R. Girder et al., [1], p. 477.
9. Typical Procedure of Determining the Economy of Capital Expenditures [in Russian], Ékonomicheskaya Gazeta, No. 39 (1969).
10. A. N. Kondrat'ev et al., Management of Low- and Intermediate-Level Radioactive Wastes, IAEA, Vienna (1971), p. 397.

11. Price List No. 05-01. Wholesale Prices of Chemical Products [in Russian], Pt. I, Preiskurantgiz, Moscow (1970).

LONGITUDINAL INSTABILITY OF A CIRCULATING
BEAM INTERACTING WITH A PASSIVE RESONATOR

V. I. Balbekov and P. T. Pashkov

UDC 621.384.6.01:621.384.634

A 70 GeV beam circulating in a steady magnetic field in the accelerator of the Institute of High-Energy Physics with the accelerating voltage disconnected exhibited longitudinal instability [1, 2]. It was found that the instability arose as a result of the interaction of the beam with the resonators of the accelerating stages. The linear stage in the development of such instabilities was considered theoretically in [3-5] when the particle distribution differed little from the uniform state. In this paper we shall refine the equations of the linear theory and reduce them to a form convenient for specific calculations. In addition to this we shall analyze the nonlinear stage of the instability numerically, i.e., we shall consider a strongly bounced beam. The calculation will be carried out using the parameters of the Institute of High-Energy Physics accelerator.

Threshold and Increment of the Instability

Let us consider a wave of beam current $\sim \exp(ikx - i\omega t)$, where k is the number of the harmonic, $\omega \approx k\Omega_0$; Ω_0 is the average angular velocity of the particle. Following the usual method [3-5] we obtain the dispersion equation

$$(u + iv) \int_{-1}^1 \frac{F'(x) dx}{x + r + i\varepsilon} = 1, \quad (1)$$

where $x = p - p_0 / \Delta p_m$ is the deviation of the particle momentum from the average value, referred to the half-width of the momentum spread with respect to the base, $F(x)$ is the normalized equilibrium distribution function;

$$r + i\varepsilon = \left(\frac{\omega}{k\Omega_0} - 1 \right) \left(\eta \frac{\Delta p_m}{p_0} \right)^{-1}; \quad \eta = \alpha - \gamma^{-2}; \quad (2)$$

α is the expansion coefficient of the orbits; γ is the relativistic factor;

$$u + iv = \frac{ie^2 N Z_K}{4\pi^2 R p_0 \eta k} \left(\frac{\Delta p_m}{p_0} \right)^{-2}; \quad (3)$$

R is the average radius of the machine; N is the number of accelerated particles; Z_K is the total impedance of the accelerating stages at the frequency $k\Omega_0$.

For a detailed analysis we chose a smooth function consisting of sections of parabolas:

$$F(x) = \frac{3}{2(1-a)} \begin{cases} (1 - |x|)^2 / (1-a), \\ a < |x| < 1; \\ 1 - x^2/a, & |x| \leq a; \\ 0, & |x| \geq 1, \end{cases} \quad (4)$$

where the parameter a is capable of varying from 0 to 1. Figure 1 shows the lines of constant values of r and ε in the u, v plane for $a = 0.5$. The diagram is symmetrical with respect to the real axis. In order to calculate the frequency and increment of the oscillations we must find u and v from Eq. (3), plot this point on the graph, determine r and ε by interpolation, and then use Eq. (2).

The inner region of the diagram bounded by the curve $\varepsilon = 0$ corresponds to the stable state. The broken lines in Fig. 1 indicate the region of stability for a equal to 0.1 and 0.9. For the limiting values of the parameter a (0 and 1) there is no threshold since the derivative distribution function exhibits

Translated from *Atomnaya Energiya*, Vol. 37, No. 4, pp. 332-335, October, 1974. Original article submitted November 10, 1973; revision submitted February 14, 1974.

© 1975 Plenum Publishing Corporation, 227 West 17th Street, New York, N.Y. 10011. No part of this publication may be reproduced, stored in a retrieval system, or transmitted, in any form or by any means, electronic, mechanical, photocopying, microfilming, recording or otherwise, without written permission of the publisher. A copy of this article is available from the publisher for \$15.00.

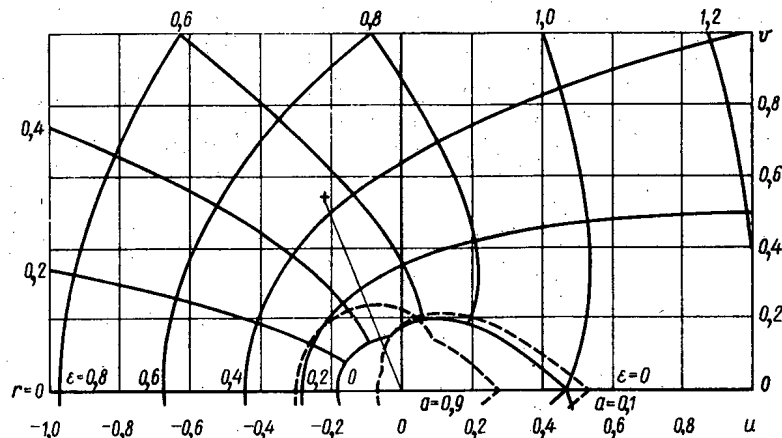


Fig. 1. Diagram for calculating the threshold and increment of the instability ($\alpha = 0.5$).

discontinuities. The break in the boundary to the stability region may be attributed to a discontinuity in the second derivative of $F(x)$.

We see that the threshold depends quite strongly on the form of the distribution, especially for $v \approx 0$ (reactive impedance). This is realized, for example, in the case of negative mass instability (the part of the ray $v = 0$, $u < 0$ situated outside the region of stability). To a coarse approximation the stability condition may be expressed as

$$\sqrt{u^2 - v^2} < 0,1 \div 0,2$$

or in ordinary form

$$N < (0,1 \div 0,2) \frac{4\pi^2 p_0 R}{e^2} \left| \frac{k\eta}{Z_{\kappa}} \right| \left(\frac{\Delta p_m}{p_0} \right)^2, \quad (5)$$

which approximately coincides with the estimate used in [5].

If the intensity greatly exceeds the threshold value, Eq. (1) may be solved in general form:

$$r + ie \approx \pm \left(\sqrt{u + iv} + \frac{3x^2}{2\sqrt{u + iv}} \right), \quad (6)$$

where the stroke denotes averaging with respect to the distribution. For distribution (4) $\bar{x}^2 = 0.1(1 + \alpha^2)$. In the ordinary form of writing, the instability increment takes the form

$$\text{Im } \omega \approx \Omega_0 \left(\sqrt{\frac{e^2 N |k\eta Z_{\kappa}|}{4\pi^2 R p_0}} - \frac{3}{2} \eta^2 k^2 \left(\frac{\Delta p}{p_0} \right)^2 \sqrt{\frac{4\pi^2 R p_0}{e^2 N |k\eta Z_{\kappa}|}} \right) \left| \sin \left(\frac{1}{2} \text{Arg } Z_{\kappa} + \frac{\pi}{4} \cdot \frac{|k\eta|}{k\eta} \right) \right|. \quad (7)$$

Let us find the increment for the Institute of High-Energy Physics accelerator using the following parameters: $N = 10^{12}$; $R = 236$ m; $p_0 = 70$ GeV/c; $\alpha = 0.0111$; $\Delta p_m/p_0 = 4 \cdot 10^{-4}$. The total impedance of the accelerating stages calculated on the basis of measurements made on the natural frequencies of the resonators has a maximum value at the thirteenth harmonic of the rotation frequency $Z_{13} = (170 + i70)$ k Ω . From Eq. (3) we find: $u = -0.22$, $v = 0.54$; hence $r = 0.55$; $\epsilon = 0.43$, $(\text{Im } \omega)^{-1} = 32$ msec. Equations (6) and (7) with $\alpha = 0.5$ give almost exactly the same values: $r = 0.57$, $\epsilon = 0.45$. The measured value of $(\text{Im } \omega)^{-1} = 30$ msec [2]. The calculated instability threshold is also close to the measured value: $2.7 \cdot 10^{11}$ and $\sim 3 \cdot 10^{11}$ respectively.

Nonlinear Stage in the Development of Instability

The exponential growth of the perturbation continues until the azimuthal distribution of the particles differs little from uniformity. The subsequent behavior of the beam may be studied by numerical methods.

For the Institute of High-Energy Physics accelerator the total impedance of the resonators at the twelfth and fourteenth harmonics is approximately three times less than at the thirteenth. For numerical analysis we therefore chose the case in which the instability initially developed at the thirteenth harmonic. Subsequently (in the nonlinear stage), harmonics of the current constituting multiples of 13 appeared; however, no corresponding voltage harmonics arose, since the impedance of the resonators at such high frequencies was very small. The accelerating voltage may accordingly be expressed thus:

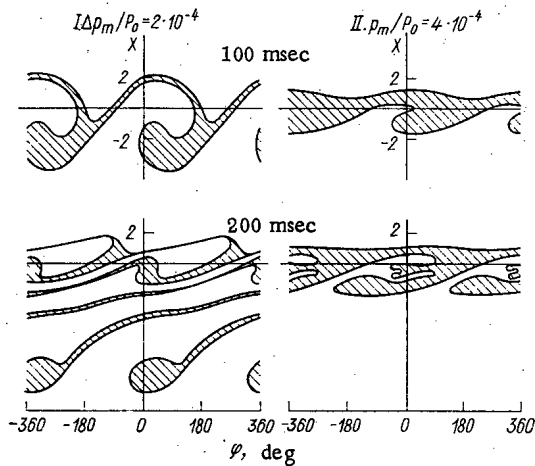
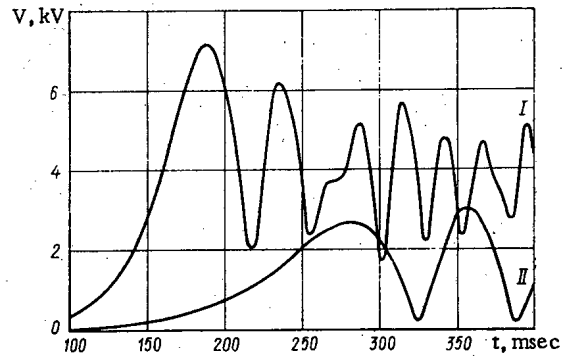


Fig. 2. Phase instability diagrams.

Fig. 3. Total amplitude of the voltage induced by the beam in the resonators of the Institute of High-Energy Physics accelerator: I) $\Delta p_m/p_0 = 2 \cdot 10^{-4}$; II) $\Delta p_m/p_0 = 4 \cdot 10^{-4}$.

$$V(t) = -|Z_q J_q(t)| \cos [q\Omega_0 t + \psi_q(t) + \text{Arg } Z_q], \quad (8)$$

where $q = 13$ is the number of the resonance harmonic; ψ_q is the phase of the beam current. The processes taking place in the beam have characteristic times greatly exceeding the attenuation times of the oscillations in the resonators, i. e., in this sense $J_q(t)$ and $\psi_q(t)$ are slowly varying functions.

The motion of the particles in the circulating beam is described by the phase equation [6]:

$$\ddot{\varphi} = -\frac{eq\eta |Z_q J_q(t)|}{2\pi m\gamma R^2} \cos [\varphi + \psi_q(t) + \text{Arg } Z_q], \quad (9)$$

which was solved in the following manner. Four hundred macroparticles were placed in the phase plane in such a way as to obtain a parabolic momentum distribution [distribution (4) with $a = 1$]. An initial accelerating voltage in the range 0.5–5 kV was specified. Then Eq. (18) was integrated in the range $\Delta t \leq 0.5$ msec for a constant beam current. At the end of the step the macroparticle coordinates so found were used to calculate the amplitudes and phases of the current and voltage, after which the process was repeated.

We also employed other methods of specifying the initial fluctuation, for example, a δ -shaped perturbation of the charge density. No qualitative differences appeared.

The development of instability in the phase plane is illustrated in Fig. 2 (the reduced momentum of the particles x is plotted along the vertical axis). The initial phase distribution is uniform and is therefore not shown in the figures.

We see that, under the influence of an induced voltage, "bunches" moving toward the center of the accelerator are separated out from the beam. Owing to the difference in the rotation frequencies of bunches with different energies, beats arise in the amplitude of the beam current and the voltage on the resonators (Fig. 3). As time progresses, the energy spread, the difference in the frequencies of rotation, and hence the frequency of the beats all increase. An increase in the initial spread slows the development of instability and reduces the maximum voltage. In the initial section the voltage rises exponentially, the increments coinciding with the values obtained from the equations of linear theory with $a = 1$: for curve I $(\text{Im } \omega)^{-1} = 25$ msec and for curve II $(\text{Im } \omega)^{-1} = 46$ msec. These curves are in good agreement with experimental results obtained in the Institute of High-Energy Physics accelerator [2].

It is interesting to follow the behavior of the beam in relation to the phase of Z for a fixed $|Z|$. Let us consider the hypercritical range of energy, for which $\eta > 0$.

For $\text{Arg } Z = -\pi/2$ instability is absent, and the initial perturbation is repeated periodically in the beam. The ray $v = 0$, $u > 0$ corresponds to this case in Fig. 1. With increasing $\text{Arg } Z$ the rate of development of the instability and the maximum voltage on the resonators increase (see upper half-plane in Fig. 1). The rate of turning of the beam also increases up to $\text{Arg } Z = 0$. Then the picture changes slightly: the grouping at the original radius increases, but the displacement of the beam along the radius is retarded. For $\text{Arg } Z = \pi/2$ the beam groups entirely in the original orbit, the form of the bunches coinciding with the form of the ordinary separatrix ($\cos \varphi_s = 0$). This kind of instability has the maximum rate of development.

This case gives a coarse representation of the limiting state of the beam for negative mass instability, although in actual fact all the harmonics of the beam current should make a considerable contribution.

The region $\text{Arg } Z > \pi/2$ (lower half-plane in Fig. 1) corresponds to negative resistance and may be realized by means of feedback circuits. The behavior of the beam differs in no way from the preceding case, except for the fact that the separating bunches collect energy in the resonators and their radius of rotation increases.

The authors wish to thank A. I. Basov, V. V. Polyakov, I. I. Sulygin, and B. K. Shembel' for information as to the results of a study of this effect in the Institute of High-Energy Physics accelerator and for fruitful discussions, and also L. A. Polyakova for help in the numerical calculations.

LITERATURE CITED

1. Yu. M. Ado et al. , Proc. Eighth Int. Conf. on High-Energy Accel. , CERN (1971), p. 14.
2. P. I. Basov et al. , Preprint Inst. High-Energy Phys. , 73-77, Serpukhov (1973).
3. A. A. Kolomenskii and A. N. Lebedev, At. Énerg. , 7, No. 6, 549 (1959).
4. S. Nielsen et al. , Proc. Int. Conf. High-Energy Accel. , CERN (1959), p. 239.
5. K. Hübner et al. , Proc. Eighth Int. Conf. on High-Energy Accel. , CERN (1971), p. 295.
6. A. A. Kolomenskii and A. N. Lebedev, Theory of Cyclic Accelerators [in Russian], Fizmatgiz, Moscow (1962), Chap. IV, p. 152.

ABSTRACTS

MEASUREMENT OF RATIO OF EFFECTIVE CROSS
SECTIONS OF CAPTURE IN ^{238}U AND FISSION OF ^{235}U
IN A FAST-THERMAL CRITICAL ASSEMBLY

M. V. Bychkov, A. V. Skobakarev,
A. P. Malykhin, I. V. Zhuk,
Yu. I. Churkin, and O. I. Yaroshevich

UDC 539.125.5.17

The procedure and results of measurement of the ratio of the effective cross sections of capture in ^{238}U and fission of ^{235}U ($\bar{\sigma}_C^8/\bar{\sigma}_f^5$) in the fast spectrum of neutrons on the critical assembly BTS-2 [1] are given. The determination of $\bar{\sigma}_C^8/\bar{\sigma}_f^5$ is based on the measurement of the intensity of ^{239}U γ -radiation ($T_{1/2} = 23.5$ min; $E_\gamma = 75$ keV) in a thin depleted uranium indicator and of the traces of fission products of ^{235}U from an enriched uranium indicator when irradiated in the investigated fast and thermal neutron spectra.

Uranium indicators 0.1 mm in thickness (27 mg/cm² uranium) and 10 mm in diameter, made of U-Al alloy (uranium depleted of ^{235}U 230 times) were used for the measurement of the rate of capture in ^{238}U . The rate of capture in ^{238}U was determined from the 75 keV photopeak with a γ -spectrometer with a 45 x 2 mm NaI(Tl) crystal and AI-128-2M analyzer. A 0.09 mm thick lead filter, proposed in [2], was used for the separation of the 75 keV γ -line against the large background of γ -radiation of the fission products of uranium. In the measurement of γ -radiation of ^{239}U γ -radiation of nonirradiated indicator, the intensity of the background of the γ -spectrometer, and the intensity of the γ -radiation of the fission products of uranium, which was determined with the use of a highly enriched uranium indicator, were taken into consideration.

Thin fission sources made of uranium enriched to 90% in ^{235}U (24 $\mu\text{g}/\text{cm}^2$ of ^{235}U) were used in the measurement of the fission rates of ^{235}U . Silicate glass of 0.1 mm thickness and 7 mm diameter was used as a detector of the fission products; the surface of the glass was specially treated for eliminating the background from the defects [3].

The uranium indicators were calibrated in the thermal column of the reactor of the Nuclear Physics Institute of the Academy of Sciences of BSSR using the constants $\bar{\sigma}_{f_0}^5 = 580.2 \pm 1.8$ barn [4] and $\bar{\sigma}_{C_0}^8 = 2.721 \pm 0.016$ barn [5].

The value of $\bar{\sigma}_C^8/\bar{\sigma}_f^5$ averaged over five measurements was 0.107 ± 0.002 .

The following errors were taken into consideration in the analysis of the results of measurements: 1) root mean square error of measurement of the ratios of the intensities of 75 keV γ -radiation and the fission products (0.8%); 2) error of the constants used (0.7%); 3) error due to different yields of fission products of ^{235}U and ^{238}U taking into consideration the γ -background of the fission products in the equipment γ -spectrum of the enriched uranium indicator (about 2%); 4) systematic error associated with different blocking of ^{238}U resonances, dispersion and scattering of neutrons during the irradiation of the indicators in the investigated and thermal neutron spectra (0.16%). The overall error of measurement of $\bar{\sigma}_C^8/\bar{\sigma}_f^5$ in BTS-2 was $\pm 2.3\%$.

LITERATURE CITED

1. V. A. Naumov et al., in: Dissociating Gases as Heat Transfer Agents and Working Substances in Power Installations [in Russian], Pt. II, ITMO AN BSSR, Minsk (1973), p. 229.

Translated from *Atomnaya Energiya*, Vol. 37, No. 4, pp. 337-342, October, 1974. Original article submitted June 19, 1973; revision submitted January 28, 1974.

© 1975 Plenum Publishing Corporation, 227 West 17th Street, New York, N.Y. 10011. No part of this publication may be reproduced, stored in a retrieval system, or transmitted, in any form or by any means, electronic, mechanical, photocopying, microfilming, recording or otherwise, without written permission of the publisher. A copy of this article is available from the publisher for \$15.00.

2. W. Davey, Nucl. Sci. and Engng., 24, No. 1, 26 (1966).
3. A. P. Malykhin, Report of AN BSSR, Phys. -Energ. Sci. Series, No. 2, 5 (1972).
4. S. Hanna et al., Atomic Energy Rev., 7, No. 4, 3 (1969).
5. C. Bigham et al., Canad. J. Phys., 47, 1317 (1969).

CALCULATION OF PRESSURE AND TEMPERATURE WITHIN THE CASING OF A WATER-WATER REACTOR

I. Mishak

UDC 621.039.584.001.2

The casing plays an important role in the trapping of radioactive fission fragments and must not be damaged even under emergency conditions. In order to estimate the casing load, a mathematical model for the calculation of the temperature and pressure in the event of damage by the emission of the primary coolant is developed. In developing the model it was important to take into consideration the partition of the inner volume of the casing by walls and constructions, and to describe this system of interconnected sections. The resistance of the openings between the sections to the flow of an expansible coolant (vapor) results in the formation of a pressure difference with the possibility of disruption in the integrity of the walls, damage to the technical safety system, and, at the worst, damage to the casing itself.

The model primarily describes the expansion of a mixture of air and vapor from a given source (break in the loop) in a system of adjacent sections. Assuming thermodynamic equilibrium of the water, water vapor, and air, the air-mass

$$\frac{dM_A^i}{d\tau} = \sum_j G_A^{i,j}, \quad (1)$$

the coolant-mass

$$\frac{dM_C^i}{d\tau} = \sum_j G_C^{i,j}, \quad (2)$$

and the internal energy balances for the mixture

$$\frac{d}{d\tau} (U_A^i + U_C^i) = Q^i + \sum_j (G_A^{i,j} h_A^{i,j} + G_C^{i,j} h_C^{i,j}). \quad (3)$$

are formulated for each section. Here M is the mass, kg; G is the flow rate, kg/sec; τ is the time from the start of the damage, sec; Q is the thermal output, J/sec; h is the specific enthalpy, J/kg; A denotes the air; C denotes the coolant; i denotes the number of the section; i, j denotes motion from the i -th to the j -th section.

The sum over "j" in Eqs. (1-3) expresses the interaction of the i -th section with the surrounding system of sections, including the emission of the coolant from the primary loop and the effect of the sprinkler and ventilation system. In Eq. (3) $h_C^{i,j}$; $h_A^{i,j}$ is the enthalpy of the coolant (air). The thermal outputs Q^i delimit the effect of random heat sources. By utilizing the equations of state for water and air, as well as the conditions for the constancy of the sections' volumes ($V^i = \text{const}$), one can convert Eq. (3) into a differential equation for the temperature of a section. The pressure is determined by the partial pressures of the air and vapor at a given temperature.

The system of differential equations obtained is solved numerically by means of a TRACO program in FORTRAN IV language. Preliminary calculations allow one to draw the following conclusions.

The division of the vacant volume into a system of sections influences substantially the behavior of the pressure inside of the casing. The pressure in the present sources in the sections exceeds significantly

Original article submitted October 22, 1973.

the mean pressure. The maximum pressure differences between the sections depend first of all on the rate of evacuation of the primary loop, the location of the damage in the loop, the cross-sectional areas of the flow between the sections, and the coefficient of transport of water droplets by the flow.

p VERSUS T PHASE DIAGRAM OF THE URANIUM-OXYGEN SYSTEM

Yu. V. Levinskii

UDC 541.01.123:546.791

On the basis of an analysis and generalization of the experimental data, a p versus T phase diagram has been proposed for the uranium-oxygen system in the temperature interval 800-3000°C and range of

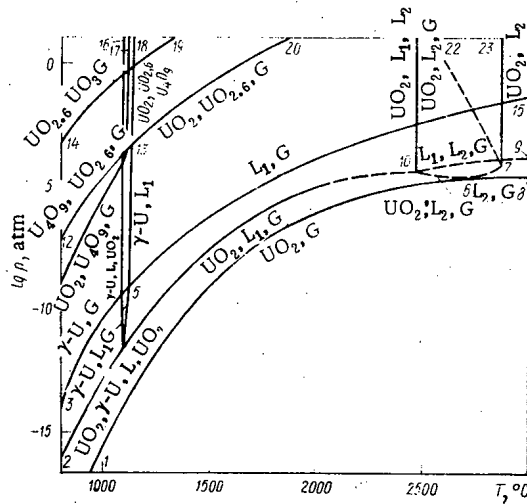


Fig. 1. p versus T phase diagram of the uranium-oxygen system.

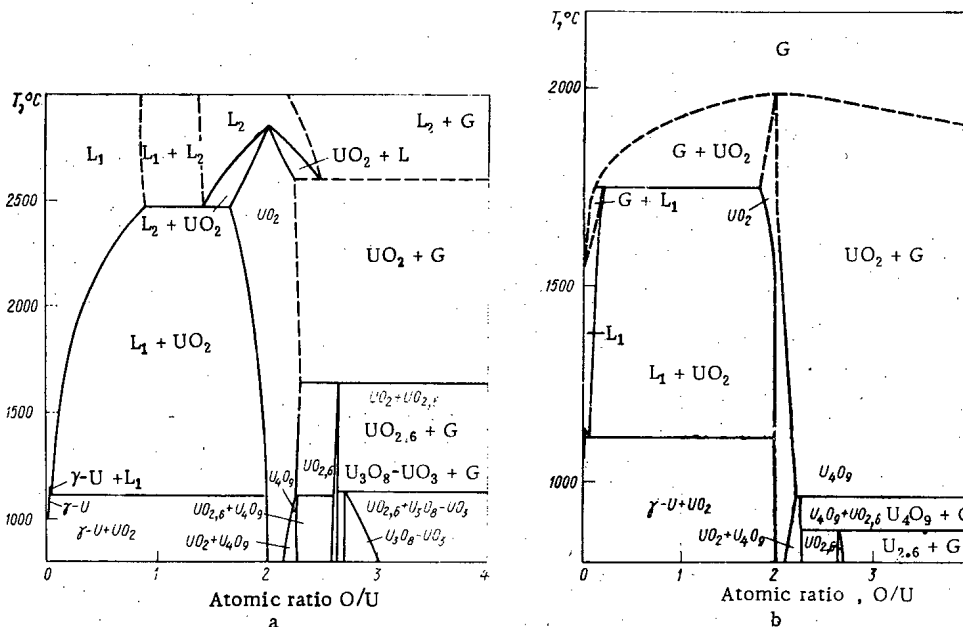


Fig. 2. Isobaric cross sections of the phase diagram of the uranium-oxygen system at pressures 1 (a) and 10^{-6} atm (b).

Original article submitted February 15, 1974.

pressures 10^{-17} –10 atm (Fig. 1), representing the projection of the isotherms–isobars of monovariant reactions onto the p versus T plane. With the aid of this diagram, using information on solubility, any isobaric and isothermal cross sections of the uranium–oxygen system can easily be constructed (Fig. 2).

CAN URANIUM BE REDUCED FROM THE HEXAFLUORIDE TO THE ELEMENTARY STATE BY HYDROGEN?

Yu. N. Tumanov and N. P. Galkin

UDC 546.791.6.161:669.094.1

The work analyzes the results of unsuccessful attempts to reduce elementary uranium from the hexafluoride with plasma hydrogen according to the scheme cited in Fig. 1. The basic reduction products are uranium tetrafluoride or a mixture of the latter with lower fluorides of uranium, the gross composition of which lies in the range 3.68–4.0. The composition of these products depends little on the temperature of the reduction (it reaches 3000–5000°K), the mole ratio $H_2:UF_6$ (6.4–640), or the consumption of electric power.

To explain the experimental results, the thermodynamics of the reactions in the system UF_6-H_2 are discussed, as well as the kinetics of recombination processes and phase transitions in the receiver of the reaction products. It was shown that the large values of the equilibrium constants of the summary reactions of reduction of uranium from the hexafluoride by molecular and atomic hydrogen are due chiefly to the first two cofactors in the product $K_{eq} = \prod_i k_{pi}$, where k_{pi} represents the equilibrium constants of the intermediate reactions. The subsequent reactions do not go to completion thermodynamically, even at temperatures of 3000–5000°K, where the equations of reduction are essentially formal. Actually, at temperatures above 300°K hydrogen loses its reducing ability, since it does not form a thermodynamically stable compound with fluorine. The lowering of the valence of uranium in the system UF_6-H_2 occurs as a result of thermal decomposition of uranium fluoride, which dissociates under conditions of plasma temperatures. Therefore, in the interaction of uranium hexafluoride with plasma hydrogen, at temperatures above 3000°K the latter plays the role not of a reducing agent, but of a heat carrier.

Since the reactions in plasma heat carriers proceed under conditions close to thermodynamic equilibrium, while the reduction of uranium from the hexafluoride by hydrogen does not go to thermodynamic completion even at 5000°K (as yet it is technically difficult to heat hydrogen even up to this temperature), it is concluded that the use of hydrogen reduction for the production of elementary uranium from the hexafluoride is unpromising.

Elementary uranium can be produced from the hexafluoride if the latter is heated (at $p = 1$ atm) to

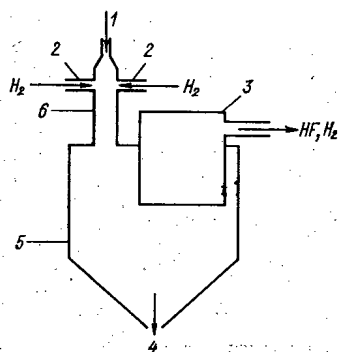


Fig. 1. Scheme of reactor for the reduction of uranium from uranium hexafluoride with plasma hydrogen. 1) Uranium hexafluoride; 2) plasma-tron; 3) filter; 4) uranium tetrafluoride; 5) receiver of reaction products; 6) plasma reactor-mixer.

Original article submitted February 18, 1974.

$\sim 6000^\circ\text{K}$. However, uranium or fluorides in which the valence of uranium is ≤ 3 can be isolated only under the condition that the rate of condensation at the exit from the reactor is greater than the rate of gas phase recombination of uranium or uranium fluorides. An estimate shows that this condition can be fulfilled for lower fluorides of uranium, and evidently for uranium.

The results of the investigation show why uranium tetrafluoride is the basic product of the reaction of uranium hexafluoride with hydrogen in the absence of special quenching: at the exit from the plasma reactor there is a condensation of the reduction products and a recombination of uranium fluorides in the heterophase region to the most thermodynamically stable compound under these conditions — uranium tetrafluoride.

CALCULATION OF SOME DIFFUSION PARAMETERS AND GAS GENERATION OF PARTICLES ON HEATING THE SAMPLES AFTER IONIC BOMBARDMENT

A. A. Pisarev and V. A. Pisarev

UDC 539.12.17:533.15

The results of machine calculations of the diffusion and gas generation of particles injected into the metal during the ionic bombardment are given. The calculations are based on the solution of the simultaneous equation of diffusion determined on the semiinfinite straight line having zero limiting conditions. The initial Gaussian distribution function of the particles $c(x, 0)$ is cut off at a certain distance x_0 from the vacuum surface $x = 0$ for satisfying the limiting condition $c(0, t) = 0$. The gas flux j from the metal in a vacuum is determined by Fick's first equation. The diffusion equation was solved for the case of linear increase of temperature T with time when the velocity was a . The distribution of the particles in the sample was considered in the dimensionless coordinates $\vartheta = x/x_m$, where x_m is the coordinate of the center $c(0, t)$.

According to [1], the activation energy for the diffusion Q can be expressed according to any characteristic temperature T^* in the bell-shaped curve $j(T)$. Figure 1 gives the isoenergetic curves which simplify

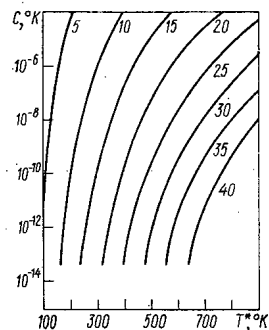


Fig. 1

Fig. 1. Isoenergetic curves of the dependence of the parameter C on the characteristic temperature T^* for different values of the activation energy for diffusion $Q = 5$ to 40 kcal/mole.

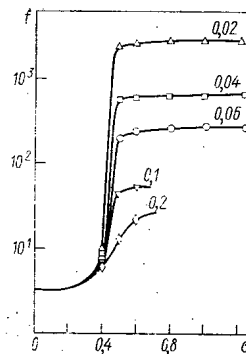


Fig. 2

Fig. 2. Dependence of the gas-generation parameter f on σ_1 for different values of ϑ_0 .

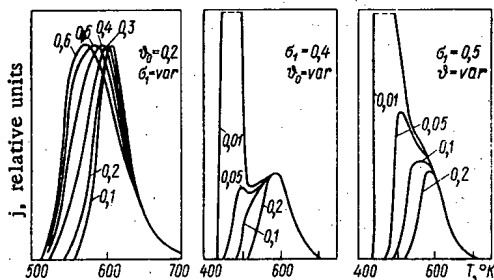


Fig. 3. The function $j(T)$ for different combinations of the parameters ϕ and σ_1 .

the determination of Q according to the value of T^* and the parameter $C = p_m^2 a / Fk_0$ (F is a parameter depending on the choice of T^* , k_0 is the lattice vibration frequency, $p_m = x_m / \lambda$, and λ is the lattice parameter).

For T^* we preferably use the temperature T_{\max} of the occurrence of the maximum of $j(T)$; in this case $F = f$. It has been shown that T_{\max} and f depend on the shape of $c(0, t)$. Figure 2 shows the relation $f(\sigma_1)$ for different values of ϕ_0 , where σ_1 is the relative half-width of the Gaussian function $c(0, t)$; $\phi_0 = x_0 / x_m$. It is important that for small values of σ_1 , the parameter f and the value of T_{\max} are practically constant.

The calculations of $j(T)$ (Fig. 3) explain the small variation of the tail of the function $j(T)$, observed experimentally [2], and its displacement in the low-temperature region on increasing the width $c(0, t)$; moreover, they indicate that a sharp increase of $f(\sigma_1)$ and a decrease of $f(\phi_0)$ are associated with the occurrence of the false low-temperature maximum of $j(T)$.

It has been shown that the diffusion model used in the calculations cannot be applied for wide original distributions because of the occurrence of false peaks in $j(T)$; these are caused by the abnormally large concentration gradients close to the vacuum limit, which arise in the initial stage of heating. From Fig. 4, it follows that for a small value $\phi_0 = 0.01$, we observe two maxima $\partial c / \partial x$: at 450 and 600°K, which correspond to the false peak and the real peak in the curve $j(T)$. For $\phi_0 = 0.1$, when $c(x, 0)$ is cut off far from the limit, the maximum $\partial c / \partial x$ occurs only at 600°K.

In the determination of Q , it is recommended that the experiments be carried out with low doses and high ionic energies; the ascending branch of $j(T)$ should not be used for the calculations.

In the study, we observe some peculiarities of the variation of the concentration profile and the rate of gas generation during the process of heating of the sample. In particular, we observe a shift of the maximum of $c(x, t)$ in the depth of the sample on heating and a decrease in the height and an increase of the width of the profile. It has been shown that for $T > T_{\max}$ the diffusing particles "forget" their previous history, and the concentration profile and the gas-generation curves practically do not depend on the shape of initial distribution.

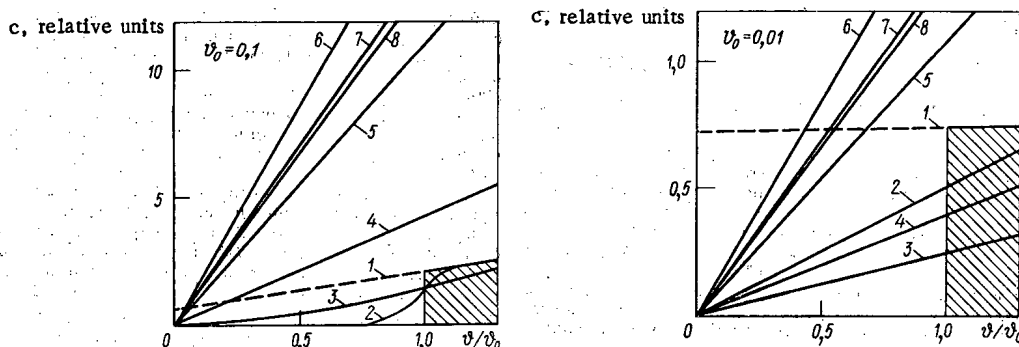


Fig. 4. Dependence of the particle concentration in the sample on the depth ϕ/ϕ_0 close to $\phi = \phi_0$ in different stages of heating for $\sigma_1 = 0.3$: 1) part of the initial distribution; curves 2 to 8 were plotted correspondingly for the temperatures 450 to 750°K with intervals of 50°K; the values of c in curves 6 to 8 increase correspondingly by 10, 100, and 1000 times.

LITERATURE CITED

1. L. B. Begrambekov et al., *At. Énerg.*, **31**, No. 6, 625 (1971).
2. A. A. Pisarev, V. M. Sotnikov, and V. G. Tel'kovskii, in: *Second All-Union Symposium on the Interaction of Atomic Particles with Solids (Moscow, October 9-11, 1972) [in Russian]*, Izd. ONTI IAÉ im I. V. Kurchatova, Moscow (1972), p. 240.

ALLOWANCE FOR GEOMETRY IN ACTIVATION ANALYSIS
INVOLVING FAST NEUTRONS GENERATED IN A CYCLOTRON
BY THE REACTIONS ${}^9\text{Be}(d, n){}^{10}\text{B}$ AND ${}^9\text{Be}(p, n){}^9\text{B}$

V. A. Muminov, B. Akabirov,
and N. Abibullaev

UDC 543.53

It is extremely important in neutron-activation analysis to take due account of the sample-irradiation geometry, especially in the case in which a thick target bombarded with cyclotron-accelerated fast particles forms the neutron source.

Using existing functions for the angular distributions of the neutrons arising from the reactions ${}^9\text{Be}(d, n){}^{10}\text{B}$ and ${}^9\text{Be}(p, n){}^9\text{B}$ and an auxiliary geometrical construction, an elementary equation is derived with this end in view and used for calculating the fall in neutron flux corresponding to various target-sample distances, and also the flux variation along the sample radius.

The fall in neutron flux is given in tabular and graphical form in relation to these two parameters. The calculated fall in neutron flux along the radius is compared with experimental results, and the fall expressed as a function of distance, corresponding to isotropic radiation. Certain conclusions are drawn.

Original article submitted January 3, 1974.

LETTERS TO THE EDITOR

OBSERVATION OF ANOMALOUSLY LARGE PORES IN
NICKEL BOMBARDED BY CARBON IONSV. I. Krotov, S. Ya. Lebedev,
and V. N. Bykov

UDC 621.039.531:546.74

At the present time, there is great interest in simulation of radiation-induced swelling by irradiating structural metals and alloys with accelerated ions [1-3]. The use of accelerators for this purpose makes it possible to obtain such a dislocation density in the surface layer of test specimens, within a few hours, as would be achieved only in the course of several years' testing in a reactor. But further theoretical and experimental investigations will be required to justify the validity of extrapolating the results obtained through simulation of reactor irradiation conditions.

It was in this context that we undertook studies of the special features of development of porosity in nickel exposed to bombardment by argon ions and carbon ions of 70 keV energy. The irradiation experiments were carried out on an ILU-100 accelerator [4]. A nickel specimen (0.1 mm thick and 3 mm in diameter) was annealed at 800°C for one hour in a 10^{-5} torr vacuum prior to irradiation. The specimen was then thinned down electrolytically and examined under an electron microscope in order to monitor the quality of the thinning operation. Irradiation conditions were: a) 70 keV carbon ions to doses of $5 \cdot 10^{17}$ and 10^{18} ions/cm² at 550°C; b) 70 keV argon ions to doses of 10^{17} and $7 \cdot 10^{17}$ ions/cm² at 550°C; c) helium ions to a dose of $2 \cdot 10^{16}$ ions/cm² followed by irradiation with 70 keV carbon ions to a dose of $5 \cdot 10^{17}$ ions/cm² at 550°C. The results of electron microscope studies of the test irradiated specimens are entered in Table 1.

Figures 1 and 2 show electron micrographs of specimens irradiated with carbon ions to a dose of 10^{18} ions/cm², as well as of specimens irradiated with helium ions and subsequently irradiated with carbon ions.

Micrographs of portions of the specimens whose thickness was greater than the path of the ions, calculated at 1000-1100 Å and ~200-300 Å in the case of carbon ions and argon ions, respectively, were used in processing the results.

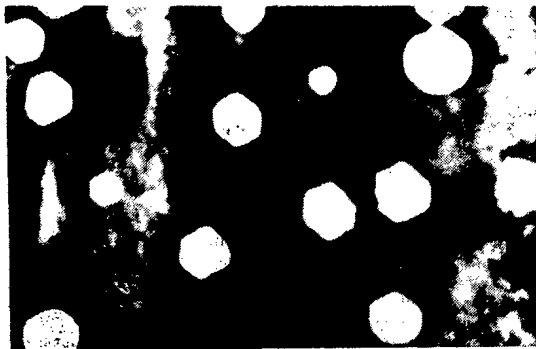


Fig. 1

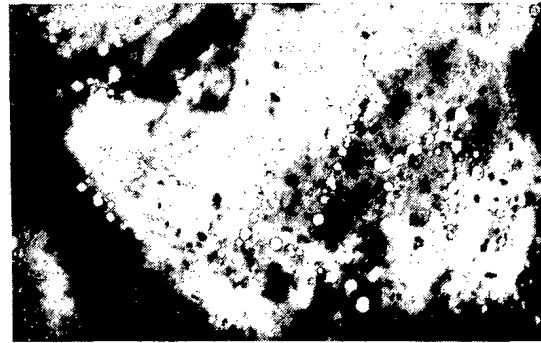


Fig. 2

Fig. 1. Electron microscopic photograph of nickel specimen irradiated by 70 keV carbon ions at 550°C, dose 10^{18} ions/cm² (magnification $\times 90,000$).

Fig. 2. Electron micrograph of nickel specimen irradiated by 50 keV helium ions at room temperature, dose $2 \cdot 10^{16}$ ions/cm², with subsequent irradiation by 70 keV carbon ions at 550°C and dose $5 \cdot 10^{17}$ ions/cm² (magnification $\times 90,000$).

Translated from *Atomnaya Énergiya*, Vol. 37, No. 4, pp. 343-344, October, 1974. Original letter submitted September 12, 1973.

© 1975 Plenum Publishing Corporation, 227 West 17th Street, New York, N.Y. 10011. No part of this publication may be reproduced, stored in a retrieval system, or transmitted, in any form or by any means, electronic, mechanical, photocopying, microfilming, recording or otherwise, without written permission of the publisher. A copy of this article is available from the publisher for \$15.00.

TABLE 1. Results of Electron Microscopic Investigation of Irradiated Specimens

Characteristic	Bombarding ion			
	carbon		argon	
Dose, cm ⁻²	5·10 ¹⁷	10 ¹⁸	10 ¹⁷	5·10 ¹⁷
Pore concentration, cm ⁻³	~10 ¹⁴	~10 ¹⁴	~10 ¹⁶ -10 ¹⁷	~10 ¹⁶ -10 ¹⁷
Maximum dimension of pores, Å	1500	2200	200	400
Minimum dimension of pores, Å	300-500	500-1000	—	—
Porosity, %	5	13	—	0,5

No pores were observed on portions of the specimens of sufficiently small thickness (respectively < 500-800 Å and < 150-200 Å for irradiation by carbon ions and argon ions). Clearly, with decreasing specimen thickness the relative yield of vacancies on the surface increases, while the thickness of the specimen becomes less than the path length of the ion, so that the dislocation density decreases abruptly. Starting with the specified thicknesses, the equilibrium concentration of vacancies in the specimen proves to be insufficient to support the growth of pores. But even when specimen thicknesses are in a very low range ~200-300 Å (in the case of irradiation by argon ions), when it would appear that vacancies must lead off to the surface at a high rate, a sufficiently high dislocation density would ensure the vacancy concentration required for pore growth. Apparently, the increase in the yield of interstitial atoms of the target material on the surface as specimen thickness decreases also has a definite role to play, and that also contributes to the rise in vacancy concentration through lowered recombination.

The pore concentration in specimens irradiated with carbon ions to doses of $5 \cdot 10^{17}$ and 10^{18} ions/cm² is practically identical at a level of $\sim 10^{14}$ cm⁻³ (see Table 1). Clearly, this is due to the concentration of active centers available for condensation of vacancies. As the irradiation dose is stepped up, new pores do not form, but instead we find a further growth of the pores already present. This point is confirmed by the minimum dimension of the pores (see Table 1). A certain spread in pore dimensions would seem due either to the different effectiveness of vacancy condensation centers or to local inhomogeneities in the structure of the specimen such as would affect the rate at which vacancies drain off to the given center.

The maximum dimension of the pores (~2200 Å) is roughly double the calculated path length of the carbon ion traversing nickel. The random yield in the direction of channeling as a result of collisions with lattice ions on the part of either the initial ion or the secondary and subsequent atoms from collision stages can cause damage at a depth far in excess of the ion path length.

The emergence of pores beyond the damage zone may also account for the diffusion redistribution of vacancies and lattice atoms with the formation of a closer to equilibrium pore configuration. In addition, the clearly defined faceting and pore orientation in the crystal lattice also show a similar effect. We get the impression that the pore growth was limited only by the specimen thickness, which averages ~1500 Å. Coarser pores not emerging at the surface were observed in the thicker portions of specimens.

In specimens irradiated by argon ions, we note an extremely high concentration of pores ($\sim 10^{16}$ - 10^{17}). A count of the number of pores becomes more difficult because of the abundance of all sorts of fine pores whose dimensions do not exceed 30 to 50 Å, as well as intense overlap of pore images on the electron micrographs. In this case the penetration of argon atoms into the specimen metal brings about the formation of an appreciable number of active vacancy condensation centers during the irradiation process. The spread in pore dimensions can be accounted for in terms of the difference in pore "age", whereas all the pores are of identical "age" in bombardment by carbon ions.

In specimens irradiated sequentially by helium ions and carbon ions (see Fig. 2), a certain orderedness in the pore arrangement was observed on some portions.

Hence, ion irradiation makes it possible to discern some regularities of pore development which are needed in the study of radiation-induced swelling of materials.

LITERATURE CITED

1. R. Nelson and D. Mazey, AERE-R 6046 (1969).
2. R. Nelson et al., J. Nucl. Materials, 37, 1 (1970).
3. D. Norris, Radiation Eff., 14, 1 (1972).
4. S. Ya. Lebedev et al., Pribory i Tekh. Eksperim., No. 4, 225 (1968).

KINETIC INSTABILITY OF AN INTENSE BEAM OF CHARGED PARTICLES IN A STORAGE RING

N. N. Naugol'nyi

UDC 621.384.61

Many papers have appeared on the longitudinal motion of beams of charged particles in circular accelerators, taking account of space-charge forces. An extensive bibliography on this problem is given in [1].

The so-called "negative mass" instability (NMI) of a beam can arise in a smooth nonresonant perfectly conducting cavity. The instability develops at energies above a critical value $[\eta \equiv \gamma^{-2} - \alpha < 0$, where $\gamma = (1 - \beta^2)^{-1/2}$ is the familiar relativistic factor; $\alpha = (1 - n)^{-1}$, where n is the exponent in the expression for the radial decrease of the magnetic guide field [2]] at frequencies $\omega = \nu\omega_0(1 + \delta)$ close to integral multiples of the rotational frequency ω_0 ($|\delta| \ll 1$). For a small equilibrium beam density ρ_0 the growth rate of the oscillations $\text{Im } \nu\omega_0\delta$ is proportional to $\rho_0^{1/2}$. Our results show, however, that as the ring current increases, a kinetic instability of the beam rather than a hydrodynamic NMI develops. It is clear that a kinetic instability can appear earlier than the NMI since an appreciable threshold current is generally required for the development of an NMI because of the thermal spread in momenta.

Let us consider a circular beam of radius a circulating in a metal toroidal chamber of minor radius b . The general dispersion relation for longitudinal oscillations in such a system is rather complicated. In the ultrarelativistic case good accuracy is ensured by using the long-wavelength approximation $|\kappa^2|b^2 \ll 1$, where $\kappa^2 = k_{\perp}^2 - k^2$ is the square of the transverse wave number, k_{\parallel} is the longitudinal wave number, $k = \omega/c$, and c is the velocity of light. There is no need to present a detailed derivation of the dispersion equation. Following the procedure of the self-consistent approximation and satisfying the appropriate boundary conditions on the surface of the beam and the chamber we obtain

$$\frac{a^2}{2} (\epsilon_{\parallel} - 1) \kappa^2 \ln b/a + 1 = 0. \quad (1)$$

$\epsilon_{\parallel} = 1 + (\omega_e^2/\omega) \int [dpp \partial_p u(p-p_0)] / [\gamma(\omega - k_{\parallel}v)]$ is the dielectric constant of the beam, $\omega_e = (4\pi\rho_e^2/m)^{1/2}$ is the Langmuir frequency, and $\partial_p u(p-p_0)$ is the derivative of the background distribution function with respect to the longitudinal momentum p . In evaluating the Cauchy type integral in the expression for ϵ_{\parallel} in accord with the form for writing the Fourier expansions of perturbed quantities $\sim \exp i(k_{\parallel}z - \omega t)$, the pole at $\omega = k_{\parallel}v$ is bypassed below. Limiting ourselves to analytic distribution functions $u(p-p_0)$ with small dispersions (δp^2) and using the relation $\partial_p u_0 = \eta\omega_0/p_0$ [3] it is easy to find

$$\frac{dpp \partial_p u(p-p_0)}{\gamma(\omega - k_{\parallel}v)} = -\gamma^{-1} \{ \eta\omega_0 |(\omega - \nu\omega_0)^2 + i\pi p^2 \partial_p u_{\text{res}} | v | \eta | \omega_0 \},$$

where $\partial_p u_{\text{res}}$ is the resonance value of the derivative $\partial_p u(p-p_0)$ at the point $p-p_0 = p_0(\omega - \nu\omega_0)/\eta\nu\omega_0$.

We now write Eq. (1) in the form

$$\frac{\omega_e^2 a^2}{2\omega\gamma} \kappa^2 \ln b/a \{ \eta\nu\omega_0 |(\omega - \nu\omega_0)^2 + i\pi p^2 \partial_p u_{\text{res}} | v | \eta | \omega_0 \} = 1. \quad (2)$$

The solution of this equation must be sought in the form $\omega = \nu\omega_0(1 + \delta)$. Neglecting the thermal spread in the beam we have for $|\delta| \ll 1$

$$\delta_{\pm}^{(0)} = [-\xi \pm \sqrt{\xi^2 - (\xi + \gamma^{-2})}] (1 + \xi)^{-1}, \quad (3)$$

where $\xi = (\omega_e^2 a^2 / 2\gamma c^2) \ln(b/a)$. If $\xi < 0$ the NMI develops with a growth rate for $-\xi \ll \gamma^{-2}$ equal to [3]

Translated from *Atomnaya Energiya*, Vol. 37, No. 4, pp. 344-346, October, 1974. Original letter submitted October 12, 1973.

© 1975 Plenum Publishing Corporation, 227 West 17th Street, New York, N.Y. 10011. No part of this publication may be reproduced, stored in a retrieval system, or transmitted, in any form or by any means, electronic, mechanical, photocopying, microfilming, recording or otherwise, without written permission of the publisher. A copy of this article is available from the publisher for \$15.00.

$$\text{Im } \nu \omega_0 \delta \approx \nu \omega_0 \frac{\omega_e a}{\nu} (-\eta \ln b/a/2\gamma^3)^{1/3}. \quad (4)$$

Assuming that the imaginary part of (2) is much smaller than the real part (for $\text{Im } \omega = 0$) and taking $\delta = \delta^{(0)} + (\delta)^{(1)}$, we find the correction to the frequency ω :

$$\delta_{\pm}^{(1)} = i\pi p^2 \delta^{(0)4} \partial_p u_{\text{res}} / 2 |\eta| |\eta| \pm \sqrt{\xi \beta^{-2} (\xi + \gamma^{-2})}; \quad (5)$$

$$|\delta^{(1)2}| \ll |\xi \beta^{-2} (\xi + \gamma^{-2})|.$$

Since for decreasing distributions, symmetric with respect to p_0 , $\partial_p u_{\text{res}} \approx -\delta/\eta$, in view of the obvious inequalities

$$-\xi > \sqrt{\xi \beta^{-2} (\xi + \gamma^{-2})} \quad (\xi < 0),$$

$$\xi < \sqrt{\xi \beta^{-2} (\xi + \gamma^{-2})} \quad (\xi > 0)$$

it follows from Eq. (5) that $\text{Im } \delta^{(1)} < 0$ for $|\xi| < \gamma^{-2}$, i. e., in this case the oscillations are damped as a result of the thermal spread in the beam. According to (5) the kinetic instability appears for $-\xi > \gamma^{-2}$, and for decreasing distributions solution (3) is unstable with a negative value of the root $\delta^{(0)}$. If $-\xi \rightarrow \gamma^{-2}$ Eq. (5) no longer holds. For $|\xi \beta^{-2} (\xi + \gamma^{-2})| \ll |\delta^{(1)2}|$ we obtain directly from Eq. (2)

$$\delta^{(1)} = (\pi/2 |\eta|)^{1/2} p \delta^{(0)2} [i \partial_p u_{\text{res}} / \eta]^{1/2}, \quad (-\xi = \gamma^{-2}). \quad (6)$$

In the last expression there is always a value of the root with a positive imaginary part which corresponds to growing oscillations. Thus an instability arises if $-\xi \geq \gamma^{-2}$, or in explicit form

$$\omega_e^2 \geq -\frac{2c^2}{\eta \gamma a^2 \ln b/a}. \quad (7)$$

It should be noted that the instability under consideration is possible only for energies above the critical value ($\xi < 0$), i. e. it is a kinetic NMI. The solution with $\xi > 0$ can be unstable only if the momentum distribution functions of the particles increase to the limits (two-beam instability).

The results of Eqs. (5) and (6) can be written in a more descriptive form by carrying out an analogy with the propagation of longitudinal waves in a homogeneous medium with $\epsilon = 0$. We introduce a complex function ϵ whose real and imaginary parts in accord with (2) are

$$\text{Re } \epsilon = 1 - \kappa^2 \xi c^2 / (\omega - \nu \omega_0)^2;$$

$$\text{Im } \epsilon = -i\pi p^2 \partial_p u_{\text{res}} \kappa^2 \xi c^2 / \eta |\eta| \nu^2 \omega_0^2.$$

Hence

$$\partial_\omega \text{Re } \epsilon (\delta^{(0)}) = 2 (\xi + \delta^{(0)} \xi + \delta^{(0)}) / \nu \omega_0 \delta^{(0)2}.$$

If $|\text{Re } \epsilon| \gg |\text{Im } \epsilon|$ ($\text{Im } \delta^{(0)} = 0$) Eq. (5) takes the form

$$\delta' = -i \text{Im } \epsilon / \partial_\omega \text{Re } \epsilon \nu \omega_0 (\delta = \delta_{\pm}^{(0)}).$$

Since for $-\xi \geq \gamma^{-2}$ the value of $\partial_\omega \text{Re } \epsilon (\delta_{\pm}^{(0)}) \leq 0$ (anomalous dispersion) and $\text{Im } \epsilon (\delta_{\pm}^{(0)}) > 0$ (for decreasing distributions) the solution $\delta_{\pm}^{(0)}$ is unstable and describes a "slow" wave with a "negative" energy. Equation (6) corresponds to the instability of "zero" energy oscillations: $\partial_\omega \text{Re } \epsilon (\delta_{\pm}^{(0)}) = 0$.

In addition it should be noted that condition (7) may be insufficient to ensure the initiation of an instability because of the finite conductivity of the chamber walls surrounding the beam. Taking this into account leads to a decrease in the absolute value of the growth rates (5) and (6) since a dissipative instability at energies above critical develops in waves of "positive" energy [1]. By applying Leontovich boundary conditions at the surface of the chamber and making appropriate calculations we obtain an equation similar to (1) if we make the substitution

$$\kappa^2 \ln b/a \rightarrow \kappa^2 \ln b/a - i \zeta k/b,$$

where $\zeta = (e^{-i\pi/4}/2)(\omega/\sigma)^{1/2}$ is the impedance of the chamber material and σ is the static conductivity in reciprocal seconds. Then under these same assumptions we write instead of (5) and (6)

$$\delta_{\pm}^{(1)} = i \left[\frac{\pi p^2}{\eta |\eta|} \delta^{(0)4} \partial_p u_{\text{res}} - \xi \text{Re } \zeta / kb \ln b/a \right] / [\pm 2 \sqrt{\xi \beta^{-2} (\xi + \gamma^{-2})}], \quad (8)$$

$$\delta_{\pm}^{(1)} = [i\pi p^2 \delta^{(0)4} \partial_p u_{\text{res}} / \eta |\eta| - i \xi \text{Re } \zeta / kb \ln b/a]^{1/2}. \quad (9)$$

The instability threshold is determined from the condition that $\delta_{\pm}^{(1)}$ be real and for $-\xi \approx \gamma^{-2}$ has the form

$$\pi b \ln b / a k p^2 \xi^3 \partial_p \mu_{res} \gg |\eta| \eta Re \zeta.$$

In conclusion we consider some numerical examples. For the parameters of the electron storage ring at the Physicotechnical Institute of the Academy of Sciences of the Ukr SSR [4] with a reduced energy $\gamma \approx 100$ -200 the instability according to (7) develops for a density $\rho_0 \approx 10^{12} \text{ cm}^{-3}$. The growth rate close to the point $-\xi \approx \gamma^{-2}$, calculated from Eq. (6) for a normal momentum distribution with a relative spread $\langle \delta p^2 \rangle^{1/2} / p \approx 10^{-4}$, is 10^3 sec^{-1} . For a high-current electron storage ring [5] with $\gamma = 12$ and a design current $I = 10^3$ A inequality (7) is satisfied if the linear charge density $\pi a^2 \rho_0 \gtrsim 10^{11} \text{ cm}^{-1}$, which corresponds to a ring current $I \approx 500$ A.

LITERATURE CITED

1. A. A. Kolomenskii and A. N. Lebedev, Proceedings of an All-Union Conference on Charged Particle Accelerators [in Russian], VINITI, Moscow (1970), p. 261.
2. A. A. Kolomenskii and A. N. Lebedev, The Theory of Circular Accelerators [in Russian], Fizmatgiz, Moscow (1962), p. 145.
3. H. Bruck, Circular Charged Particle Accelerators [Russian translation], Atomizdat, Moscow (1970), p. 254.
4. Yu. N. Grigor'ev et al., Atomnaya Énergiya, 23, No. 6, 531 (1967).
5. I. Beal et al., Proc. of 8th Intern. Conf. on High-Energy Accelerators, CERN 1971, IAEA, Geneva (1971), p. 600.

EFFECT OF ENERGY DEGRADATION ON THE ENERGY
SPECTRUM OF FAST ELECTRONS IN MATTER

V. S. Remizovich

UDC 539.124.17

In passing through matter fast electrons lose their energy as a result of collisions with atomic electrons. For fast particles with a kinetic energy $T \gg I(Z)$, where $I(Z)$ is the ionization potential of the atoms of the medium, the distribution of particles in depth x and energy T was first obtained by Landau [1] for thin absorbers. In subsequent papers [2-4] refinements were introduced into Landau's theory taking account of scattering, radiation losses, the effect of density etc. In all these papers it was assumed that the energy loss

$$\Delta = T_0 - T \ll T_0 \quad (1)$$

is small. Here T_0 is the initial kinetic energy of the beam particles. It was assumed that the probability of energy loss per unit path length $w(T/\epsilon)$ is independent of the final energy: i. e.

$$w(T/\epsilon) \approx w(T_0/\epsilon), \quad (2)$$

where ϵ is the energy lost by a particle in one collision. Condition (2) is not satisfied at deep penetrations, and condition (1) is too general. Therefore it is desirable to define more accurately for just what energy losses Δ and to what depths the substitution (2) can be used in the transport equation, and also to refine the expression for the distribution function. To do this let us consider the next term in the expansion of the relaxation of the probability of energy loss

$$w(T/\epsilon) \approx w(T_0/\epsilon) - \Delta \frac{dw(T_0/\epsilon)}{dT_0} \quad (3)$$

which is accurate to terms of the order $\sim \Delta/T_0$. Then the transport equation can be written in the form

$$\begin{aligned} \frac{\partial N(x, \Delta)}{\partial x} = & -N \left[w(T_0) - \Delta \frac{dw}{dT_0} \right] + \int_0^\Delta d\epsilon w(T_0/\epsilon) N(x, T_0 - \epsilon) \\ & - \Delta \int_0^\Delta \frac{dw(T_0/\epsilon)}{dT_0} N(x, \Delta - \epsilon) d\epsilon + \int_0^\Delta \frac{dw(T_0/\epsilon)}{dT_0} \epsilon N(x, \Delta - \epsilon) d\epsilon; \end{aligned} \quad (4)$$

$$N(x=0, \Delta) = \delta(\Delta),$$

where $N = v(T)f(x, T)$ is the flux density of electrons of energy T at depth x , v is the velocity of the particles, and $f(x, T)$ describes the distribution in depth x and energy T . Equation (4) can be solved exactly by taking the Laplace transform with respect to Δ :

$$N(x, \Delta) = \frac{1}{2\pi i} \int_{-i\infty+\sigma}^{i\infty+\sigma} dp \exp \left\{ p\Delta - \int_{g(p, x)}^p dp' W(T_0/p') \left(\frac{dW(T_0/p')}{dT_0} \right)^{-1} \right\}, \quad (5)$$

where, as in [1],

$$W(T_0/p) = \int d\epsilon w(T_0/\epsilon) [1 - e^{-p\epsilon}], \quad (6)$$

and the function $g(p, x)$ is given by

$$\int_g^p dp' \left(\frac{dW(T_0/p')}{dT_0} \right)^{-1} = x. \quad (7)$$

Translated from *Atomnaya Energiya*, Vol. 37, No. 4, pp. 346-347, October, 1974. Original letter submitted December 11, 1973.

© 1975 Plenum Publishing Corporation, 227 West 17th Street, New York, N.Y. 10011. No part of this publication may be reproduced, stored in a retrieval system, or transmitted, in any form or by any means, electronic, mechanical, photocopying, microfilming, recording or otherwise, without written permission of the publisher. A copy of this article is available from the publisher for \$15.00.

The solution (5) is applicable in the nonrelativistic and relativistic cases. However, it is a priori evident that the nonrelativistic case $T \ll 1$ (the energy is measured in units of mc^2) is the most interesting. In this case the specific energy loss depends strongly on energy, $\bar{\varepsilon}(T) = (dT/dx)_{ion} \sim (1/T) \ln T_0$, and the effect of energy degradation begins to manifest itself at relatively small depths. In this case by using $W(T_0/\rho)$ from [1], and solving Eq. (7) we obtain from Eq. (5) the following expression for $N(x, \Delta)$:

$$N\left(\xi, \frac{\Delta}{T_0}\right) = \frac{1}{2\pi i} \int_{-i\infty+\sigma}^{i\infty+\sigma} ds \exp\left\{s \frac{\Delta}{T_0} + s[1 - \exp\{(1 - e^{-\xi})(L_i + 0.423 - \ln s)\}]\right\}, \quad (8)$$

where

$$\xi = \frac{x}{2R_0L_i} = \frac{\pi n_0 Z r_e^2}{T_0^2} x; \\ R_0 = \int_0^{T_0} \frac{dT}{\varepsilon(T)}; \quad L_i = \ln 1.34 \frac{T_0^2}{I^2(Z)}; \quad (9)$$

Z is the charge of the nucleus, r_e is the classical radius of the electron, n_0 is the atomic density of the medium, L_i is the ionization logarithm, and R_0 is the range of electrons of energy T_0 in the continuous loss approximation. In this notation Landau's solution has the form

$$N_L\left(\xi, \frac{\Delta}{T_0}\right) = \frac{1}{2\pi i} \int_{-i\infty+\sigma}^{i\infty+\sigma} ds \exp\left\{-s \frac{\Delta}{T_0} - s\xi(L_i + 0.423 - \ln s)\right\}. \quad (10)$$

Analysis shows that Eq. (8) goes over into (10) if

$$x \ll R_0/L_i; \quad \Delta \ll T_0/L_i. \quad (11)$$

We note that L_i is large in light elements. Thus for 50 keV electrons in helium $L_i \approx 15$. Conditions (11) define a domain of depths and effective energy losses where Landau's distribution can be used. In addition we see from Eq. (8) that the distribution obtained is not expressed in terms of any universal function, in contrast to Eq. (11) which is expressed in terms of the universal function [1] $\varphi_L(\lambda)$, where $\lambda = \lambda(\xi, \Delta)$. Thus the property of universality of the distribution function is not general, but is related only to the use of approximation (2). Numerical calculations performed by using Eq. (8) show that as the depth increases the energy spectrum is displaced into the region of larger energy losses Δ . The most probable value of the energy lost by particles increases with depth somewhat more rapidly than following from Eq. (10) since the slowing down power of the medium increases with a decrease in particle energy.

For relativistic electrons ($T \gg 1$) the refined distribution function (10), as before, is expressed in terms of a universal function

$$N\left(\xi, \frac{\Delta}{T_0}\right) = \frac{2}{1 - e^{-2\xi}} \varphi_L(\lambda), \quad (12)$$

where

$$\xi = \frac{x}{R_0L_i} = \frac{2\pi n_0 Z r_e^2}{T_0} x,$$

and the parameter λ is defined by

$$\lambda\left(\xi, \frac{\Delta}{T_0}\right) = \frac{2 \frac{\Delta}{T_0} + [1 - e^{-2\xi} - 2\xi e^{-2\xi}]}{1 - \exp(-2\xi)} - \left[L_i + 0.423 + \ln \frac{1 - e^{-2\xi}}{2}\right], \quad (13)$$

which for $\xi \ll 1$ goes over into the familiar expression for λ_L

$$\lambda_L\left(\xi, \frac{\Delta}{T_0}\right) = \frac{\Delta}{T_0} - [L_i + 0.423 + \ln \xi]. \quad (14)$$

The author thanks A. S. Kompaneits and M. I. Ryazanov for their interest in the work and for helpful comments.

LITERATURE CITED

1. L. D. Landau, Ionization Losses of Fast Particles [in Russian], Collected Works, Vol. 1, Nauka, Moscow (1969).

2. F. Ziemia et al. , Phys. Rev. , 118, 1552 (1960).
3. O. Blunck, Z. Phys. , 130, 641 (1951).
4. E. Goldwasser et al. , Phys. Rev. , 88, 1137 (1952).

SPECIFIC HEATS OF YTTRIUM AND GADOLINIUM AT HIGH TEMPERATURES

I. I. Novikov and I. P. Mardynkin

UDC 536.63

The prospect of using elements of the lanthanum series in nuclear power installations [1, 2] necessitates an investigation of their properties over a wide range of temperatures. The experimental studies of these elements have been confined to a small number of the metals and to limited temperature ranges. The published data in a number of cases differ by more than the total systematic errors and are often contradictory [1-3].

There is practically no information on the thermal properties of the heavy lanthanides of the yttrium subgroup at high temperatures.

Measurements of the specific heats of yttrium and gadolinium in the 1100-1800°K temperature range, including the liquid phase for gadolinium, were undertaken as a part of the ongoing investigation of the thermal and electrical properties of the lanthanides [3].

The specific heat at constant pressure C_p was measured with apparatus based on one of the various regular thermal regimes of the third kind — the method of radial temperature waves [4]. These studies were performed simultaneously with measurements of the theoretic conductivity.

In the variant of this method used [3] measurements of C_p are reduced to measurements of the amplitude of the temperature oscillations of the outer surface of a hollow cylindrical sample. These oscillations are produced by modulating the inner surface of the sample, or crucible in the study of liquid metals, by electron heating. The systematic error of the data on the volumetric heat capability is ~7%.

The specific heat of yttrium was measured because of the divergence of the estimated and experimental values [5] noted in [3]. The specific heats of yttrium [5] and gadolinium [6] have also been measured by the method of mixtures. It is interesting to compare these results with data obtained by the method of radial temperature waves.

Experiments were performed in vacuo (10^{-5} - 10^{-4} torr) on samples of 99.8% pure yttrium and 99.75%

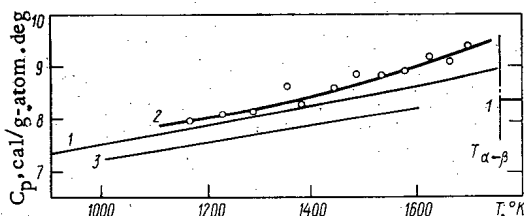


Fig. 1

Fig. 1. Specific heat of α yttrium at high temperatures. 1) Data from [5]; 2) our data; 3) estimate from [9].

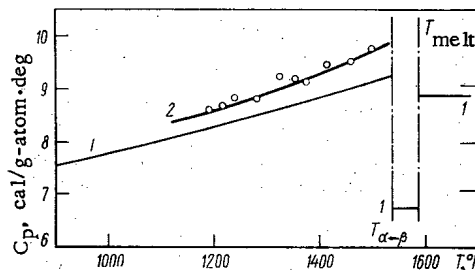


Fig. 2

Fig. 2. Specific heat of gadolinium at high temperatures. 1) Data from [6]; 2) our data.

Translated from *Atomnaya Energiya*, Vol. 37, No. 4, pp. 348-349, October, 1974. Original letter submitted December 17, 1973.

© 1975 Plenum Publishing Corporation, 227 West 17th Street, New York, N.Y. 10011. No part of this publication may be reproduced, stored in a retrieval system, or transmitted, in any form or by any means, electronic, mechanical, photocopying, microfilming, recording or otherwise, without written permission of the publisher. A copy of this article is available from the publisher for \$15.00.

TABLE 1. Volumetric Heat Capacity of Liquid Gadolinium

T, °K	C, cal/cm ³ ·deg	T, °K	C, cal/cm ³ ·deg
1600	0,442	1750	0,438
1650	0,440	1800	0,435
1700	0,440		

pure gadolinium in the form of hollow cylinders 7 cm long having outside diameters of ~15 mm and inside diameters of ~6 mm.

The percentages of the impurities in yttrium were: Gd, Tb, Dy, Ho < 0.1; Fe < 0.01; Ca < 0.03; Cu < 0.05; Ta ~ 0.06; in gadolinium: Y ~ 0.08; Tb ~ 0.07; Eu ~ 0.04; Cu ~ 0.025; Fe ~ 0.02; Ca < 0.004.

A polymorphic α - β phase change occurs in gadolinium at ~1535°K and in yttrium at ~1760°K. The resulting softening of the samples made it impossible to obtain stable results for the β phase. The results obtained for the α phase of the metals studied are shown in Figs. 1 and 2.

The mean-square deviation of the experimental points from the smoothed values (curve 2 of Figs. 1 and 2) is ~4%, which agrees with the estimated values of the random errors.

The values of C_p were determined by using the values of the density ρ measured in the 300-1200°K range for yttrium, and in the 200-920°K range for gadolinium [7]. Since no polymorphic transformations are observed in the 1100-1500°K range for gadolinium, and up to ~1750°K for yttrium, the density was estimated by interpolation relations [7].

Table 1 lists values of the volumetric heat capacity of liquid gadolinium. The data on the heat capacity of α yttrium for $T > 1100^\circ\text{K}$ agree with the results obtained by the method of mixtures [5].

The data on the heat capacity of α gadolinium in the 1150-1500°K range are 6-8% higher than the published values [6]. This difference is close to the total systematic error.

The extrapolation of the data to lower temperatures leads to results in agreement with [8].

The lattice, electronic, and other contributions to the specific heat of α gadolinium at 400 and 1000°K calculated in the same way as for yttrium at 1000°K are shown in Table 2.

It should be noted that the almost total lack of data on the physical and chemical properties of gadolinium, particularly at high temperatures, necessitates purely qualitative estimates. This applies particularly to an estimate of the contribution of the f electrons which is performed primarily to determine the characteristics of the lanthanides in comparison with elements of nontransition groups.

The analysis of the specific heat is based on the assumption that the value of C for $T > \theta_D$, where θ_D is the Debye temperature, is described by the expression

$$C = C_v^0 + C_{el} + \delta C + C', \quad (1)$$

where C_v^0 is the lattice specific heat at constant volume, C_{el} is the electronic specific heat, δC is defined by the relation $\delta C = (\alpha^2 V / \beta_T) T$, where α is the volume coefficient of expansion, V is the atomic volume, β_T is the isothermal compressibility, C' is the contribution from the formation of thermal vacancies and from anharmonic vibrations. C_v^0 is computed in the Debye approximation.

The lack of published information on β_T for gadolinium at high temperatures makes it impossible to determine δC directly. The Nernst-Lindemann relation $\delta C = A C_p^2 T$, where A is a parameter, was used to estimate δC . A is approximately constant over a wide range of temperature [9]. The contribution of the conduction electrons, C_{el}^{con} is estimated by the standard method.

The value of the coefficient in the expansion for the electronic specific heat of γ gadolinium in the paramagnetic region agrees closely with the values for other lanthanides [9-11]. In analyzing the electronic specific heat of gadolinium there is the problem of determining the contributions of the 4f electrons, C_{el}^f ,

TABLE 2. Calculated Contributions to the Specific Heat of Gadolinium

θ_D , °K	$A \cdot 10^6$, g-atom/cal	C_p , cal/g-atom·deg		C_v^0 , T = 400°K	δC		C_{el}^{con}	
		T = 400°K [8]	T = 1000°K [6]		T = 400°K	T = 1000°K	T = 400°K	T = 1000°K
173	1,48	6,9	7,75	5,92	0,03	0,11	1,15	2,87

related to the transition of these electrons to higher energy levels of the multiplet, to levels formed as a result of the ground-state splitting in the trivalent Gd^{3+} ion in the field of the crystal lattice [12].

It has been established that this contribution can be appreciable at $\sim 1000^\circ K$ and higher in cerium, neodymium, and samarium [13, 14]. The value of C_{el}^f for gadolinium cannot be calculated directly because of a lack of the necessary data. Attempts to estimate C_{el}^f by starting from the experimental values of C_p and the calculated values of C_v^0 , C_{el}^{con} , and δC given in Table 2 do not give acceptable results.

Thus the procedure which generally satisfactorily describes the experimental data for other (light) lanthanides is inadequate for gadolinium. There are other anomalies characteristic of gadolinium [2]. A satisfactory explanation of this fact has not yet been found.

LITERATURE CITED

1. F. Spedding and A. Daane, Rare Earth Metals, in: Progress in Nuclear Energy, Vol. 1, Pergamon, New York (1956).
2. K. Taylor and M. Darby, The Physics of Rare Earth Solids, Halsted, New York (1972).
3. I. I. Novikov and I. P. Mardykin, Teplofiz. Vys. Temp., 11, 527 (1973).
4. L. P. Filippov, Measurement of the Thermal Properties of Solid and Liquid Metals at High Temperatures [in Russian], MGU, Moscow (1967).
5. J. Berg, F. Spedding, and A. Daane, US AEC Doc., No. IS-327 (1968).
6. D. Dennison, K. Gschneidner, and A. Daane, J. Chem. Phys., 44, 4273 (1966).
7. F. Spedding, J. Hanak, and A. Daane, J. Less Common Metals, 3, 110 (1961).
8. M. Griffel, R. Skochdopole, and F. Spedding, Phys. Rev., 93, 657 (1954).
9. K. Gschneidner, Solid State Phys., 16, 275 (1964).
10. I. I. Novikov and I. P. Mardykin, Teplofiz. Vys. Temp., 12 (1974).
11. I. P. Mardykin, V. I. Kashin, and P. P. Sbitnev, Izv. AN SSSR, Metally, 6, 78 (1973).
12. B. Wybourne, Phys. Rev., 148, 317 (1966).
13. S. Arajs and R. Colvin, J. Less Common Metals, 4, 159 (1962).
14. F. Spedding, J. MacKeown, and A. Daane, J. Phys. Chem., 64, 289 (1960).

THE METHOD OF RECURSIVE SUMS AND INTEGRALS
FOR SOLVING MULTIGROUP NEUTRON DIFFUSION
EQUATIONS

V. Yu. Vasil'ev and A. D. Dymnikov

UDC 539.125.5.172:621.039.512.4

We present a method for calculating the spatial distribution of one-dimensional group neutron fluxes and currents based on writing the solution of a standard system of equations equivalent to the initial system of diffusion equations as nonlinear recursive integrals. Such integrals are similar to ordinary integrals (linear quadratures) and are in fact nonlinear quadratures. This way of writing facilitates the solution of multizone problems, some problems of optimization, perturbation theory problems etc.

The multigroup neutron diffusion equations in a reactor, written in vector-matrix form

$$\frac{d}{dr} \left[r^\alpha D(r) \frac{d}{dr} \Phi(r) \right] = r^\alpha [\Sigma(r) - \lambda F(r)] \Phi(r), \quad (1)$$

$$r \in [r_0, r_n], \quad \alpha = 0, 1, 2,$$

are transformed to the standard form

$$\frac{d}{dr} X(r) = T(r, \lambda) X(r), \quad (2)$$

by the substitutions

$$X(r) = \begin{pmatrix} X_1(r) \\ X_2(r) \end{pmatrix} = \begin{pmatrix} r^\alpha D(r) \frac{d}{dr} \Phi(r) \\ \Phi(r) \end{pmatrix}; \quad (3)$$

$$T(r, \lambda) = \begin{pmatrix} 0 & T_{12}(r, \lambda) \\ T_{21}(r) & 0 \end{pmatrix}; \quad (4)$$

$$T_{12}(r, \lambda) = r^\alpha [\Sigma(r) - \lambda F(r)]; \quad (5)$$

$$T_{21}(r) = r^{-\alpha} D^{-1}(r).$$

Here $\Phi(r)$ is a vector-function whose components $\varphi_l(r)$ describe the group neutron fluxes, $D(r)$ is the diffusion coefficient matrix, $\Sigma(r)$ is the group removal cross sections and intergroup transfer cross sections matrix, $F(r) = \{\chi_l [\nu \Sigma_f(r)]_k\}$, ($l, k = 1, 2, \dots, N$), λ is the eigenvalue of the problem $\lambda_{\min} = 1/K_{\text{eff}}$. The rest of the notation is standard.

It is assumed that the neutron group cross sections are piecewise continuous functions of the coordinate and satisfy the boundary conditions

$$X_1(r_0) = X_{10} = 0, \quad X_2(r_n) = X_{2n} = 0 \quad (6)$$

or for a plane region without symmetry with respect to the center

$$X_2(r_0) = X_{20} = 0, \quad X_2(r_n) = X_{2n} = 0. \quad (7)$$

The solution of Eq. (2) has the form

$$\begin{pmatrix} X_1(r) \\ X_2(r) \end{pmatrix} = R(r/r_0) \begin{pmatrix} X_{10} \\ X_{20} \end{pmatrix},$$

$$R(r/r_0) = \begin{pmatrix} R_{11}(r/r_0) & R_{12}(r/r_0) \\ R_{21}(r/r_0) & R_{22}(r/r_0) \end{pmatrix}, \quad (8)$$

Translated from *Atomnaya Energiya*, Vol. 37, No. 4, pp. 350-351, October, 1974. Original letter submitted December 13, 1973.

© 1975 Plenum Publishing Corporation, 227 West 17th Street, New York, N.Y. 10011. No part of this publication may be reproduced, stored in a retrieval system, or transmitted, in any form or by any means, electronic, mechanical, photocopying, microfilming, recording or otherwise, without written permission of the publisher. A copy of this article is available from the publisher for \$15.00.

where the elements of the matrizant $R_{pt}(r/r_0)$ ($p, t = 1, 2$) are $N \times N$ matrices and the matrizant itself satisfies the matrix differential equation

$$\frac{d}{dr} R(r/r_0) = T(r, \lambda) R(r/r_0), \quad R(r_0/r_0) = E. \quad (9)$$

By substituting (6) into (8) we obtain an equation for λ :

$$|R_{22}(r_n/r_0)| = 0. \quad (10)$$

Similarly for condition (7) we have

$$|R_{21}(r_n/r_0)| = 0. \quad (11)$$

We now write the solution for $R_{pt}(r/r_0)$ in the form of nonlinear recursive integrals. We introduce the ordered sequence of m elements a_i ($i = 1, 2, \dots, m$). We divide the domain of the argument r in Eq. (2) into n parts (generally unequal), and denote the matrix-function $T(r, \lambda)$ at a certain point ξ_j of the j -th interval ($j = 1, 2, \dots, n$) by $T(\xi_j, \lambda) = T(j, \lambda)$ where $\xi_j \in (r_{j-1}, r_j)$. We assume that all points of discontinuity of the function $T(r, \lambda)$ are among the points of subdivision. We choose the elements of the sequence in the form

$$a_{2j+1} = (1-\kappa) T_{n_1 n_2}(j) \Delta r_j + \kappa T_{n_1 n_2}(j+1) \Delta r_{j+1}; \quad (12)$$

$$a_{2j} = T_{n_2 n_1}(j) \Delta r_j.$$

Here κ is an arbitrary real parameter generally chosen close to 0.5 in practice. The subscripts n_1 and n_2 form one of the two possible combinations: $n_1 = 1, n_2 = 2$; $n_2 = 1, n_1 = 2$.

We call the recursive operation S_k^m on the elements of our sequence of recursive sum from k to m and define it as

$$S_k^m = a_m S_k^{m-1} + S_k^{m-2}; \quad S_k^{k-1} = E; \quad S_k^{k-2} = 0. \quad (13)$$

With the notation $R_{n_p n_t}(r_j/r_0) = R_{n_p n_t}(j)$ for the matrix elements we write Eq. (9) in the following difference approximation:

$$\bar{R}_{n_p n_t}(j) - \bar{R}_{n_p n_t}(j-1) = \Delta r_j \sum_{s=1}^2 \{ (1-\delta_{1p}) T_{n_p n_s}(j) \bar{R}_{n_s n_t}(j) + \delta_{1p} T_{n_p n_s}((1-\kappa) \bar{R}_{n_s n_t}(j) + \kappa \bar{R}_{n_s n_t}(j-1)) \}; \quad (14)$$

$$(p, t = 1, 2).$$

$$R_{n_p n_t}(j) = \lim_{\substack{\Delta r_j \rightarrow 0 \\ i \rightarrow \infty}} \bar{R}_{n_p n_t}(j); \quad (i = 1, 2, \dots, j).$$

Here δ_{1p} is the Kronecker symbol. It can be shown that this equation is solved by recursive sums:

$$\bar{R}_{n_p n_t}(j) = S_{3-t}^{2j+2-p}. \quad (15)$$

It should be noted that in evaluating the recursive sum for $\bar{R}_{n_p n_t}(j)$ it is necessary to set $\Delta r_0 = \Delta r_{j+1} = 0$ ($j = 0, 1, 2, \dots, n$).

We call the limit of the recursive sum S_{3-t}^{2n+2-p} as $n \rightarrow \infty$ ($\Delta r_j \rightarrow 0$) the Riemann pt recursive integral [1] and denote it by

$$\lim_{\Delta r_j \rightarrow 0} S_{3-t}^{2n+2-p} = \langle pt | \int_{r_0}^r T(r) dr. \quad (16)$$

As $\Delta r_j \rightarrow 0$ ($n \rightarrow \infty$) the difference equation (14) goes over into Eq. (9), and the matrix elements of the matrizant can be written as recursive integrals

$$R_{n_p n_t}(r/r_0) = \langle pt | \int_{r_0}^r T(r) dr. \quad (17)$$

We note that the multiplicative integral [2] which is also a solution of Eq. (9), corresponds to the Euler difference scheme

$$\bar{R}(j) - \bar{R}(j-1) = \Delta r_j T(j) \bar{R}(j-1). \quad (18)$$

A comparison of schemes (14) and (18) shows that the first should converge more rapidly. Actually

a numerical realization showed that for a homogeneous reactor ($\alpha = 0, 1, 2$) the relative error in λ is proportional to $1/n^{1.9-2.0}$ and in the neutron flux distribution $|1 - \frac{\sum_j \varphi(j)}{\sum_j \varphi^{\text{exact}}(j)}| \sim 1/n^{1.7-2.1}$. It should be noted that even for a small number the method of nodes gives a reasonable approximation. Thus for a homogeneous reactor the solution of Eq. (10) for $n = 1$ ($N = 1, 2$) leads to an expression for K_{eff} which is well known from general theory [3], with the geometrical buckling $B^2 = 2/R^2$ for all α . An increase in n gives a better value of B^2 . Therefore for a large core where B^2 is small the convergence is more rapid than for a small core. It is easy to see also that the amount of calculation is determined only by the number of nodes, and does not depend on the number of discontinuities in the macroscopic cross sections. The continuity conditions at the surfaces of discontinuity are satisfied automatically.

The first step in solving Eq. (2) is to find λ_{min} from the critical conditions (10) or (11). Then the components of the vectors X_{20} and X_{10} are determined from the appropriate linear systems. Then it is possible to proceed to the calculation of the spatial shape of the neutron flux or current from Eq. (15). Here for convenience in constructing the program it is necessary to choose in each case the one of two possible algorithms which is not related to the calculation of the $(2j + 1)$ -th element a_{2j+1} .

It is important to note that the algorithm of the recursive sums preserves the Wronskian of system (2) equal to unity in each elementary interval.

The recursive sums (13) have useful properties permitting various analytic transformations such as differentiation with respect to any of its elements, resolution into partial recursive sums etc. These properties facilitate the analysis of problems and give the solution certain advantages generally characteristic of solutions in explicit form.

LITERATURE CITED

1. A. D. Dymnikov, in: Abstracts of Papers Presented at the Second Ukrainian Conference on Electron Optics and Its Applications [in Russian], IRE AN UkrSSR, Kharkov (1971), p. 31.
2. F. R. Gantmacher, The Theory of Matrices, Chelsea, New York (1959).
3. R. Megreblain and D. Holmes, Reactor Analysis, McGraw-Hill, New York (1960).

TEMPERATURE DEPENDENCE OF TOTAL COLD NEUTRON
CROSS SECTION IN LIGHT WATER AND BENZENE

S. B. Stepanov, V. E. Zhitarev,
F. M. Zelenyuk, and V. Ya. Krasil'nikov

UDC 539.171.02;162.2

A comparison of an experimentally measured total scattering cross section with a calculated cross section based on some scattering model can serve as a supplementary, and often very useful check on the correctness of the approximations used in construction of the model. Unfortunately, such a comparison is usually limited to the neutron energy region above 10^{-3} eV ($\lambda \approx 9$ Å) and to scatterer temperatures of $\sim 293^\circ\text{K}$. At the same time, it is precisely in the description of the scattering of long-wave neutrons that great difficulty arises and a definite tendency toward divergence of theoretical and experimental data is noted. The latter also applies to the temperature dependence of the cross sections. This situation mainly results from the sparseness of experimental material in the region of low neutron energies and over a broad temperature range.

The aim of the present work is to fill this gap partially. The total interaction cross section in water and benzene was measured for fluid temperatures of 294–523 and 295–543°K respectively for neutrons of wavelengths 8–14 Å ($E = 0.00128$ – 0.000420 eV).

The cross section was determined from measurements of sample transmission for a given material. Measurements were made with equipment set up at the IRT reactor of the Moscow Engineering Physics Institute [1].

A doubly-bent copper neutron pipe was used as a neutron filter with a limiting wavelength $\lambda_l \approx 6.5$ Å

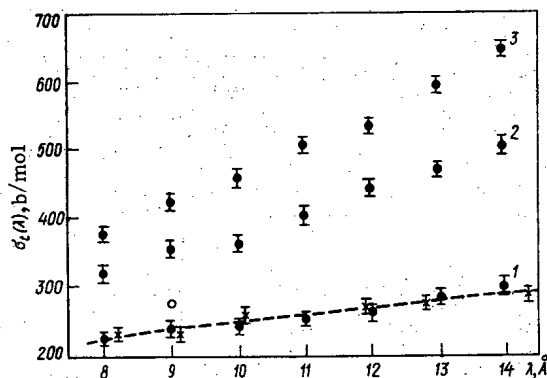


Fig. 1

Fig. 1. Total interaction cross section for water: \bullet) present work; 1) $T = 294^\circ\text{K}$; 2) $T = 453^\circ\text{K}$; 3) $T = 532^\circ\text{K}$; ---) atlas [3]; \times) data from [7]; \circ) calculation [5] for $T = 550^\circ\text{K}$.

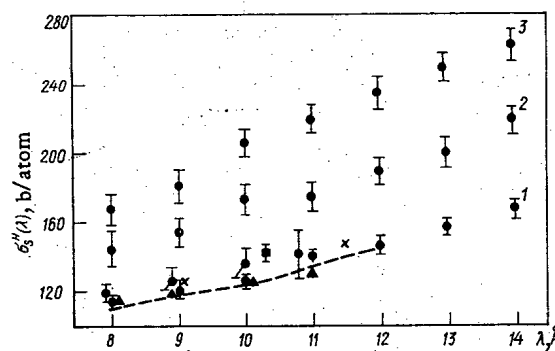


Fig. 2

Fig. 2. Scattering cross section per hydrogen atom for benzene: \bullet) present work; 1) $T = 295^\circ\text{K}$; 2) $T = 453^\circ\text{K}$; 3) $T = 543^\circ\text{K}$; \blacktriangle , \blacksquare) experiment [4, 7], $T = 294$ – 296°K ; upper points \bullet 8–11 Å at 295°K [8]; ---) calculation based on the Krieger–Nelkin model [4], $T = 295^\circ\text{K}$; \times) calculation [6], $T = 295^\circ\text{K}$.

Translated from *Atomnaya Energiya*, Vol. 37, No. 4, pp. 351–353, October, 1974. Original letter submitted December 27, 1973.

© 1975 Plenum Publishing Corporation, 227 West 17th Street, New York, N.Y. 10011. No part of this publication may be reproduced, stored in a retrieval system, or transmitted, in any form or by any means, electronic, mechanical, photocopying, microfilming, recording or otherwise, without written permission of the publisher. A copy of this article is available from the publisher for \$15.00.

TABLE 1. Total Interaction Cross Section for Water, b

Temperature, °K	$\lambda, \text{Å}$						
	8	9	10	11	12	13	14
294	222±8	241±11	242±10	253±9	260±10	286±12	299±12
403	311±13	321±15	335±11	380±14	390±11	396±11	434±10
453	317±13	357±11	363±11	405±14	446±11	468±12	507±14
488	362±8	382±7	433±9	463±10	500±7	537±7	574±8
523	377±11	423±12	460±14	507±10	536±10	594±11	647±10

TABLE 2. Total Interaction Cross Section for Benzene, b

Temperature, °K	$\lambda, \text{Å}$						
	8	9	10	11	12	13	14
295	694±25	736±30	769±20	848±25	893±30	960±30	1024±30
348	800±40	857±20	870±40	906±30	980±40	1030±40	1105±35
403	800±30	858±40	928±30	968±30	1094±25	1126±40	11266±40
453	897±57	931±47	1050±54	1060±30	1156±40	1280±47	1345±40
488	852±40	1013±40	1084±40	1161±40	1263±40	1351±40	1390±55
523	910±30	1060±40	1220±40	1235±40	1330±40	1450±30	1560±30
543	1012±59	1100±63	1253±50	1340±48	1431±58	1527±48	1603±63

and a crystal monochromator made of a fluorophlogopite plate ($2d_{001} = 19.97 \text{ Å}$) was used to select monochromatic neutrons [2]. The wavelength resolution of the device was about 3% over the entire range covered.

The samples studied were placed in the neutron beam after it emerged from the neutron pipe. The samples were in a hermetically sealed, electrically heated container. The body of the container was made of stainless steel. Two plane-parallel aluminum-alloy disks sealed with Teflon gaskets were inserted in the central portion of the body perpendicularly to the axis of the neutron beam. The disks were separated by a ring which created the required gap for the liquid sample under study; a thermocouple was located in the gap. The size of the gap was 1 and 1.5 mm for water and 1.5 and 2 mm for benzene to an accuracy of ± 0.01 mm. Sample transmission varied from 0.1-0.6. The thickness of the aluminum disks was selected in accordance with the pressure within the container — up to 15 mm. The transmission of the empty container was 0.5-0.9. The thermal expansion of the gap with change in temperature was taken into account in the calculations, but it had practically no effect on the results because of its smallness. The uncertainty in the temperature was no more than 3° in all measurements.

A counter filled with a mixture of 97% ^3He and 3% Ar was used as a neutron detector.

Figure 1 shows the dependence of the total interaction cross section $\sigma_t(\lambda)$ for water at three sample temperatures. Also shown are experimental and theoretical data from other authors.

Based on the measured total cross sections for benzene molecules, the scattering cross section per hydrogen atom in benzene, σ_s^H , was calculated. In such calculations, the following procedure is usually used: subtraction from the experimentally measured total interaction cross section for a molecule of the absorption cross section of hydrogen and of the total cross section of carbon, each multiplied by the corresponding number of atoms in the molecule, and subsequent division of the result by the number of hydrogen atoms. Such an operation was justified in this case by the need for a comparison with the results of others and by the smallness of the contribution to the cross section from carbon and absorption in hydrogen (less than 2%). The total cross section for carbon atoms and for absorption in hydrogen was taken into account by using the data in [3]. The dependence $\sigma_s^H(\lambda)$ at three temperatures is shown in Fig. 2 together with other results.

The error in the values obtained for the cross sections including uncertainties in sample thickness varied within the limits of 1.5-6%. The complete results are shown in Tables 1 and 2.

The figures indicate a marked rise in the cross sections for water and benzene with temperature. However, the slope of the dependence for benzene varies considerably less. A qualitative connection between the slope and the nature of the dynamics of the scatterer established in [4] can be explained by the existence in water of a strong intermolecular interaction leading to the formation of a complex structure which determines the formation of the low-energy portion of the frequency spectrum. The excitation of this spectral region at elevated temperatures strongly affects the scattering of the longer wavelength neutrons.

The agreement between the different experimental results and between experimental and calculated results is satisfactory at room temperature. However, calculated data for water at 550° K [5] differ greatly from the present results (see Fig. 1). For benzene, there is a calculation [6] at 295° K based on the model of a free gas of semirigid molecules covering the neutron energy range 0.00062-1.0 eV. The excellent agreement between theoretical and experimental data for liquid benzene confirms the concept of weak intermolecular interaction in benzene. How well the model can describe the temperature dependence of the cross section is unclear, however.

From the data given, there is an obvious interest in the comparison of experimental and theoretical data in the low-energy region ($E < 10^{-3}$ eV) over a broad temperature range. It arises out of the lack of such a possibility at the present time and from the divergence of such results as do exist. This situation ought to stimulate the performance of calculations and experiments under the conditions specified.

LITERATURE CITED

1. V. E. Zhitarev et al., *Pribory i Tekh. Éksperim.*, No. 4, 43 (1973).
2. F. M. Zelenyuk et al., *idem*, No. 2, 57.
3. D. J. Hughes and R. B. Schwartz, *Atlas of Neutron Cross Sections* [Russian translation], 2nd Ed., Atomizdat, Moscow (1959).
4. J. Rush et al., *J. Chem. Phys.*, 37, 243 (1962).
5. B. K. Haywood and D. I. Page, *Slow-Neutron Spectra* [Russian translation], Atomizdat, Moscow (1971), p. 74.
6. R. S. Marsden and H. L. MacMurray, *idem*, p. 142.
7. K. Heinloth, *Z. Phys.*, 163, 218 (1961).
8. B. Antonini et al., *Physica*, 32, 119 (1968).

COMPARISON OF ACCIDENT DOSIMETRY SYSTEMS AT HPRR

I. B. Keirim-Markus, V. A. Knyazev,
and S. N. Kraitor

UDC 539.12.02

To select the dosimeter most suitable for providing accident monitoring of personnel, a cycle of international comparisons of accident dosimetry systems was carried out under the auspices of the IAEA. A second comparison was made in 1971 at Oak Ridge (USA) at the pulsed reactor HPRR [1]. Specialists from 12 countries participated in this comparison including those from Great Britain, Canada, USSR, USA, France, and others; from the USSR, there were specialists from the Institute of Biophysics of the USSR Ministry of Public Health (IBF), from FÉI, and from GKAÉ USSR.

At the present time, final results of the comparison have been published [2-5]. It is of interest to compare them and to determine the state of personnel accident dosimetry.

Various kinds of accident dosimeters were represented at Oak Ridge. Thermoluminescent, photoluminescent, and film dosimeters were used for gamma dosimetry. Neutron dosimeters were based on the use of activation and track detectors. At the same time, there was a comparison of the measurement of neutron kerma with area dosimeters and spectrometric sets of resonance and threshold detectors.

IBF was represented in the comparison by the IKS-A personnel accident gamma dosimeter [6], by the neutron track dosimeter DINA [7], and by the neutron spectrometer DISNEI [8] based on fissile isotopes; FÉI was represented by the personnel accident gamma-neutron dosimeters AIDA [9] and TIDA [10] in which the IKS-A gamma dosimeters are also used.

The dosimetric systems were irradiated at 3 m from the center of the reactor core. Furthermore, the dosimeters were located both in air and on the surface of phantoms. There was a total of four pulsed irradiations in two of which (first and fourth) there was no shielding; the second was performed behind an iron shield 13 cm thick and the third behind a plastic shield 12 cm thick. The shielding was 2 m from the center of the core.

For a quantitative evaluation of the results of the comparison, the average and maximum errors

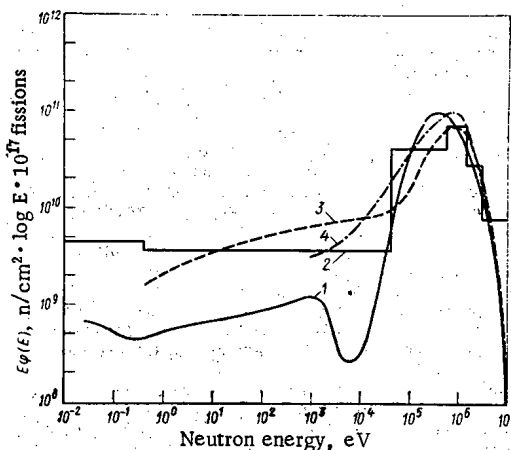


Fig. 1. Spectrum of HPRR neutrons outside an iron shield by calculation (1) as measured by the neutron spectrometers DISNEI (2) and SNAC (3), and as measured with a set of threshold detectors using iteration analysis (4).

Translated from *Atomnaya Énergiya*, Vol. 37, No. 4, pp. 353-356, October, 1974. Original letter submitted January 7, 1974.

© 1975 Plenum Publishing Corporation, 227 West 17th Street, New York, N.Y. 10011. No part of this publication may be reproduced, stored in a retrieval system, or transmitted, in any form or by any means, electronic, mechanical, photocopying, microfilming, recording or otherwise, without written permission of the publisher. A copy of this article is available from the publisher for \$15.00.

TABLE 1. Maximum Measurement Error for Accident Dosimetric Systems, %

Country	Neutron spectrometers, threshold detector sets, area dosimeters	Personnel neutron dosimeters	Personnel gamma dosimeters
Canada (AECL)	0 to +13	-21 to -1,8	-25 to +17
Great Britain (AERE)	-2,2 to +15	-34 to +19	+7,0 to +57
France (CEA)	-20 to +0,8	-0,5 to +19	-24 to -6,3
Czechoslovakia	-2,0 to +40	—	-4,2 to +23
Hungary	-43 to -17	-28 to +18	-15 to +28
India	-65 to -18	-70 to +13	-12 to +14
Italy	-8,7 to +96	-7,0 to -120	-1,3 to +22
West Germany	-7,8 to +31	-15 to +26	—
Poland	-49 to +6,4	-70 to -26	-26 to +13
USA (SRL)	-24 to +6,0	—	-33 to +13
USA (1)	—	—	-14 to +26
USA (2), ORNL	-9,0 to -1,9	—	-2,1 to +6,9
USSR (1), IBF	-6,7 to +5,0	+1,2 to +9,8	-12 to +6,3
USSR (2), FEI	-15 to +2,3	-20 to +8,5	-6,9 to -1,9
Jugoslavia	-14 to +25	+2,3 to +23	-12 to -1,6

TABLE 2. Average Measurement Error for Accident Dosimetric Systems, %

Country	Neutron spectrometers, threshold detector sets, area dosimeters	Personnel neutron dosimeters	Personnel gamma dosimeters
Canada (AECL)	5,2	10	13
Great Britain (AERE)	6,8	20	29
France (CEA)	9,1	15	17
Czechoslovakia	17	—	10
Hungary	21	18	13
India	32	32	6,9
Italy	35	48	23
West Germany	14	15	8,2
Poland	59	50	15
USA (SRL)	11	—	18
USA (1)	—	—	12
USA (2), ORNL	5,0	—	3,0
USSR (1), IBF	5,2	5,1	7,0
USSR (2), FEI	11	10	4,4
Jugoslavia	15	11	4,2

were calculated for measurements of neutron kerma and gamma dose by the various dosimeters for all measurements during three of the pulses (soviet specialists did not participate in the experiments during the first pulse and therefore the corresponding data were obtained from that for the fourth pulse by conversion relative to the number of fissions per pulse). The errors were determined with respect to the average value for each pulse based on the measurement results for all dosimeters with the exception of isolated deviations in neutron measurements (for example, the Polish data for the first pulse and the Italian data for the third pulse). In addition, in measurements behind the iron shield, the average value of neutron kerma in air was determined from the spectrometric detector sets submitted by Great Britain, Canada, USSR, USA, and France. In the method of analysis used by their specialists, there is no assumption about the Fermi nature of the neutron spectrum in the energy region 0.4 eV to 0.7 MeV, which can lead to a large underestimate of the dose. The results of the calculations are shown in Tables 1 and 2.

The tables indicate that the errors are basically within the limits of $\pm 20\%$ although there are also rather significant deviations (60-120%). This is more clearly visualized in Table 3 where the results of measurements in air are shown along with the region of 10% deviation from the average value. The spread of the readings may be associated with dosimeter characteristics, calibration with different sources, and nonequivalent locations of the dosimeters.

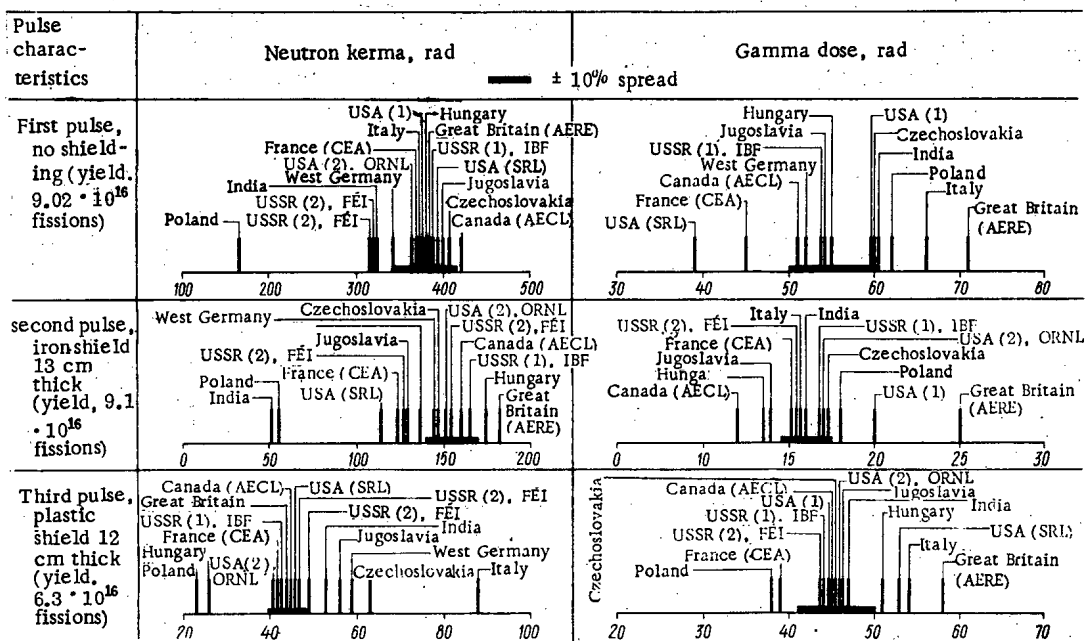
Of the neutron spectrometric systems, the least error in measurement of neutron kerma was noted for the various versions of the Hurst set of threshold detectors [11] submitted by Great Britain, USSR (IBF), and USA (ORNL) when modern methods of analysis for determination of the readings were used (for example, the modified method of effective cross section and threshold energy [12] or iteration [13]). The average error for these spectrometers was no more than 5-7%, and the maximum error was 7-15%. Approximately the same error applied to the SNAC activation spectrometer (France) and the set of detectors submitted by the Canadians, which included isomeric rhodium and indium detectors.

As an example, we show in Fig. 1 the results of measurements by different methods of neutron spectra in air behind an iron shield 13 cm thick [4, 13, 14] normalized to 10^{17} fissions per pulse. A calculated spectrum [5] is also shown for comparison. It is clear that the calculated and measured results are in good agreement in the neutron region above ~ 100 keV. At the same time, all the measured spectra are above the calculated spectrum for slow and intermediate neutrons. This is because the scattering of neutrons by surrounding objects, equipment, phantoms, etc. was not taken into account in the calculation.

Of the personnel neutron dosimeters, the DINA dosimeter consisting of ^{237}Np behind a filter of 0.1 g/cm² of ^{10}B and ^{235}U together with track detectors exhibited the greatest accuracy.

The gamma dose was measured most accurately with thermoluminescent and photoluminescent dosimeters submitted by the USSR (IKS-A) and by the USA (ORNL dosimeters) and by the film dosimeters used in Jugoslavia.

TABLE 3. Measurement of Neutron Kerma and Gamma Dose in Air for Various Dosimetric Systems



We note with satisfaction that our dosimetric systems were among the best.

The comparisons indicate that at the present time there are dosimeters for the measurement of gamma—neutron radiation doses in accident situations. In the choice of gamma dosimeters, preference should be given to glass thermoluminescent (IKS-A) and photoluminescent (ORNL) dosimeters since photographic films are sensitive to climatic factors.

In the choice of neutron dosimeters, the DINA dosimeter is preferable, and for rapid determination of neutron dose, the isomeric rhodium detector is recommended.

LITERATURE CITED

1. J. Auxier, *Health Phys.*, **11**, 89 (1965).
2. H. Delafield, S. Boot, and J. Dennis, AERE-R7008, Harwell (1972).
3. G. Makra and P. Zarand, KFKI-71-82, Budapest (1971).
4. I. A. Bochvar et al., Accident Dosimetric Systems in the Experiment at the HPRR [in Russian], AINFI 138, TsNIAtominform, Moscow (1972).
5. F. Haywood and J. Poston, ORNL-TM-3770 (1973).
6. I. A. Bochvar et al., Handling of Radiation Accidents, Proc. Symp. IAEA, Vienna (1969), p 235.
7. I. B. Keirim-Markus et al., *At. Énerg.*, **34**, No. 1, 11 (1973).
8. T. V. Koroleva, K. K. Koshaeva, and S. N. Kraitor, *At. Énerg.*, **32**, No. 2, 157 (1972).
9. V. F. Kozlov and G. V. Shishkin, Radiation Safety at Nuclear Critical Assemblies [in Russian], Atomizdat, Moscow (1969).
10. I. B. Keirim-Markus et al., Nuclear Accident Dosimetry Systems, Proc. Panel IAEA, Vienna (1970).
11. J. Hurst et al., *Rev. Sci. Instrum.*, **27**, 153 (1956).
12. K. K. Koshaeva, S. N. Kraitor, and L. B. Pikel'ner, JINR Preprint PZ-5421 (1970).
13. S. Boot, AERE-R7294, Harwell (1972).
14. F. Fasso et al., SESR/SESRCI N70/S2, AF/BS, Cădarache (1970).

OPTIMAL SAMPLE DIMENSIONS FOR GAMMA ACTIVATION ANALYSIS

S. P. Kapitsa, Yu. T. Martynov,
V. N. Samosyuk, V. V. Sulin,
and Yu. M. Tsipenyuk

UDC 543.53

One of the main advantages in the use of γ -rays in activation analysis is their great penetrating power. From that follows two extremely important consequences for many applications: 1) the entire volume of a sample is analyzed; 2) the weight of the analyzed sample may be taken sufficiently large, which is absolutely necessary, for example, to ensure representativeness in the analysis of the elemental composition of rocks and ores. We consider factors that limit the dimensions of samples analyzed.

Analyzed samples are usually irradiated with bremsstrahlung having a maximum energy of 10-20 MeV produced in electron accelerators (betatrons, microtrons, linear accelerators), and the induced activity measured with a single-crystal scintillation spectrometer. The energy of the γ -rays from the activation products ordinarily lies in the range 0.1-1 MeV. Therefore, although the primary radiation penetrates rather deeply into the sample, the secondary γ -rays from the internal regions, which are of considerably lower energy, are absorbed. It is completely obvious that under such conditions it is difficult to make a judgement about the accuracy of the analysis and its representativeness.

For efficient use of the primary and secondary γ -rays, the geometric dimensions of samples during irradiation and measurement ought not to be the same in view of the features of a photonuclear reaction mentioned. It is rather simple to solve these requirements. The sample is selected in the form of a cylinder (or nearly so) the dimension h of which along the axis is determined by the degree of absorption of the activating γ -radiation in the sample material, i. e., the value of h should be approximately equal to the length over which the intensity of the activating radiation is reduced by a factor e ; the radius r of the cylinder is estimated from the absorption of the γ -rays emitted from nuclei in the material for which analysis must be made. This radius is selected equal to that sample thickness for which the attenuation of the γ -ray intensity from the desired isomer is also a factor e , (Fig. 1a).

Secondary γ -radiation is measured with a ring crystal having internal cavity dimensions equal to the dimensions of the analyzed sample (Fig. 1b). Thus the geometric dimensions during irradiation and

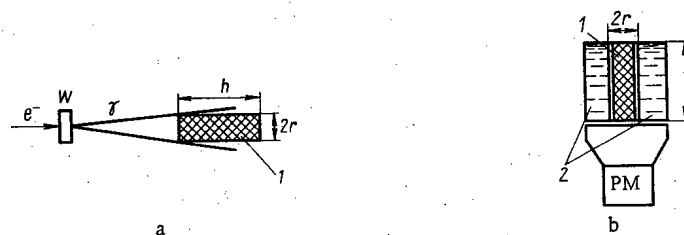


Fig. 1. a) Diagram of irradiation of sample to be analyzed in the bremsstrahlung beam of an electron accelerator; b) measurement of induced γ activity with a ring detector: e^-) electron beam; W) bremsstrahlung target; γ) bremsstrahlung; 1) sample to be analyzed; 2) scintillation crystal.

Translated from *Atomnaya Energiya*, Vol. 37, No. 4, pp. 356-357, October, 1974. Original letter submitted February 1, 1974.

© 1975 Plenum Publishing Corporation, 227 West 17th Street, New York, N.Y. 10011. No part of this publication may be reproduced, stored in a retrieval system, or transmitted, in any form or by any means, electronic, mechanical, photocopying, microfilming, recording or otherwise, without written permission of the publisher. A copy of this article is available from the publisher for \$15.00.

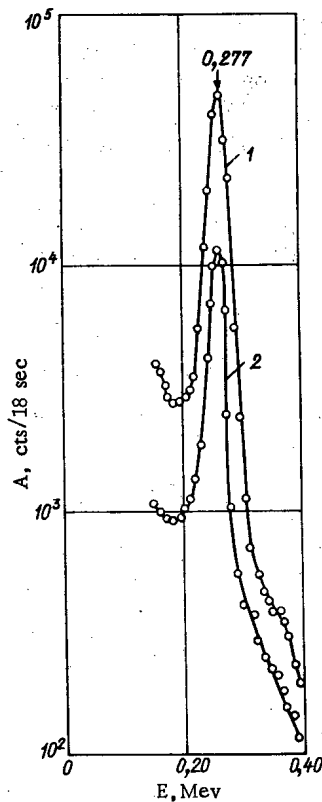


Fig. 2. Instrumental γ -ray spectra from induced activity of the two portions of a gold-ore sample: 1, 2) sample in container with "optimal" and standard dimensions respectively.

measurement are different which reflects the nuclear physics characteristics of these radiations. The dependence of the dimensions of the sample and γ -spectrometer on the energy of the irradiating and recorded γ -radiation makes it possible in each specific case of γ -activation analysis to set up the best conditions for activation of the sample and for recording the γ -radiation from the induced activity. In this way the maximum permissible sample weight is also determined; exceeding this weight leads to no significant improvement in the sensitivity or accuracy of the analysis.

For experimental confirmation of the statements made above, a comparison was made of activation results for samples with a varying content of gold selected from a gold deposit. A portion of each sample weighing from 200-300 g was packed in a "standard" cylindrical container 60 mm high and 60 mm in diameter, and the remaining portion packed in an "optimal" cylindrical container 35 mm high and 18 mm in diameter (these dimensions are not entirely optimal; they were dictated by the dimensions of a crystal on hand). Each loaded container was irradiated by microtron bremsstrahlung radiation with $E_{\max} = 9$ MeV and an average current of accelerated electrons equal to $30 \mu\text{A}$. The sample irradiation time, the "cooling" time, and the measurement time were 18, 3, and 18 sec. A mechanical transporter [1] was used to transfer the loaded containers.

Activity of the samples in a standard container was measured with a γ -spectrometer having a 70×70 mm NaI(Tl) crystal, and the samples in optimal containers were measured with a similar spectrometer having an NaI(Tl) crystal of the same dimensions but with a well 18×35 mm in size. The γ -ray spectra from induced activity in the samples were recorded with a multichannel pulse-height analyzer in an energy interval corresponding to the γ -rays from gold activation products resulting from the (γ, γ') reaction ($E = 277$ keV).

Figure 2 shows the instrumental γ -ray spectra of the induced activity from two such portions of a single sample containing 50 g/ton of gold. Despite the reduction in sample weight by a factor of four, it is clear that useful information about gold content in the sample was increased by a factor of five in the case of the "optimal" container, which confirms our assertions. Indeed, as has been shown [2], the detection efficiency for γ -rays with an energy of 0.3 MeV is about 20% for ore and rock samples packed in the "standard" container we used. This means that in counting the γ -activity of such a sample under 4π conditions, the number of recorded decay events can be increased by a factor of four to five at the most. At the same time, with improved sample geometry, we have obtained experimentally an increase in useful information per unit weight by a factor of 20.

LITERATURE CITED

1. S. P. Kapitsa et al. , *At. Énerg.* , 34, No. 3, 199 (1973).
2. A. K. Berzin et al. , in: *Regional, Exploration, and Industrial Geophysics [in Russian]*, No. 6, Izd. ONTI BIÉMS, Moscow (1967), p. 30.

DETERMINATION OF ^{234}Am HALF-LIFE

V. G. Polyukhov, G. A. Timofeev,
P. A. Privalova, V. Ya. Gabeskiriya,
and A. P. Chetverikov

UDC 539.163:546.799.5

Until the present time, a large uncertainty has been observed in the value for the α -decay half-life of ^{243}Am ($T_{\alpha 243}$). This is very apparent from Table 1. Another determination of it was made because of the importance of the knowledge of the value of $T_{\alpha 243}$ for both scientific and purely practical purposes.

Americium samples of two isotopic compositions were used in the present work (Table 2). All the experimental results are given for the 95% confidence interval.

The chemical and radiochemical purification of the samples, the methods of source preparation, and the radiometric measurements were similar to those described previously [8]. Americium concentration in the original solutions was established through the results of weight and complexometric [9] determinations.

Isotopic composition of the samples was determined on an MI-1311 mass spectrometer with ion recording by means of a BEU-1A secondary electron multiplier. Analysis of each sample was performed three times over the mass range from 238 to 244. Masses other than those indicated in Table 2 were not observed.

Alpha spectrometry was accomplished on an alpha spectrometer having a surface barrier Si(Au) detector. The overall resolution of the alpha spectrometer obtained with working sources prepared from samples 1 and 2 was no worse than 25 keV. Figure 1 shows a typical α -spectrum from a source prepared from sample 1.

In order to eliminate the effect of the low-energy distribution on the analytical results, the α -spectra were analyzed by comparison of proportional parts of the areas under the peaks of the most intense α lines in ^{241}Am and ^{243}Am ($E = 5486$ and 5275 keV) allowing for relative yield. The relative yields of these α lines, which were obtained by averaging previous results [2, 10-15], were respectively 85.0 ± 0.74 and $87.3 \pm 0.34\%$.

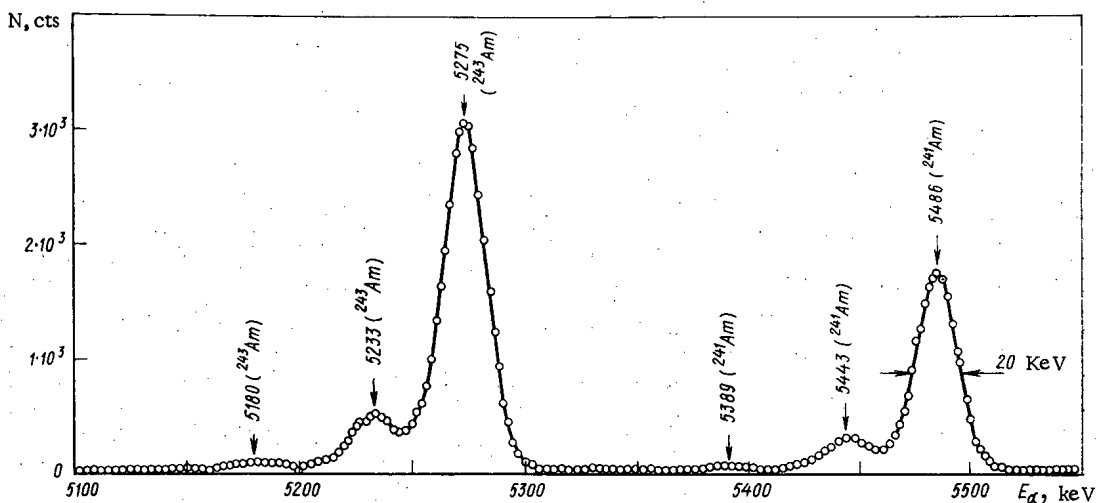


Fig. 1. Alpha-spectrum from source prepared from sample 1.

Translated from *Atomnaya Energiya*, Vol. 37, No. 4, pp. 357-359, October, 1974. Original letter submitted March 14, 1974.

© 1975 Plenum Publishing Corporation, 227 West 17th Street, New York, N.Y. 10011. No part of this publication may be reproduced, stored in a retrieval system, or transmitted, in any form or by any means, electronic, mechanical, photocopying, microfilming, recording or otherwise, without written permission of the publisher. A copy of this article is available from the publisher for \$15.00.

TABLE 1. Summary of Data for $T_{\alpha 243}$

Date of determination	$T_{\alpha 243}$, yr.	Reference
1953	8800 ± 600	[1]
1954	7600	[2]
1956	7600 ± 370	[3]
1958	7951 ± 48	[4]
1959	7720 ± 160	[5]
1960	7650 ± 50	[6]
1968	7370 ± 40	[7]

TABLE 2. Characteristics of Americium Samples Used in the Determination of $T_{\alpha 243}$

Characteristic	Sample 1	Sample 2
Americium concentration in original solution after dissolving sample, mg/g of solution	$0,2750 \pm 0,0010$	$0,3950 \pm 0,0018$
Content of inert impurities, wt. %	$\leq 0,3$	$\leq 0,5$
Contamination by extraneous α -emitters, % of total α -activity	$\leq 0,1$	$\leq 0,09$
Mass spectrum, at. %		
	²⁴¹ Am	²⁴¹ Am
	²⁴³ Am	²⁴³ Am
	$3,379 \pm 0,050$	$0,524 \pm 0,019$
	$96,621 \pm 0,050$	$99,476 \pm 0,019$
Alpha-spectrum, % of total α -activity		
	²⁴¹ Am	²⁴¹ Am
	²⁴³ Am	²⁴³ Am
	$37,39 \pm 0,47$	$7,98 \pm 0,30$
	$62,61 \pm 0,47$	$92,02 \pm 0,30$

The data from α -spectrometric analyses of samples 1 and 2 (see Table 2) are the average of 17 measurements.

From the original solutions, eight series of $4\pi\alpha$ sources were prepared for sample 1 and four series for sample 2 (in accordance with the number of separate dilutions).

Values of the specific α -activity $Q_{\Sigma\alpha}$ were calculated from $4\pi\alpha$ measurements of the individual sources. The results of the determination of $Q_{\Sigma\alpha}$ for the separate series of $4\pi\alpha$ sources were checked by means of dispersion analysis [16], and having established their membership in the appropriate general set, they were combined and analyzed by the least-squares method for measurements of unequal accuracy (Table 3). The total error of $Q_{\Sigma\alpha}$ includes the error in the determination of the weight concentration of americium in the original solutions (0.60 and 0.46% for samples 1 and 2 respectively).

Values of $T_{\alpha 243}$ were calculated by the following three methods: from the $Q_{\Sigma\alpha}$, α -spectra, and mass spectra obtained; from the $Q_{\Sigma\alpha}$ and the α -spectrum obtained and the known value of the ²⁴¹Am specific α -activity $Q_{\alpha 241}$; from the known half-life of ²⁴¹Am and the measured α - and mass spectra.

TABLE 3. Results of $Q_{\Sigma\alpha}$ Determination for Americium Samples, $\text{dis} \cdot \text{sec}^{-1} \cdot \text{g}^{-1}$

Sample 1										Sample 2			
A *	$Q_{\Sigma\alpha} \times 10^{-9}$	A	$Q_{\Sigma\alpha} \times 10^{-9}$	A	$Q_{\Sigma\alpha} \times 10^{-9}$	A	$Q_{\Sigma\alpha} \times 10^{-9}$	A	$Q_{\Sigma\alpha} \times 10^{-9}$	A	$Q_{\Sigma\alpha} \times 10^{-9}$	A	$Q_{\Sigma\alpha} \times 10^{-9}$
1	11,514	12	11,753	23	10,897	34	11,554	45	10,957	1	8,062	12	7,620
2	11,522	13	11,480	24	11,198	35	11,058	46	10,591	2	7,706	13	7,911
3	11,496	14	11,506	25	11,251	36	11,595	47	11,630	3	8,009	14	8,175
4	11,423	15	11,824	26	11,445	37	11,581	48	11,760	4	7,912	15	8,019
5	11,145	16	11,560	27	11,397	38	11,843	49	11,217	5	8,003	16	8,160
6	11,386	17	11,636	28	10,757	39	10,782	50	11,246	6	8,021	17	7,887
7	11,520	18	11,376	29	11,339	40	11,599	51	11,306	7	7,959	18	8,146
8	11,439	19	11,049	30	11,309	41	10,950	52	11,647	8	8,011	19	7,977
9	11,233	20	11,005	31	10,858	42	11,672	53	11,553	9	8,076	20	8,186
10	11,408	21	11,282	32	11,000	43	11,477	54	11,508	10	7,820	21	8,103
11	11,574	22	11,278	33	11,176	44	11,765			11	8,175	22	7,710

$$\bar{Q}_{\Sigma\alpha} = (11,358 \pm 0,103) \cdot 10^9 \text{ dis} \cdot \text{sec}^{-1} \cdot \text{g}^{-1}$$

$$\bar{Q}_{\Sigma\alpha} = (7,984 \pm 0,079) \cdot 10^9 \text{ dis} \cdot \text{sec}^{-1} \cdot \text{g}^{-1}$$

* A) number of $4\pi\alpha$ source.

TABLE 4. Determination of $T_{\alpha 243}$

Method of determination	Sample 1	Sample 2
From the values found for $Q_{\Sigma\alpha}$, the α - and mass spectra	7393 \pm 87	7369 \pm 77
From the values found for the α -spectrum and $Q_{\Sigma\alpha}$ and from the known $T_{\alpha 241}$	7397 \pm 88	7371 \pm 78
From the α - and mass spectra obtained and the known $T_{\alpha 241}$	7390 \pm 190	—

In the calculations, we assumed the following: $T_{\alpha 241} = 432.7 \pm 0.7$ yr ($Q_{\alpha 241} = 1.26830 \cdot 10^{11}$ dis \cdot sec $^{-1}$ \cdot g $^{-1}$) [17]; the atomic weights of ^{241}Am and ^{243}Am are respectively 241.057 and 243.061 [18] (on the ^{12}C scale); 1 year = $3.15567 \cdot 10^7$ sec; $\ln 2 = 0.693147$; $N_0 = 6.02252 \cdot 10^{23}$ mol $^{-1}$.

Sample 2 is the most suitable for the determination of $T_{\alpha 243}$ by the first two methods, but because of the strong dependence of the final result on the accuracy of the α - and mass-spectrometric analyses, the value obtained by the third method of calculation is not given.

Values of $T_{\alpha 243}$ calculated from the data in Tables 2 and 3 by the three methods mentioned are shown in Table 4. The data in Table 4 are not of equal accuracy (obtained by different methods) [19] and therefore the final value $T_{\alpha 243} = 7380 \pm 34$ yr ($Q_{\alpha 243} = 7.374 \pm 0.034 \cdot 10^9$ dis \cdot sec $^{-1}$ \cdot g $^{-1}$) was determined as a weighted mean value.

The resultant value of $T_{\alpha 243}$ is practically in agreement with the value given by Brown and Propst [7] and is considerably lower than data in [1-6].

LITERATURE CITED

1. H. Diamond et al., Phys. Rev., 92, 1490 (1953).
2. F. Asaro and I. Perlman, Phys. Rev., 93, 1423 (1954).
3. E. Hyde, I. Perlman, and C. Seaborg, Nuclear Properties of Heavy Elements [Russian translation], No. 1, Atomizdat, Moscow (1967).
4. J. Wallman, P. Graf, and L. Goda, J. Inorg. and Nucl. Chem., 7, 199 (1958).
5. R. Barnes et al., J. Inorg. and Nucl. Chem., 9, 105 (1959).
6. A. Beadle et al., J. Inorg. and Nucl. Chem., 12, 359 (1960).
7. L. Brown and R. Propst, J. Inorg. and Nucl. Chem., 30, 2591 (1968).
8. V. G. Polyukhov et al., At. Énerg., 36, No. 4, 319 (1974).
9. E. M. Piskunov, A. G. Rykov, and G. A. Timofeev, Byull. Izobret., No. 3, 178 (1973).
10. L. L. Gol'din, G. I. Novikova, and E. F. Tret'yakov, Izv. Akad. Nauk SSSR, Ser. Fiz., 20, 868 (1956).
11. S. Rosenblum, M. Valadares, and J. Milsted, J. Phys. Radium, 18, 609 (1957).
12. S. A. Barabov, V. M. Kulakov, and V. M. Shatinskii, Zh. Éksp. Teor. Fiz., 45, 1811 (1963).
13. L. Magnusson, Phys. Rev., 107, 161 (1957).
14. W. Michaelis, Z. Phys., 186, 261 (1965).
15. K. Doerfel, Statistics in Analytic Chemistry [Russian translation], Mir, Moscow (1969).
16. F. Oetting and S. Gunn, J. Inorg. and Nucl. Chem., 29, 2659 (1967).
17. V. A. Kravtsov, Atomic Masses and Nuclear Binding Energies [in Russian], Atomizdat, Moscow (1965), p. 97.
18. V. M. Shchigolev, Mathematical Analysis of Observations [in Russian], Fizmatgiz, Moscow (1962).

COMECON NEWS

**XXVI SESSION OF THE COMECON PERMANENT
COMMISSION ON THE PEACEFUL USES OF ATOMIC ENERGY**

V. A. Kiselev

The XXVI session of the COMECON Permanent Commission on the peaceful uses of atomic energy was held in Leningrad, June 18-21, 1974. Participating in the work of the Commission were delegations from Bulgaria, Hungary, the German Democratic Republic, the Republic of Cuba, Poland, Rumania, the Soviet Union, and Czechoslovakia.

Reports were heard from the chairman of the Commission on "COMECON activities over 25 years and realization of the integrated developmental program in the field of peaceful uses of atomic energy," by the USSR delegation on the Leningrad nuclear power station, and the discussion covered further developments in collaboration between COMECON member-nations in monitoring and control of nuclear reactor facilities, radiation technology and radiation equipment, including procedural and instructions documents on radiation sterilization of materials and medical wares, standardization of instruments and nucleonic instrumentation.

Appropriate recommendations and resolutions were adopted on all of these topics.

Translated from *Atomnaya Energiya* Vol. 37, No. 4, p. 361, October, 1974.

© 1975 Plenum Publishing Corporation, 227 West 17th Street, New York, N.Y. 10011. No part of this publication may be reproduced, stored in a retrieval system, or transmitted, in any form or by any means, electronic, mechanical, photocopying, microfilming, recording or otherwise, without written permission of the publisher. A copy of this article is available from the publisher for \$15.00.

COLLABORATION DAYBOOK

The twenty-seventh session of the work team on nuclear instrumentation was held April 2-5, 1974, in Dresden. Reports of the science and engineering conference on "Monitoring and control of nuclear reactors and nuclear power stations" were discussed, and proposals were prepared for further collaboration in this field. The overall concept and the structural layout of the system designed for monitoring leaks in fuel elements and the radiation safety of nuclear power stations were discussed and approved. The development of common standards and requirements for the design of systems of nuclear instrumentation and equipment for laboratory use and industrial use was discussed in detail. A list of integrated circuits recommended for use in nuclear instrumentation and equipment for laboratory use and industrial use was discussed in detail. A list of integrated circuits recommended for use in nuclear instrumentation was agreed upon. Standardization topics were also discussed.

* * *

The fourth session of the KNTS [Science and Engineering Coordinating Council] on nuclear power station water management was held in Budapest May 13-16, 1974. The draft work plan for 1975-1976, for this KNTS, was discussed and approved, and a draft program of scientific and technical collaboration in the field of nuclear power station water management was drawn up for the 1976-1980 period. Reports from delegations of specialists of the various participating nations on water conditions of the primary and secondary loops of VVÉR-1000 reactors and on the selection of structural materials, on the development of instruments for measuring boric acid concentration in the reactor primary loop coolant, and on the status of work in the field of monitoring the seal of fuel-element cladding and radiometric analysis of reactor loop coolants, were heard and discussed. Suggestions on basic principles in the organization of chemical water treatment at nuclear power stations were discussed, and recommendations on how best to organize work in this area were worked out. Topics pertaining to improvements in the activities of the KNTS were also discussed.

* * *

The third session of the KNTS on research reactors was held May 14-17, in Sofia. Reports from delegations of specialists of the various countries on the progress of work on the program of collaboration on the topics "Improvements in existing research reactors, expansion of their experimental potentialities, and coordination of their use in various lines of research," and "Development of new research reactors with improved neutron-physics characteristics" were heard and discussed.

A delegation of specialists from Rumania reported to the session participants on progress in preparations for the symposium entitled "Experience in the operation and use of research reactors," which is scheduled for September 30 through October 4, 1974, in Rumania.

Topics associated with the fulfillment of distinct stages of the 1974-1975 work plan for the KNTS were also discussed, as were proposals put forth by delegations of specialists on the 1975-1976 work plan. A draft plan of scientific and technical collaboration between COMECON member-nations in the field of nuclear research reactors for the years 1976-1980 was also discussed.

* * *

The eighteenth session of the work team on reactor science, reactor engineering, and nuclear power was held May 21-24, 1974, at Bialobrzeg near Warsaw. The work team discussed and agreed upon a

Translated from Atomnaya Énergiya, Vol. 37, No. 4, pp. 361-362, October, 1974.

© 1975 Plenum Publishing Corporation, 227 West 17th Street, New York, N.Y. 10011. No part of this publication may be reproduced, stored in a retrieval system, or transmitted, in any form or by any means, electronic, mechanical, photocopying, microfilming, recording or otherwise, without written permission of the publisher. A copy of this article is available from the publisher for \$15.00.

realization plan for the program of collaboration between COMECON member-nations in the field of dissociating gases as coolants for fast reactor facilities. The first draft of a plan of scientific and technical collaboration in the field of reactor science and engineering and nuclear power for the 1976-1980 period was discussed. Information put forth by a delegation of USSR specialists on the progress and results of research conducted in COMECON member-nations within the framework of the program of collaboration in the area of the VVER-1000 reactor facility was discussed, as well as a balance sheet on the conference "Monitoring and control of nuclear reactors and nuclear power stations." Proposals dealing with further collaboration in this area were also heard and accepted.

Proposals were presented by delegations of specialists on the preparation and holding of a seminar to expedite exchanges of experience on the installation and operation of VVER type reactor facilities, and a seminar planned to familiarize specialists of COMECON member-nations with specific topics concerning the building and integration of nuclear power stations with KS-150 reactor facilities cooled by carbon dioxide gas.

* * *

The third session of the KNTS on radiation safety was held in Moscow, May 21-24, 1974.

Reports were heard on work being done within the framework of the program of collaboration (on requirements for protection of the environment in normal operation of nuclear power plants, methods for taking air samples, radiometry of gases and aerosols in the surroundings, etc.), and on the progress of work on documents stipulating regulations and procedures in the COMECON member-nations for the area of radiation safety (procedures to be followed in determining limits of permissible discharges of radioactive products to the surroundings at nuclear power stations and research reactors, recommendations on monitoring the state of the external environment when ^{131}I gains access to atmospheric air in industrial effluents and discharges, etc.). After the materials presented had been discussed, the Council decided to concentrate the work of specialists under its guidance on developing recommendations pertaining to permissible doses, including population doses, and on procedures for determining scaling coefficients between the concentration of radioactive materials in the air and the dose with migration taken into account — principles underlying the determination of a public health zone. The Council brought greater precision into coordination and further collaboration involving working bodies of the Commission (KNTS 1-3, work team on reactor science and engineering and nuclear power, and section 5 PK on electric power), the siting and scheduling of a conference on radiation safety in connection with the operation of nuclear power stations (CSSR, September, 1975), and a tentative agenda for the fourth session of the KNTS-RB [KNTS on radiation safety] (now scheduled for Leipzig, GDR, September 24-27, 1974); resolutions were adopted on a variety of topics.

* * *

A conference of specialists from COMECON member-nations on methods in shielding design and on the properties of materials used in nuclear power station reactors was held in Moscow, June 3-5, 1974. Reports from specialists of COMECON member-nations were heard and discussed. These reports dealt with "Development of unique methods for the design of shielding for reactor facilities. Research, development, and verification of systems of nuclear constants for nuclear shielding design," and "Searches and investigation of the properties of materials for reactor shielding." Proposals submitted by delegations of specialists of COMECON member-nations on further work in this area were agreed upon.

* * *

A conference of specialists from COMECON member-nations on programs and methods in the physical design of fast reactors was held in Dimitrovgrad on July 1-5, 1974.

Reports presented by specialists on the work being done on "Optimization of the physical characteristics of fast power reactors," and "Development of programs and sets of programs for physical design calculations of fast power reactors," were heard and discussed at this conference. The program of collaboration between COMECON member-nations on the topic "Physics research with fast reactors" was also discussed.

The conference participants drew up proposals on further collaboration in this area.

INFORMATION

SILVER JUBILEE OF THE SOVIET OF MUTUAL
ECONOMIC AID

A. F. Panasenkov

The Soviet of Mutual Economic Aid, the first interstate economic organization of socialist countries, completes twenty five years of its activity this year. The formation and the major periods of activity of SMEA have been inseparably linked with the economic development of the socialist countries and of the world wide socialist system as a whole.

Creating the SMEA in 1949 its members expressed determination to develop extensive economic collaboration based on gradual development of international socialistic division of labor for building a thoroughly developed socialistic society in the member countries, and for ensuring world stability.

The objective of the Soviet of Mutual Economic Aid is to contribute through coordination of the efforts of the member countries toward a further intensification and perfection of the collaboration and development of socialistic economic integration, a balanced development of the national economy, an acceleration of the economic and technical progress in these countries, an increase in the level of industrialization of the countries with less developed industry, a gradual approach and equalization of the levels of economic development, and a steady rise of the welfare of the people of the member countries.

The best index of the fruitful activity of SMEA is provided by the notable achievements of the socialist countries during the past 25 years. The countries of the socialist commonwealth comprise the most dynamically developing region of the world. At present these countries including 18.5% of the territory and 9.6% of the population of the world (over 366 million people), account for about 33% of the world's industrial production compared to 18% in 1950.

The problems of providing fuel and energy to the member countries of SMEA have been successfully solved through making joint efforts in the development of energy resources. A general agreement has been signed for collaboration in the exploitation of Orenburg condensed gas deposits and joint construction of a main gas pipeline from the Orenburg region to the western border of the USSR (about 3000 km in length) and also of a gas treatment plant. These developments are an important addition to the largest oil pipeline of the member countries "Druzhba" and the gas pipeline, which have been in existence for ten years.

An important measure toward the realization of the complex program is the agreement for the construction of a 750 kV power supply line (PSP-750) 900 km in length, which would permit parallel operation of unified power systems (UPS) "Mir" of the member countries and the unique European power system of the USSR. By 1980 PSP-750 will increase the power of UPS of the member countries of SMEA to 205,000 MW which offers the possibility of making large unit power blocks.

Scientific-technical collaboration is also being developed extensively. The members of SMEA have prepared (and member countries signed) 48 multilateral agreements on joint solution of the most important scientific and technical problems. Thirty eight coordinating centers, seven scientific-technical coordinating councils (STCC), and a number of international associations of scientists and laboratories have been formed. Over 700 scientific organizations are participating in solving more than 150 scientific and technical problems. At present the number countries of SMEA are in the forefront of many important areas of world scientific and technical progress. Over 1.6 million scientists, i. e. a third of the total number of scientists in the world are working in these countries.

The composite program of further intensification and improvement of collaboration and development of socialistic economic integration of the member countries of SMEA, adopted at the XXV session of SMEA,

Translated from *Atomnaya Energiya*, Vol. 37, No. 4, pp. 363-366, October, 1974.

© 1975 Plenum Publishing Corporation, 227 West 17th Street, New York, N.Y. 10011. No part of this publication may be reproduced, stored in a retrieval system, or transmitted, in any form or by any means, electronic, mechanical, photocopying, microfilming, recording or otherwise, without written permission of the publisher. A copy of this article is available from the publisher for \$15.00.

stresses the introduction of atomic energy in the national economy on an industrial scale.

In a short period the collaboration has made possible the creation of atomic scientific-research centers, each equipped with an appropriate scientific experimental base. This has undoubtedly aided the extensive growth of scientific research, engineering development and emergence of new institutes, laboratories, and enterprises for the use of atomic energy in different areas of national economies.

Research atomic reactors, cyclotrons, radiochemical and physical laboratories equipped with modern equipment have been constructed and put into operation.

Taking an active part in the work of the permanent commission of SMEA on the peaceful uses of atomic energy (CPUAE SMEA) the delegates from Bulgaria, Hungary, GDR, Poland, Rumania, USSR, and Czechoslovakia, and from 1972 also of the Republic of Cuba, have made significant contributions in developing collaboration in respect of nuclear energetics, nuclear instrument manufacture, isotopes and tracer compounds, radiation safety and protection technology, use of radioisotope methods and equipment in different branches of national economies etc.

The commission has worked out and adopted recommendations on standardization and specialization of production of about 80 groups of parts used in nuclear instrument manufacture, about 1000 isotopes, tracer compounds, and radiation sources, and about 20 denominations of articles of protection technology.

A prominent place in the collaboration in peaceful uses of atomic energy has been occupied by the scientific-technical collaboration, in particular, the coordination of scientific-technical research, design and constructional developments in nuclear engineering, and the determination of the most efficient use of atomic energy in different branches of national economies (electric power, metallurgical, textile, chemical, food and agricultural industries, public health).

Within the framework of the coordinated scientific-technical themes the commission has adopted a series of scientific-technical measures. During the past ten years it has organized 14 science conferences, 31 symposia and seminars, about 160 meetings of specialists for the discussion of specific scientific and technical problems, and also three exhibitions. Representatives of IAEA have participated in a number of these events.

An important event of 1974 was the scientific-technical conference held on 25-27 June at Obninsk, dedicated to the twentieth anniversary of the inauguration of the first atomic power plant in the USSR and the world, which marked the beginning of a new era in the industrial use of the enormous resource of nuclear power for peaceful purposes.

In the last sessions of SMEA, the highest body of the Soviet of Mutual Economic Aid, in 1972-1974 the importance and special significance of an accelerated development of nuclear energetics and of the improvement of collaboration in this field have been stressed. This attention to nuclear energetics is reflected in the fact that an appreciable increase in the electric power production by atomic power plants is planned in the structure of the fuel energy balance of the countries up to 1980 and in a preliminary prognosis of fuel and energy needs up to 1990.

Agreements and protocols have been signed, according to which the Soviet Union will provide technical assistance in the construction of atomic power plants in Bulgaria, Hungary, GDR, Poland, Rumania, and Czechoslovakia with a total power in excess of 8000 MW. Construction of over 20 power blocks with atomic reactors WWPR-440 has been planned. The total electrical power of the atomic power plants being constructed in the member countries of SMEA, including the Soviet atomic power plants, will be 30-35 thousand MW by 1980 and will be several times more by 1990.

For ensuring such a growth of nuclear power an all-encompassing collaboration in the development of the WWPR-1000 reactor has acquired a special significance. Within the framework of SMEA scientific-technical, constructional, and design measures have been worked out and approved for accelerating the work for the construction of WWPR-1000. These measures envisage a collaboration of the member countries of SMEA in 1973-1975 in a more intensive scientific-technical validation of the solutions used in the design of the reactor equipment, in the development of improved constructions of individual forms of the basic and auxiliary equipment, and also in conducting a number of seminars, meetings, and two-day consultations with the specialists of the countries.

The endurance characteristics of construction materials and equipment of this reactor installation, for example, steam generators, circulating and other pumps, valves with remote control etc., are being

studied in the USSR, Czechoslovakia, and Poland. Low- and high-efficiency sensors for measuring energy releases and temperatures in the active zone (as well as other instruments) are being developed in GDR, Poland, and Rumania. Considerable work on the investigation of the water regime in boric control of the reactor installation is being carried out in Bulgaria, Hungary, GDR, and USSR.

The construction of the WWPR-1000 reactor has started with the building of the fifth block of the Novovoronezhsk atomic power plant.

Proposals on possible directions of collaboration in the development of reactor installations with 2000-3000 MW electric power and multipurpose reactor installations are being studied within the framework of the commission.

A temporary international scientific-research association for carrying out investigations on the critical assembly of water-moderated, water-cooled power reactors has been formed on the recommendations of CPUAE SMEA. This association functions at the Central Institute of Physical Research (CIPR) of the Hungarian Academy of Sciences in Budapest, where a large physical installation has been constructed in a short time through the joint efforts of the member countries. A program has been devised which provides for conducting a wide range of investigations by specialists of the member countries.

On the experimental side, in 1973-1974, the international association conducted measurements on the statics of reactors for the possibility of choosing the most suitable methods of measurements and for further procedural developments, on the kinetics of reactors for comparing different methods of measuring reactivity, on the determination of macro- and microparameters as a function of the concentration of boric acid in the moderator and the temperature effect of the reactivity etc. Theoretical investigations included the development of a two-dimensional diffusion program for hexagonal geometry, creation of a library of group constants, and comparison of computations with experimental results obtained on the critical assembly. A system of computational programs for accurate description of the geometrical relations of WWPR type grids has been compiled.

With the creation of the temporary international scientific-research association a transition occurred in the work of the commission from coordination of scientific-technical investigations to a more effective form of conducting joint work on a definite scientific-laboratory basis. The completion of all the work envisaged in the program will make it possible to obtain important experimental data which will be subsequently used in developments in the design of atomic power plants with the WWPR-1000 reactor.

One of the basic problems is to equip atomic power plants with instruments and electronic equipment of the control and protection system, dosimetric and radiometric control for water-moderated, water-cooled reactors. A scientific-technical conference of the member countries of SMEA with the theme "Control and Management of Nuclear Reactors and Atomic Power Plants" was held in December, 1973 in Warsaw. It revealed new stages in the growth of work in this field.

The most important problem in developing collaboration of the member countries of SMEA in the field of atomic energetics is supplying equipment for the atomic power plants and providing technical assistance in the construction of the plants. An international economic union "Interatoménergo" was created in December, 1973 with its headquarters in Moscow. This union organizes cooperation in the production and delivery of the equipment, instruments, and materials for atomic power plants, ensures necessary technical assistance in design, construction, and operation of the plants, participates in engineering and production training of the personnel and so forth. The establishment of trade and scientific-technical relations with other countries that do not belong to the union also falls within the scope of "Interatoménergo."

With the signing of the agreement for the creation of "Interatoménergo" a very important stage has been completed in the solution of a great problem posed by the composite program of socialistic economic integration of the member countries of SMEA concerning the creation of the necessary prerequisites for the industrial growth of atomic energy.

In 1973-1974 significant progress was achieved in the work on the water regimes of atomic power plants. The STCC, created by the commission in GDR, developed and examined a series of data and reports on water regimes, corrosion and water cleaning of WWPR type reactors, on the results and prospects of further development work on deactivation of the first contours of power blocks, on supplying ion-exchange resins to the plants of the member countries of SMEA and so forth. On the basis of these data the commission took appropriate decisions and adopted recommendations.

In accordance with a resolution of the XXVI session of SMEA the commission formulated proposals

and is implementing collaboration in the field of scientific-research and design—construction work on high-power, fast reactors, and is organizing exchange of scientific and technical experience by conducting symposia and seminars and through other forms of collaboration. For this problem an STCC has been created at Obninsk at the Physicopower Institute and a program for scientific and technical collaboration has been worked out. In October 1973 the second symposium on "The Present State and Prospects of Work on Construction of Atomic Power Plants with Fast Neutron Reactors" was held at Obninsk, at which 95 scientific papers were presented. The symposium made a large contribution toward further growth of collaboration in this field and toward accelerating the development of high-power, fast reactors.

In recent years more extensive efforts have been made toward collaboration in the development and improvement of research-type nuclear reactors. The STCC created to take care of this problem, in 1972, in Rumania has initiated a number of scientific and technical programs including the development of intra-reactor research, control and management of research-type nuclear reactors, improvement of the existing research reactors and enlargement of their experimental potentials, and the development of new reactors with improved neutron-physical characteristics.

In the field of treatment of irradiated fuel for atomic power plants the following technical and procedural matters have been developed or are being developed along with the scientific research work within the competence of the commission.

- 1) Technical conditions for the assembly of depleted fuel elements of atomic power plants with WWPR-440 reactors approved by the commission and recommended for use as a typical document in closing contracts for the delivery of depleted assemblies of fuel elements among the countries owing the plants, and the USSR.
- 2) General instructions for the transport of depleted nuclear fuel from the plants.
- 3) Technological scheme of control of extraction treatment of depleted fuel elements of WWPR type.
- 4) Methods and equipment for determining the content of fissionable elements in the depleted fuel and their isotope composition.
- 5) Technical requirements on the development of equipment for the unit of fluorination of the nuclear fuel.

The activity of the commission and the STCC on radioactive wastes and deactivation in 1973-1974 centered around the development of industrial technology and equipment, treatment and burial of radioactive wastes, and also the development of such procedural materials as lists of unique analytical and technical—economical indices for evaluating the results of existing installations for treatment of liquid wastes of low and intermediate levels of activity, technical requirements on the design of atomic power plants from the point of view of deactivation, techniques of simulating modes of operation of underground storage of radioactive wastes on analog computers, which can be used both for simulating the modes of operation of underground storage of radioactive wastes and for solving problems of safe burial of other highly toxic industrial wastes.

The work of this STCC also included a large complex of investigations of radioactive contamination of the Danube river, including the preparation of annual summaries. These summaries showed that the observed levels of radioactive contamination of the Danube as of 1973 did not exceed the mean annual permissible concentrations and did not present a danger to the environment. However, the mean values of the overall activity showed a tendency toward continuous increase.

A prominent place in the activity of SMEA in 1973-1974 is occupied by the extensive collaboration in specialization of the isotope manufacturing industry, use of isotopes and radiation, radioisotope instruments and radiation technology, and the technology in different branches of national economies.

On the recommendation of the commission an agreement on multilateral international specialization and cooperative formation of the industry for isotope production articles was signed in January 1974. The nomenclature of the agreement covers more than 1000 denominations including 52 isotopes and inorganic compounds, 396 organic tracer compounds, 29 radiopharmaceutical preparations, 19 types of sealed radiation sources, two types of constant action phosphors, and 514 denominations of stable isotopes and their tracer compounds. According to agreement, Hungary will manufacture and meet the needs of the member countries of SMEA in respect of 65 denominations, GDR 247, Poland 28, Rumania 20, USSR 551, and Czechoslovakia 101.

The commission has turned its attention to the need of further coordination of the development and supply to the industry of new tracer compounds for stable and radioactive isotopes; the proposals for further specialization of the industry will be worked out on the basis of these results.

The groundwork for the coordination of the plans of development of the isotope industry in 1976-1980 has been done and a program has been adopted which provides for the following: working out proposals for the solution of the most important problems in this field in 1974-1975, which include ensuring the production capacity of the industry of isotope articles, development of special cyclotron equipment for producing short-lived isotopes for medicine, coordination and cooperative formation of scientific-research and design-construction work on the technology of isotope manufacture and development of industrial capacities etc.

In December, 1973 a symposium on the methods of measurement and testing of sources of ionizing radiation was held in Moscow and future problems in the field of standardization, control, and methods of testing sealed radiation sources were determined.

The STCC on radiation engineering and technology, created in 1971, formulates and solves the problems of industrial realization of processes of sterilization of medical articles, for which eight procedural documents have been prepared and approved, that are unique to the member countries of SMEA. A technical proposal for organizing industrial manufacture of radiation-modified wood has been prepared and plans have been made for work on radiation treatment of polymer materials and industrial rubber articles, sterilized medical articles and materials, and food and agricultural products. These problems were discussed at the symposium on radiation treatment of food and agricultural products held in October, 1973 in Bulgaria. Representatives of IAEA also presented papers at this symposium.

The collaboration in the field of protection and improvement of the environment has been developed more extensively during the past few years in accordance with the composite program. Working out measures for nature conservation is one of the main scientific-technical problems being investigated jointly with the use of the most effective forms of collaboration. A program for scientific and technical collaboration on the problem of ensuring radiation safety up to 1980 and the main directions for the collaboration in this field up to 1990 have been worked out within the framework of the commission.

It is becoming increasingly more important to link the work on radiation safety done by the SMEA bodies with the measures adopted by IAEA and other international organizations. The recommendation of the commission on the transportation of radioactive materials is one of the manifestations of this link. The work of the commission on the development of collaboration in the field of manufacture of elements of radiation protection technology by working out a number of recommendations on standardization and other documents of standards also contributes to radiation safety.

Due to the growth of nuclear power and reactor technology, and also more widespread use of radioactive isotopes and radiation in scientific research, the national economy, and medicine there has been a significant increase in the demand for nuclear physics instruments and radioisotope equipment including instruments and equipment for nuclear medicine. Here a significant role is played by the international economic union "Interatominstrument" (IAI), created in 1972, as a new form of collaboration. The main task of this union is to ensure the most complete coverage of the needs of the countries in dosimetric radio-metric, and nuclear-physics equipment including multidimensional and multichannel systems for nuclear research and nuclear power plants, and also in radioisotope, radiomedical, and fault detection equipment, nuclear radiation detectors and special instruments for isotope laboratories conforming to the world's scientific and technical standards. The tasks of this union also include organization of scientific-technical, industrial, and trade collaboration among the economic organizations of the interested member countries of SMEA and assistance in trade with other countries. The number of the members of the union has now increased from 11 to 15. The soviet of the union has prepared and approved a list of nomenclature groups of instruments in nuclear engineering and has drawn up proposals for specialization of more than 150 types of instruments and materials for long-term agreements in 1976-1980.

Helping the development and use of atomic energy in all branches of the national economy of the member countries, the commission is continuously improving and intensifying its activity, taking an active part in the unique process of socialistic economy integration.

The jubilee session of the Soviet of Mutual Economic Aid, held in June, 1974, noted that the activity of SMEA is accompanied by a steady increase of the prestige of this organization in the world. The underlying principles of its operation: equality, independence, free will, respect of sovereignty, mutual convenience and aid, and high efficiency of collaboration for all participating countries, are making an increasingly greater international impact.

The session expressed the conviction that the gradual completion of the composite program of socialist economic integration will render significant help to all the brotherly countries in the creative work of building socialism and communism.

LITERATURE CITED

1. N. V. Faddeev, Soviet of Mutual Economic Aid [in Russian], *Ékonomika*, Moscow (1974).
2. Soviet of Mutual Economic Aid: 25 Years [in Russian], SMEA Secretariat (1974).
3. On the Silver Jubilee of the Soviet of Mutual Economic Aid. Resolution of the Jubilee Session of SMEA [in Russian], *Pravda*, 20 June 1974.
4. Communiqué on XXVIII Session of the Soviet of Mutual Economic Aid [in Russian], *Pravda*, 22 June, 1974.
5. A. M. Petros'yants, Collaboration in the Field of Uses of Atomic Energy (Special Issue): Economic Collaboration of Member Countries of SMEA [in Russian], SMEA Secretariat (1974).
6. A. F. Panasenkov, "Silver jubilee of SMEA. Information bulletin of the International Economic Union on Nuclear Instrument Manufacture 'Interatominstrument', " No. 1, Warsaw (1974).

CONFERENCES AND MEETINGS

CONFERENCE ON PHYSICAL ASPECTS OF ATMOSPHERIC
POLLUTION

B. I. Styro

An international conference was held in Vilnius on 18-20 June, 1974, in which the physical aspects of atmospheric pollution were discussed. The conference was organized by the Institute of Physics and Mathematics of the Academy of Sciences of the Lithuanian SSR. About 250 scientists from Bulgaria, Hungary, GDR, Poland, USSR, and Czechoslovakia participated in the conference; over 200 papers were presented. Review papers were presented at the plenary session. Four to five parallel sections held their meetings, in which the following problems were discussed:

- neutron activation, chemical, electrochemical, radiochemical, and spectrometric analysis of samples of atmospheric air, and rain;
- radiometric instruments and methods of analysis of radioactive samples of atmospheric objects;
- instruments, methods, and filters for the investigation of atmospheric aerosols and radioactive ions in air;
- natural short- and long-life isotopes in the atmosphere;
- fission products and their behavior in the atmosphere;
- atmospheric aerosols and their chemical composition;
- pollution of the atmosphere by cities;
- cosmic radioisotopes in the atmosphere and their use for the investigation of the problems in the physics of the atmosphere;
- meteorological processes and atmospheric pollution;
- chemical composition of rain and distribution of contaminants in atmospheric fall-outs;
- record of atmospheric pollution in glaciers;
- washing out of pollutants from the atmosphere and self-cleaning of the atmosphere;
- mathematical modeling of the processes of atmospheric pollution;
- exchange of radioactive pollutants between the atmosphere and the oceans;
- physical aspects of normalization of atmospheric pollution.

The methodological papers stressed the need for developing and improving the physical methods of investigation of the pollutants in the atmosphere, the use of neutron-activation determinations, the improvement of accurate chemical and physicochemical techniques for determining small impurities in air, and, more importantly, the development of automatic methods of continuous monitoring of pollution and computable systems. Some of the papers were devoted to the improvement of the techniques of studying gaseous radioactive contaminants in the atmosphere (^{85}Kr) whose concentration in the terrestrial atmosphere is increasing as a result of the growth of nuclear power.

The investigation of atmospheric pollution by fission products needs to be followed in greater detail. In order to improve the methods of pollution prediction it is necessary to study the spatial distribution over

Translated from *Atomnaya Énergiya*, Vol. 37, No. 4, pp. 367-368, October, 1974.

© 1975 Plenum Publishing Corporation, 227 West 17th Street, New York, N.Y. 10011. No part of this publication may be reproduced, stored in a retrieval system, or transmitted, in any form or by any means, electronic, mechanical, photocopying, microfilming, recording or otherwise, without written permission of the publisher. A copy of this article is available from the publisher for \$15.00.

large territories and search for the connection with meteorological processes. This is caused by local peculiarities of the place of prognosis, since the density of fall-out of radioactive contaminants depends substantially on the geographic location. Apparently, relationships can be established between different observation points.

In recent years the investigation of natural (radon) radioactivity of the atmosphere has consisted of studying long-life products. It is found that along with the products of decay of radon the atmosphere contains the same products which enter with terrestrial dust and occur in radioactive equilibrium with ^{222}Rn .

The investigation of cosmic radioisotopes in the atmosphere was also represented at the conference. Because of the nuclear tests conducted earlier, some of these isotopes (^{14}C) have not yet reached their natural values. The rates of formation of such isotopes in the atmosphere depend on action of cosmic rays on the atmospheric matter, volcanic dust, meteoric material penetration into the atmosphere etc. The concentrations and fall-out values of cosmic radioisotopes at the Earth's surface and their relationship with meteorological processes and also with the mixing of the stratospheric and tropospheric air masses were investigated. Considerable interest was generated by the communications concerning the characteristics of the behavior of $^{14}\text{CO}_2$ and tritium oxide in the surface and high layers of the atmosphere and the relationship of their concentrations with meteorological processes.

A number of papers were devoted to the use of radioactive isotopes as tracers in the study of physical processes occurring in the atmosphere. Radioactive tracers allow a study of the air mass exchange between the stratosphere and troposphere, the laws and amount of turbulent exchange in the atmosphere, dispersal of contaminants in cloud systems and the atmosphere over large distances, coagulation of cloud particles with solid aerosols, washing out of the contaminants by rain etc. It was noted that tracer methods of investigation of the atmosphere should be developed, since the current period is characterized by local ejections of radioactive isotopes into the atmosphere. In the near future, due to the growth of nuclear power, the contamination from a complex of nuclear power industries will create a general "background"; then the unique possibility of investigating certain physical properties of the atmosphere would be irrevocably lost.

In the analysis of the processes of self-cleaning of the atmosphere from radioactive and neutral contaminants, it was shown that thermophysical processes occurring near the evaporating drops play a significant role in the process of removal of aerosol contaminants by rain. The following aspects were also discussed: the effect of collisions of rain drops with aerosols, change in radioactivity of the falling drops due to evaporation, determination of the numerical parameters characterizing the wash-out of the contaminants from the atmosphere, laboratory modeling of these processes, the role of fog and ground condensations in the washing-out of contaminants, wash-out characteristics of molecular radioactive iodine by falling rain drops etc.

Mathematical investigations mainly covered the problems of diffusion spreading the radioactive and neutral contaminants in a turbulent atmosphere. The radioactive dust cloud was regarded as an active contaminant interacting with the aerosols and rain drops in the atmosphere. This was the main feature of some theoretical papers.

Lately, interest has developed in the pollution from cities and pollution prediction, for which further investigations are required. This is caused by the fact that with a large complexity and "turbulence" of the pollution sources the study of their dispersal and concentration in different areas of the cities requires methodical analysis of the measurements as well as an analysis and evaluation of the obtained results. The problems of smogs are closely related to the problems investigated in this field. They should be investigated in laboratories in model experiments as well as in natural conditions. Furthermore, it is necessary to investigate the phenomena of photochemical reactions in the atmosphere, which can lead to large and stable concentrations of harmful contaminants. Certain meteorological conditions also play an important role in these phenomena.

In the section devoted to the exchange of radioactive contaminants between the atmosphere and ocean, the global fall-outs and the fields of artificial radiostopes in the surface layer of the ocean and their statistical structure were discussed. It was shown that ^{18}O may serve as an indicator in the exchange process and in the self-cleaning of the atmosphere above oceans one must take into consideration the washing of the surface layer by sea sprays. The radioactive contamination of the Baltic Sea was discussed. "Lenses" of increased ^{137}Cs concentrations have been detected at some depths along the coast of Sweden. In view of the planned growth of construction of atomic power plants in the countries surrounding the Baltic sea, a detailed study of the contamination is necessary, where the concentrations are an order of magnitude higher than in the Pacific Ocean.

Finally, the aspects and physical bases of sanitary and ecological settings of permissible content of harmful pollutants in the atmosphere, were discussed in one of the sections. The areas investigated were: dilution of the pollutants entering into the atmosphere and estimation of the dilution factor as a function of the averaging period; statistical probability estimates of pollution potential; methods of determining optimum level of content of chemical materials in multicomponent contamination etc. It was concluded that there is a need for setting limits of contamination taking into consideration their effect of living organism and the change in the form of their existence during their distribution throughout the atmosphere.

The conference represents an important stage in reviewing the study of the entire complex of atmospheric pollution and the ways of further investigation of these problems. The conference succeeded in establishing agreements and differences in the study of individual components of atmospheric pollution and the projection of the prospects for further investigations.

VIII INTERNATIONAL SYMPOSIUM ON THERMONUCLEAR REACTOR TECHNOLOGY

V. S. Strelkob

The VIII Symposium on thermonuclear reactor technology was held from 17-21 June, 1974 in Holland. About 230 scientists from 75 laboratories and firms of 15 countries of Western Europe and also representatives from USSR, USA, Japan, and Canada participated in the symposium. Seventy five original papers and two review papers were presented at the symposium. Problems mainly related to reactor technology were considered. The program consisted of five sections.

Experiments in Plasma Physics. (Installations in operation, those under design and construction, plans). The papers presented in this section described the construction of the following installations: NOVA (tokamak with diverter, Japan), TOSCA (tokamak with noncircular cross section and adiabatic compression, England), DITE (tokamak with injector of neutrals and diverter, England), ASDEX (tokamak with noncircular cross section and diverter, FRG), TORSO (torstron with turbulent heating, England), HBS (stellarator with large β , FRG), W-VII (large stellarator, FRG), Ring-Boog (tokamak with gaseous blanket, Holland), and FT (tokamak with strong magnetic field, Italy). The characteristics of these installations are given in Table 1

These installations have been constructed or are in the stage of construction that will be completed during 1975-1976. As is already known, besides these installations several large toroidal installations are already in operation in European laboratories engaged in thermonuclear research. These are TFR (large tokamak) in France, belt-pinch in FRG, superconducting levitron and CLEO stellarator in England. Stellarator WEGA and tokamak PETULA are being made ready for operation in France.

Energy Sources. This section is traditional. In view of the plans for large installations the interest in high-power supply sources having large reserve energy has increased.

Plasma Heating. This was the shortest section of the program with four papers, where injectors of fast neutral atoms for heating the plasma in toroidal installations CLEO, TFR, and W-VII were described.

Systems of Data Acquisition and Analysis. Seven papers were presented in this section; in most of these systems of data analysis on experimental equipment were described. Such systems are being successfully used in many experimental installations, where relatively slow processes are realized. An automated system based on a small computer permits recording of the basic technological parameters of the installation and also the main characteristics of the plasma.

Reactors of Synthesis. This section includes: predraft development, interaction with the wall, blanket, and work with tritium, neutrons, and radiation damages, and coils of superconducting materials. This was the most extensive section (33 papers). The general predraft development of the reactor was presented in a review article on the Wisconsin tokamak and in the papers on the Italian project FINTOR, where a tokamak with a plasma radius equal to 2 m, large radius equal to 10 m, and 50 kOe magnetic field at the axis of the system is considered. The possibilities of using ordinary and superconducting materials in the electromagnetic system of the reactor were compared in the paper by F. Arent et al. (FRG). Several papers were devoted to the technical aspects of a reactor based on theta pinch or beam trigger. A large number of the papers in this section dealt with the problems of radiation damage, blanket construction, tritium breeding, and erosion of the first wall. The latter problem was considered only from the point of view of wear and durability of the wall and the degree of contamination of the plasma by the material of the wall was not estimated.

Translated from *Atomnaya Énergiya*, Vol. 37, No. 4, pp. 368-369, October, 1974.

© 1975 Plenum Publishing Corporation, 227 West 17th Street, New York, N.Y. 10011. No part of this publication may be reproduced, stored in a retrieval system, or transmitted, in any form or by any means, electronic, mechanical, photocopying, microfilming, recording or otherwise, without written permission of the publisher. A copy of this article is available from the publisher for \$15.00.

TABLE 1. Basic Characteristics of the Installations

Installation	a , cm	R , cm	I , kA	H , kOe
NOVA	1,5	18	1,2	10
TOSCA	10	30	100	13+13
DITE	23	113	340	28
ASDEX	40	154	500	30
TORSO	10	40	—	20
HBS	4	800	—	—
W-VII (a)	17	200	—	40
W-VII (b)	35	200	—	40
Ring-Boog	10	50	40	30
FT	<20	83	1000	100

A review article was devoted to the status of the JET (Joint European Tokamak) project being planned by a joint group at Culham laboratory (England). The location for the construction of this installation has not yet been decided. Tokamak JET, which was initially designed for 3 mA current in the plasma, is now being planned with a ring chamber, which offers the possibility of increasing the current in the plasma to 5-6 mA. The project envisages the possibility of demonstrating the self-sustaining D-T reaction. In the case of success in attaining the required parameters with hydrogen, it is proposed to conduct experiments with tens of discharges and with a mixture of deuterium and tritium. This idea provided the greatest discussion, since according to the current design the equipment is not suitable for operation with tritium.

The next symposium on this problem is planned for 1976.

INTERNATIONAL SYMPOSIUM ON THE USE OF
ISOTOPE TECHNIQUES IN GROUNDWATER HYDROLOGY

V. T. Dubinchuk and A. M. Dimaksyan

The symposium was organized by IAEA on 11-15 March, 1974 in Vienna. Participating in the symposium were 199 delegates from 38 countries and a number of international organizations presenting the most diverse directions and aspects of the use of isotope techniques in hydrology.

A group of papers was devoted to the practical use of natural and artificial tritium to estimate the nature and intensity of underground water feed, including feed through aeration zones, and also to estimate the velocity of underground water and the rate of surface and underground runoff. Many papers contained the discussion of the results obtained with the use of stable isotopes of deuterium and ^{18}O , used with success in the investigations of the conditions of feed of underground waters in their artificial filling, penetration of rain waters into ground waters, feed of cracked water-bearing beds, and feed of underground waters into deserts.

The study of the distribution of the isotopes ^{18}O , D, T, ^{14}C , available during the period, was the most characteristic feature of the field investigations in specific territories. This series of investigations provides the more complete information needed for practical hydrogeological inferences. Thus, E. Masor et al. used ^{18}O , D, T, ^{14}C for estimating the mechanism and intensity of feed of underground waters of a large desert region in Botswana; R. Gonfiantini et al. investigated the interrelation of water-bearing beds in Northern Sahara; G. Kastani et al. gave the most interesting and instructive example of estimating the regional runoff of ground waters taking the example of a large region adjoining the Senegal river; E. Salati et al. also investigated a large region and obtained valuable information on the genesis, feed, and regional runoff of underground waters and the interaction of water-bearing beds in a coastal zone; V. I. Ferronskii, Yu. B. Seletskii et al. presented a summary of investigations of different types of underground waters in the USSR using ^{18}O and deuterium; W. Shtal et al. made a very successful use of ^{18}O , deuterium, and carbon to study the origin of hot waters in Greece; V. T. Dubinchuk, V. A. Polyakov, V. M. Kuptsov et al. communicated the results of using a set isotope methods based on the use of ^{18}O , D, ^{14}C , $^{234}\text{U}/^{238}\text{U}$ for estimating the genesis and the rate of exchange of underground waters of the Mirgalimsk ore deposit region, and also for estimating the contribution of different components of mine water influxes. In the same paper a preliminary theoretical analysis of the possibilities of using isotope methods for the estimate of water flow through weakly permeable rocks was given for the first time. Another paper by G. Suze should be mentioned, which presented very interesting data on the measurement of isotope composition of tritium, deuterium, and ^{18}O in lysimeters for a comparative estimate of the amount of seepage.

Interesting data on the technology, procedure, and practical examples of use of the radiocarbon dating method were presented by W. Rawerat et al. (FRG), I. Winograd et al., F. Pearson et al., and T. Guphen et al. (USA).

Recently, methods based on the study of the change of the content ratio $^{234}\text{U}/^{238}\text{U}$ are coming into use increasingly more in hydrogeological studies as an influence of the work done in the Soviet Union; this was reflected in several papers. Besides our paper mentioned earlier, V. M. Kuptsov's results on separation of the components of underground waters flowing into mine influxes were given in detail, interesting data on the use of $^{234}\text{U}/^{238}\text{U}$ ratio as an indicator of the genesis of underground waters dated to Sinoman-Tironian carbonate rocks in the Galelian trough were presented. J. Cowart and J. Osmond (USA) carried out similar investigations and proposed an approximate quantitative model of formation of isotope composition of underground waters dated to the sandstone bed of Southern Texas.

Translated from *Atomnaya Énergiya*, Vol. 37, No. 4, pp. 369-370, October, 1974.

© 1975 Plenum Publishing Corporation, 227 West 17th Street, New York, N.Y. 10011. No part of this publication may be reproduced, stored in a retrieval system, or transmitted, in any form or by any means, electronic, mechanical, photocopying, microfilming, recording or otherwise, without written permission of the publisher. A copy of this article is available from the publisher for \$15.00.

Considerable interest was generated by the papers on the use of other isotopes, in particular ^{32}Si , cosmogenic ^{39}Ar , ^{15}N , which have been less used in earlier hydrogeological investigations.

The use of artificial radioactive indicators was discussed in a number of papers. West German specialists reported the development of experimental samples of bore equipment for the determination of the rate of filtration and direction of motion of underground waters, and also for an estimate of the vertical flow of water. Results of successful use of this equipment were presented.

The single-bore method of dilution was discussed in detail in the paper by H. Muner (Columbia). Interesting results on the theoretical validity of the two-bore indicator method of determining the effective porosity were presented by Polish specialists (A. Zuber, A. Lenda, et al.).

G. Gizerecs et al. (France) have proposed and developed a theoretical dispersion model for estimating the characteristics of transport of polluting materials in water-bearing beds and have carried out a successful experimental test. The model may be found suitable for the interpretation of bore indicator investigations.

V. T. Dubinchuk, V. S. Goncharov, et al. reported the results of the development of laboratory and field methods to determine the characteristics of diffusion transport of sodium chloride using the γ -radiating isotope ^{22}Na ; G. Mozer et al. (France) reported on indicator laboratory investigations of the characteristics of hydrodynamic dispersion as a function of the rate of filtration and the structure of the porous medium. Of all the known experiments this is perhaps the most detailed investigation of the dispersion process.

The symposium showed that a combination of both different isotope methods and of isotope and traditional hydrological and hydrogeological methods is being used increasingly more intensively. In practice the isotope methods are being used most extensively in the underdeveloped and developing countries. This is explained by the relative ease of availability of the isotope methods and by the fact that the isotope results permit obtention of the required information about the territories that have not been well investigated, without time-consuming traditional hydrogeological investigations. The isotope methods of investigation are being intensively developed by scientists and specialists in USA, France, FRG, Italy, and England, who are improving the techniques of use of the isotopes, extending their practical use in poorly investigated regions or in those cases where the traditional methods yield ambiguous results, and are using them extensively in the study of objects with disturbed hydrogeological and hydrochemical conditions.

All the material presented at the symposium demonstrated the high information capability and effectiveness of isotope methods in hydrogeology and indicated their ever increasingly widespread use in hydrogeological practice for obtaining valuable new information on hydrogeological objects and processes, which is difficult or even impossible to obtain by the traditional methods of investigation.

INTERNATIONAL CONFERENCE ON MESON
SPECTROSCOPY

V. A. Belyakov

An international conference on meson spectroscopy was held in Boston (U. S. A.) on the 26th of April, 1974. This was the fourth conference in a series of similar conferences organized since 1968 in the United States. Two hundred and forty physicists from seventeen countries took part. A series of review talks on separate problems of mesonic states was adopted without the usual division into plenary meetings and parallel sessions.

Reports concerned themselves with experimental and theoretical research on meson resonances, on the construction of new experimental apparatus (the Omega, LASS, and MPS projects), and the directions in meson spectroscopy which are at the present moment arousing the greatest interest for physicists.

M. G. Bowler (Oxford, England), D. Binnie (Imperial College, England), B. Gittelmann (Cornell University, U. S. A.), and others reported on the formation and characteristics of non-strange meson states. An attempt has been made to systematize the present mesonic resonances using a simple quark model. Beginning with masses of approximately 1700 MeV, data on mesons is inaccurate. In the mass region between 1700 and 2400 MeV, nine resonances are known, while in the region between 2400 and 3600 MeV there is evidence of 16 particularities in the meson mass spectrum. For all heavy mesons of mass greater than 1700 MeV, only estimates of isotopic spins have been made and the fact of the existence of more than four particles and their decay products ascertained. Phase shift analysis has shown evidence for the existence of the ρ' (1600) meson in e^+e^- interactions. This meson has previously been seen in the $4-\pi$ meson final state. The peak in the region of the A1 meson is explained by the collective interactions of three pions with a large admixture of diffractive mechanisms for the production of the system. In the light meson mass region detailed studies have been made with very good resolution. The following results have been obtained:

η^0 -meson	ω^0 -meson	X^0 -meson
$M=547,45 \pm 0,25 \text{ MeV}$	$M=783,8 \pm 0,3 \text{ MeV}$	$M=957,46 \pm 0,33 \text{ MeV}$
$\Gamma(\eta \rightarrow 2\gamma)=324 \pm 46 \text{ eV}$	$\Gamma=10,2 \pm 0,6 \text{ MeV}$	$\Gamma < 0,8 \text{ MeV}$

The width of the π -zero meson has been more accurately measured ($\Gamma = 7.7 \pm 0.4 \text{ eV}$). The existing data on the $3-\pi$ system has been analysed from a theoretical point of view. This was reported by T. Lasinski (Berkley, U. S. A.) and G. Ascoli (University of Illinois, U. S. A.). With the help of a partial wave analysis, agreement with experimental data has been found in the region of the A1 meson for the $1 + S\rho\pi$ final state, and in the region of the A2 meson for the $2 + D\rho\pi$ final state, and in the region of the A3 meson for the $3 + D\rho\pi$ final state. These results hold true for small momentum transfers ($t = 0-0.1 \text{ (GeV/C)}^2$). On the whole there is still no good partial wave description of the $3-\pi$ meson system. Theoretical reports did not present any new ideas about this system.

Since 1970 there has been no direct evidence for the existence of exotic meson states (D. Cohen, Columbia University, U. S. A.). In the ρ -minus- π -minus and K-minus- π -minus final states and in other final states, peaks in the effective mass distributions are found at the level of statistical fluctuations which leads to an upper limit for the production cross section of exotic states of $\leq 5-10 \mu\text{barn}$.

Cross sections for the production of π -mesons in e^+e^- interactions are very small. With increasing energies of the colliding particles from $\sqrt{s} = 1 \text{ GeV}$ to 4.8 GeV , the cross section decreases from 70 to 20 nbarns (W. Chinowsky, Berkley, U. S. A.). It was highly important to establish experimentally that the ratio of the total cross section for e^+e^- interactions to the cross section for $\mu^+\mu^-$ pair production is energy

Translated from *Atomnaya Énergiya*, Vol. 37, No. 4, pp. 370-371, October, 1974.

© 1975 Plenum Publishing Corporation, 227 West 17th Street, New York, N.Y. 10011. No part of this publication may be reproduced, stored in a retrieval system, or transmitted, in any form or by any means, electronic, mechanical, photocopying, microfilming, recording or otherwise, without written permission of the publisher. A copy of this article is available from the publisher for \$15.00.

dependent and equals two at $\sqrt{s} = 1$ GeV and six at $\sqrt{s} = 4.8$ GeV. The energy dependence of the $\mu^+\mu^-$ cross section strongly contradicts the predictions of the simple quark model (the cross section ratio should be constant and equal to 0.5) and the colored quark model (the ratio should equal two). Also unexpected was the copious six and eight particle production in e^+e^- interactions at $\sqrt{s} = 4.8$ GeV. In this case, antiproton production was down by a factor of 100 with respect to pion production while kaon production was down by a factor of 10.

R. L. Eisner (Brookhaven National Laboratory, U. S. A.) and J. W. Hansen (Copenhagen, Denmark) discussed the situation in the region of the Q meson (1250-1400 MeV) and the L meson (1770 MeV). It has been established that the mass peak in the region of the Q meson is not described by a Breit-Wigner curve and that the slope of $d\sigma/dt$ and fraction of $K\rho$ final state change by a factor of two. A light mass component (with mass of 1242 ± 10 MeV) can be separated out in the Q region but a heavy component cannot be isolated. The 1^+ state is preferred in the Q meson region while the 2^- state is preferred in the L meson region.

The accumulation of a large amount of experimental data has made possible an inclusive study of ρ^0 meson production in pp interactions at 12 GeV/C and 24 GeV/C and in πp interactions at 11.2 GeV/C, 15 GeV/C and 205 GeV/C (F. C. Winkelmann, Berkley, U. S. A.). In pp interactions at 24 GeV/C the ρ meson production cross section has been determined $\sigma(\rho) \approx 10.5$ mbarn. In πp interactions at 205 GeV/C the ρ meson production cross section is $\sigma(\rho) \approx 33$ mbarn. It has been estimated that in pp interactions at 24 GeV/C 1/7 of all pions produced are from ρ meson decay while in πp interactions at 205 GeV/C this is 1/4.

Of the 10 possible quantum states of the quark-antiquark system (from 0^- to 3^-) three have been definitely established at the present time.

$L = 0$ ($q\bar{q}$)	$J^P = 0^-$	$\pi\eta\eta'K$
$L = 0$ ($q\bar{q}$)	$J^P = 1^-$	$\rho\omega\phi K^*(890)$
$L = 1$ ($q\bar{q}$)	$J^P = 2^+$	$A_2 f' K^*(1420)$

The conference proceedings will be published.

MEETING OF THE FOUR NUCLEAR DATA CENTERS

V. N. Manokhin

The regular meeting of the four neutron nuclear data centers was held in Paris on May 6-10, 1974. The representatives from the National Center of Neutron Cross Sections (Brookhaven, USA), Center for Compilation of Neutron Data (Saclay, France), Nuclear Data Center (Obninsk, USSR), and the Nuclear Data Section (IAEA, Austria) participated in the meeting. It discussed the traditional problems: the library of experimental data in exchange format (EXFOR), bibliographic catalog SINDA, worldwide list of enquiries (WRENDA), reports on last year's activities of the centers, interaction among the centers, a review of the activity planned at the previous meeting, and recommendations for the future.

The greatest attention was devoted to the exchange format and the state of the library of experimental nuclear data in this format. At present the neutron nuclear data is collected by the nuclear data centers. Each center collects information from its geographic region, exchanges the information with the other centers, and furnishes the world library of neutron data to the users of its region. The regions served by the centers are:

USA, Canada — Brookhaven (USA);

West Europe, Japan — Saclay (France);

East Europe, Africa, South America, Australia, Asia — IAEA (Vienna);

USSR — Obninsk.

Each center abstracts the entire literature from its geographic region for the computer library catalog SINDA and writes out the factual and graphical information in the special exchange format (EXFOR). EXFOR is being improved and extended at the annual meetings of the representatives of the four centers. The methods of introducing experimental data into the library in EXFOR format of multidimensional tables (for example, as tables of resonance parameters) was discussed. As a result of the discussion some changes were incorporated in the format and rules for abstracting were approved that would make it possible to introduce tables of resonance parameters into EXFOR in a more convenient and compact form. Problems related to extending EXFOR format to nonneutron nuclear data were also discussed and recommendations were made to the centers to maintain close contacts with the groups and centers compiling nonneutron data and also to investigate the possibility of taking and developing already existing formats for nonneutron data.

At present the computer library of experimental neutron data in EXFOR format contains about 900 thousand rows of information on magnetic tape, numerical results and description of 800 experiments in neutron physics, and is equipped with a set of operational programs.

The international bibliographical catalog SINDA (about 100 thousand rows of information) is also being improved and enlarged. In the new 1974 edition the catalog will include additional information on the presence of the corresponding data in the computer library of EXFOR. The meeting also discussed the questions of identity of the words SINDA and EXFOR, completeness of SINDA catalog, and elimination of redundant and erroneous information.

The worldwide list of nuclear data enquiries WRENDA-74 was published this year and contains 1190 enquiries on the measurements of nuclear data from 21 countries. The committee limited itself to the review of the state of the enquiries and endorsed the report to the next meeting of the ICND.

Translated from *Atomnaya Énergiya*, Vol. 37, No. 4, pp. 371-372, October, 1974.

©1975 Plenum Publishing Corporation, 227 West 17th Street, New York, N.Y. 10011. No part of this publication may be reproduced, stored in a retrieval system, or transmitted, in any form or by any means, electronic, mechanical, photocopying, microfilming, recording or otherwise, without written permission of the publisher. A copy of this article is available from the publisher for \$15.00.

The National Center of Neutron Cross Sections (Brookhaven) issued the first volume of the third edition BNL-325 containing recommended resonance parameters. The work on the fourth version of the library of estimated data ENDE/B has been completed. The Center for Compilation of Neutron Cross Sections at Saclay has published "Compilation of neutron cross sections of threshold reactions for neutron dosimetry and other applications" (EANDC-95U). The nuclear data section of IAEA has published a summary of cross sections averaged from fission spectra; the work on estimating cross sections of reactions for neutron dosimetry is being continued. Conferences on nuclear data have been organized and held. The nuclear data center at Obninsk continues to publish the collections of articles "Nuclear Constants" and the collection of abstracts "Nuclear Physics Research in the USSR." A large amount of work is being done on the development of a computer library of experimental and estimated nuclear data, elaboration of the required accuracies and adjustment of the constants, and estimation and organization of estimates of nuclear data.

The meeting discussed the problems of interaction among the centers, summarized the international cooperation during the last year, worked out recommendations, and planned measures for all the aspects of this cooperation.

The next meeting of the four nuclear data centers will be held at Brookhaven (USA) in March 1975.

MEETINGS OF SPECIALISTS ON NONNEUTRON NUCLEAR DATA

F. E. Chukreev

Following the recommendations of the International Committee on Nuclear Data (ICND) the nuclear data section of IAEA (Vienna) conducted two meetings on nonneutron nuclear data (everywhere below nuclear data implies nonneutron nuclear data) in April—May of this year: a meeting of specialists on nuclear data for reactions with charged particles and photonuclear reactions and a meeting of specialists on nuclear data for applications.

The participants from our country in these meetings were the representatives from the Center for data on the structure of the atom and nuclear reactions of SCAE (State Committee for the use of Atomic Energy), (CAND) which was created in 1972 to meet the needs of Soviet scientists for nonneutron nuclear data. In both meetings the reviews of the existing needs for nonneutron nuclear data, prepared by the IAEA, were discussed. These reviews had been prepared mainly from the material presented at the symposium "Nuclear data in science and technology" (Paris, 1973) supplemented by some new uses coming into light after the symposium. Thus, for example, the needs for nuclear data for a number of "exotic" forms of thermonuclear fuel of type ^{11}B have appeared. The discussion showed that the needs for nonneutron nuclear data are so extensive and diverse that they can not be completely met by the existing groups and centers for compilation and estimate or by publications in scientific journals and handbooks. In the opinion of the participants the main difficulties are associated with the following facts: the accessible data are often incomplete and are not presented in a form suitable for use; the data are scattered in many publications; different values for the same parameters are given in different publications; the published data are rarely accompanied by an estimate of the error; the data are in practice not available in computer-readable form. The participants of the meetings agreed that there is a need for a standard source of nuclear data which would be free from the above drawbacks; they also agreed that the creation of such a data file is possible only under the condition of close international cooperation and free exchange of both experimental and estimated data. It was recommended that all nuclear data centers and groups, that would be collaborating in the creation of the international file, should use the key-word system for abstracting nuclear physics research, currently in use at the Oak Ridge center, CAND SCAE, and Nuclear data center of B. P. Konstantinov Leningrad nuclear physics institute. It was also decided that a single value together with an indication of its accuracy should be presented in the future file of estimated data.

It was decided to discuss the volume of the information in this file and the format of the presentation in the coming year.

The participants recommended that a small information bureau be created in the nuclear data section of IAEA, which must keep a count of all nuclear data, both existing and under compilation and estimate, in order to have the best coordination of the activity toward the creation of the file and also to furnish information about the compilations and estimates to interested organizations and individual scientists.

Three close meetings on problems related to the creation of the international file of estimated data are planned for 1975.

Translated from *Atomnaya Énergiya*, Vol. 37, No. 4, p. 372, October, 1974.

© 1975 Plenum Publishing Corporation, 227 West 17th Street, New York, N.Y. 10011. No part of this publication may be reproduced, stored in a retrieval system, or transmitted, in any form or by any means, electronic, mechanical, photocopying, microfilming, recording or otherwise, without written permission of the publisher. A copy of this article is available from the publisher for \$15.00.

USSR — BELGIUM — HOLLAND SEMINAR ON TREATMENT
AND BURIAL OF RADIOACTIVE WASTES

N. A. Rakov

A seminar on the treatment and burial of radioactive wastes was held from 18 to 27 June, 1974 at Dubanain in accordance with an agreement among SCAE USSR, the reactor center of Holland, and the AEC of Belgium.

Recent results covering all aspects of scientific—technical research and the existing practice of decontamination of the wastes resulting from the use of atomic energy were discussed in 25 papers presented at the seminar.

The processes of purification and concentration of low-activity liquid wastes, including the methods of ion exchange, evaporation, electro dialysis etc., occupied a prominent place in the program of the seminar. It was noted that the methods of purification, developed and employed in the purification facilities, permit the reliable attainment of the standard norms of purified water.

Considerable attention was devoted to the development of methods and equipment for the conversion of the wastes into solid materials (cement, bitumen, glass) suitable for the safe burial and also to the study of the properties of solidified wastes and the scientific justification of the radiation—sanitary safety of their burial as a function of different conditions and levels of their activity. It was confirmed that the burial of radioactive wastes in solidified form is the safest from the point of view of its effect on the environment. One of the possible places of burial of such wastes may be depleted salt mines under favorable hydrogeological conditions.

Significant interest was generated by the papers devoted to the characteristics of the method of underground burial of liquid radioactive wastes, to the requirements of hydrogeological formations and collector beds, and also to a complex of investigations necessary for ensuring radiation—sanitary safety in the design and construction of underground storage facilities. Special attention was given to the physicochemical processes in the behavior of radioactive isotopes in underground tables.

The specialists discussed problems related to the burial of radioactive wastes in salt mines. This method of burial can be promising for the disposal of solidified radioactive wastes. However, even in these cases it is necessary to impose rigid requirements on the choice of salt mines for creating burial grounds. One of the main requirements is their inaccessibility to inundation by underground water, which can occur in 15 cases out of 100 for conditions in Belgium and Holland. The methods of collecting radioactive noble gases, radioactive iodine, and aerosols from the overhead emissions of atomic installations were also discussed. It was noted that it is necessary to continue the development of more efficient systems of gas purification in view of the rapid growth of atomic power plants.

The papers on the disposal of radioactive wastes in seas and oceans generated extensive discussion. The possibility of dangerous consequences of such burial for the environment was discussed. It was pointed out that before deciding on the disposal of wastes into seawater on a large scale it is necessary to carefully study and control the behavior of radioactive wastes, packing and other aspects related to migration of radioactive materials during prolonged contact with seawater. The soviet specialists expressed the view that the use of sea and ocean waters for the disposal of radioactive wastes on an industrial scale was inadmissible because of the possibility of dangerous consequences for the environment; they also expressed doubt about the economic feasibility of this approach. In this connection a paper dealing with the radioactive contamination of the Baltic Sea generated interest. A large amount of experimental material was unified in this paper.

Translated from *Atomnaya Énergiya*, Vol. 37, No. 4, p. 373, October, 1974.

© 1975 Plenum Publishing Corporation, 227 West 17th Street, New York, N.Y. 10011. No part of this publication may be reproduced, stored in a retrieval system, or transmitted, in any form or by any means, electronic, mechanical, photocopying, microfilming, recording or otherwise, without written permission of the publisher. A copy of this article is available from the publisher for \$15.00.

Different national points of view on decontamination of wastes of all levels of activity were put forward considering both the present activity and the prospects of development of atomic energetics in the countries.

The specialists from Belgium and Holland were acquainted with the operation of the purification facilities at the Moscow Station of Purification of Radioactive Wastes, the burial of radioactive wastes at the Central Station of Radiation Safety, the solution of problems of decontamination of wastes at the Institute of Physical Chemistry and the Scientific-Research Institute of Atomic Reactors, the test bench equipment for treatment of radioactive wastes, and also with a number of other research laboratories.

The seminar was conducted at a high scientific level in a friendly atmosphere.

BOOK REVIEWS

NEW BOOKS

A. M. Petros'yants. *The Nuclear Power Industry in Foreign Countries*. Atomizdat, Moscow (1974).

Reviewed by G. Klimov

This book, of relatively restricted volume, contains a good deal of information on the past, present, and future of the nuclear power industry of the leading capitalist nations: the USA, Canada, Great Britain, France, West Germany, Italy, Sweden, Switzerland, and Japan. These and other aspects of the development of the nuclear power industry in foreign countries have been reflected in contributions by many Soviet authors. But to date there has been no systematical review publication on these topics.

The author of the book under review did not set as his task a detailed description of the basic types of nuclear power reactors, their components, subsystems, circuits and equipment for extracting and converting heat into electric power. The main purpose of the book is to analyze the principal trends, features, and scope of development of the nuclear power industry in those countries. And to the extent required by the topic and treatment, a description is given of design features of reactors and nuclear power stations as well. This part of the author's plan is well justified.

The nuclear power industry did not arrive straight off at its present state, which can be characterized in its most general form as a state of intense growth in countries with a nuclear power capability, on the basis of a fairly limited number of reactor types. The road to materialization of nuclear power has sometimes been a difficult and meandering one, and in the case of several countries, notably Britain and France, has even been marked by a dramatic reorientation in technical priorities and policies in the field of power reactor design. The author pays close attention to the elucidation and analysis of these aspects of the problem.

It should be emphasized that the author, in his presentation of the text material, not only cites numerous foreign scientific publications, including proceedings of conferences, symposia, and congresses, but to a certain extent draws upon his personal impressions formed in visits to many of those countries, and his personal familiarity with the status of the nuclear power industry and nuclear power construction projects in "real life." This enhances the reliability and persuasiveness of the material, livens the presentation, and renders the book even more interesting.

An important place is reserved for the description of the fuel and energy situation unfolding both on a worldwide basis and in particular countries. Existing reserves, and forecast reserves, of fossil fuels and power resources, rates of demand on those reserves and resources, views entertained as to the role of nuclear power in the present state of the power industry, which is characterized as quite tense on the whole, are cited in the text. In the unanimous opinion of specialists, as the author points out, the only viable option of all of the new sources of energy promising stable delivery of electric power on an economically competitive basis, and really offering an outlook for getting out of the difficulties in the disproportion between the demand for electric power and the possibilities of satisfying that demand while conserving the necessary qualities of the living environment, is nuclear power. In this connection, the author provides an analysis of the development of nuclear power, demonstrates the continuity across generations of reactor types, and refers to the orientation to breeding of nuclear fuel in the fast breeder reactors as a solution of the nuclear fuel problem.

Translated from *Atomnaya Energiya*, Vol. 37, No. 4, pp. 374-375, October, 1974.

©1975 Plenum Publishing Corporation, 227 West 17th Street, New York, N.Y. 10011. No part of this publication may be reproduced, stored in a retrieval system, or transmitted, in any form or by any means, electronic, mechanical, photocopying, microfilming, recording or otherwise, without written permission of the publisher. A copy of this article is available from the publisher for \$15.00.

The systematic nature of nuclear power development, its rigorous complexity, expressed both in the intimate relationship with the electrical power industry as a whole and, even more important, in the presence of a specific system of fuel supply (peculiar to the nuclear power industry alone), an external fuel cycle, is emphasized. Measures geared to ensure the functioning of the nuclear power system (building uranium enrichment plants, fabrication of fuel elements, recovery of spent fuel, disposal of radioactive wastes by burial, etc.) are therefore dealt with in sufficient detail. The author demonstrates that further development of the nuclear power industry would be out of the question without such a firm basis.

The book is profusely illustrated. There are numerous photographs helpful in providing a lucid picture of the external and internal appearance of nuclear power plants and their components, and of enterprises involved in the external fuel cycle. The book is also saturated with reference material in the form of tables of data and numerical data.

The publication of this book practically coincided with the twentieth anniversary of the commissioning of the World's First Nuclear Power Station in the USSR, and serves as an excellent proof and illustration of the enormous role played by the World's First Nuclear Power Station in the formation of the nuclear power industry.

The book will be useful to the majority of specialists working in the field of nuclear power, and especially so to instructors and students in power and nuclear power departments.

A. D. Turkin. *Dosimetry of Radioactive Gases*, Atomizdat, Moscow, 1973

Reviewed by Yu. V. Sivintsev

As experience has been accumulating in the operation of nuclear reactors of various types, it has become increasingly more obvious that the degree of radiation hazard regarding internal irradiation at those facilities has been greatly exaggerated. This inference refers in equal measure to radioactive aerosols and to gases of reactor origin such as tritium, ^{14}C , and radioactive isotopes of the noble gases. Still, one of the major problems in nuclear reactor radiation safety systems design remains dosimetry of radioactive gases with the object of arriving at exact quantitative estimates of the contribution made by the component in question to the total dose involved in radiation exposure. The monograph under review here deals with this much neglected topic.

Even within the space limitations of this book, A. D. Turkin manages to provide a clear and concise description of various sources of radioactive gases at reactors, to characterize methods used in the radiometry of gases, and to analyze regularities in the formation of tissue doses in the human body and the radiation hazard presented by gases vented to the atmosphere.

In the first chapter, which is devoted to discharges of radioactive gases into the atmosphere, we find mainly citations and quotes of data from the literature, and comparisons of unique information on the extent of discharges of tritium, ^{14}C , radioactive noble gases, and iodine, and their radioactivity characteristics, for nuclear reactors of various types.

Information on the extent of discharges of radioactive noble gases and iodine in underground nuclear explosions, also included in this section, fall somewhat outside the scope of the subject matter. In analyzing the formation of tritium at nuclear reactors, the author did not view it as feasible to cite data on the lithium-water chemical regime, an important and major source of tritium found at water-cooled reactor facilities.

The second chapter (entitled "Techniques in radiometry of gases") affords A. D. Turkin an opportunity to generalize and review the data in the literature, making generous use of materials originating in his own investigations. Here the reader will find a description of methods of absolute measurements of the activity of gases with the aid of internally filled counters, radiometry of β -active gases with the aid of end-window counters, ionization chambers (including determinations of the isotope composition of radioactive noble gases), and air-ash storage units. Special sections in this chapter deal with such topics as the radiometry of ^3H , ^{14}C , and radioactive iodine. The reader should take note of the very original procedure used in monitoring effective trapping of iodine by various sorption-filtration materials, as well as the results,

obtained through that procedure, of tests of activated charcoal grades. The chapter ends with sections on techniques for calibrating gas radiometers, and determinations of the extent of discharge of radioactive gases.

In the presentation of information on tissue doses brought about by radioactive gases in the human body (third chapter), the author carefully separates out the aspects of internal exposure and external exposure. The reader's attention is unquestionably attracted to the detailed presentation of materials on unique experiments staged by A. D. Turkin in collaboration with E. S. Trukhmanova and S. V. Levinskii on ten human volunteers, in the study of regularities involved in the accumulation, distribution, and secretion of ^{85}Kr and ^{133}Xe in, through, and out of the human organism. The assemblage of data features in particular the relatively long (3 to 6 h) half-lives for elimination (biological half-lives) of radioactive noble gases from fatty tissue. This information is not only helpful in making correct tissue dose estimates where tissue doses are due to radioactive noble gases taken up in internal human exposure, but also in validating a method for measuring these isotopes in the human organism in order to restore a safe radiation situation in the event of nuclear accidents or spills. Analysis of tissue doses in external β -irradiation was carried out on the basis of the Levinger formula and experimental data reported by G. B. Radzievskii and D. P. Osanov. In the section on pathways for the uptake of radioiodine, close attention is given to research findings in programs using human volunteers, in work by S. M. Gorodinskii and colleagues. Here for the first time are published experimental data on hindrance factors for gaseous radioactive iodine in human respiratory organs, obtained at a water-moderated water-cooled reactor facility. The chapter ends with sections on tissue doses brought about by ^{14}C and ^3H in the human body. Unfortunately, in this chapter A. D. Turkin often makes use of the term "maximum permissible concentration" (MPC), a term which is not recommended by ICRP, and which is to be replaced by the more correct expression "yearly average permissible concentration" (YAPC). As pointed out in the fourth chapter, the instantaneous concentration (2-3 min averaging interval) in the case of a circular wind rose can exceed the yearly average level by anywhere from 30 to 40 times.

The fourth chapter, dealing with the radiation hazard presented by gases removed from nuclear reactors and vented to the atmosphere, fits organically into the structure of the monograph. The first section analyzes regularities of scattering of gases through the ground layer of the atmosphere. Here, in addition to the broadly familiar techniques developed by Sutton and D. L. Laikhtman and others, we also find descriptions of the work done by E. N. Teverovskii, who suggested a straightforward technique for determining the yearly-average coefficients of meteorological dilution for different parts of the Soviet Union. These figures are based on material collected from extensive observations in the field and on a real scale, in districts where major sources of impurities vented to the atmosphere are found, and quite naturally lead to the fruitful concept of maximum permissible discharge (MPD). The calculated maximum permissible discharge levels for a mixture of radioactive noble gases and their individual isotopes, as well as ^{131}I and ^{14}C , are given a good deal of attention in the last part of the fourth chapter. In addition, special attention is reserved for the results of full-scale experiments on estimates of γ -radiation doses due to a jet or stream of continuous ^{41}Ar discharge into the atmosphere.

This monograph will be received with keen interest by specialists on radiation safety and reactor design. The publication of this monograph removes a large "blank space" not only in the Soviet literature, but in the worldwide literature devoted to these topics.

breaking the language barrier

WITH COVER-TO-COVER
ENGLISH TRANSLATIONS
OF SOVIET JOURNALS

in physics

SEND FOR YOUR
FREE EXAMINATION COPIES

PLENUM PUBLISHING CORPORATION
227 WEST 17th STREET
NEW YORK, N. Y. 10011

Plenum Press • Consultants Bureau
IFI/Plenum Data Corporation

In United Kingdom: 4a Lower John Street,
London W1R 3PD, England

Title	# of Issues	Subscription Price
Astrophysics <i>Astrofizika</i>	4	\$120.00
Fluid Dynamics <i>Izvestiya Akademii Nauk SSSR mekhanika zhidkosti i gaza</i>	6	\$180.00
High-Energy Chemistry <i>Khimiya vysokikh énergii</i>	6	\$155.00
High Temperature, <i>Teplofizika vysokikh temperatur</i>	6	\$150.00
Journal of Applied Mechanics and Technical Physics <i>Zhurnal prikladnoi mekhaniki i tekhnicheškoj fiziki</i>	6	\$175.00
Journal of Engineering Physics <i>Inzhenerno-fizicheskii zhurnal</i>	12 (2 vols./yr. 6 issues ea.)	\$175.00 (\$87.50/vol.)
Magnetohydrodynamics <i>Magnitnaya gidrodinamika</i>	4	\$125.00
Mathematical Notes <i>Matematicheskie zametki</i>	12 (2 vols./yr. 6 issues ea.)	\$185.00
Polymer Mechanics <i>Mekhanika polimerov</i>	6	\$140.00
Radiophysics and Quantum Electronics (Formerly Soviet Radiophysics) <i>Izvestiya VUZ, radiofizika</i>	12	\$180.00
Solar System Research <i>Astronomicheskii vestnik</i>	4	\$ 95.00
Soviet Applied Mechanics <i>Prikladnaya mekhanika</i>	12	\$175.00
Soviet Atomic Energy <i>Atomnaya énergiya</i>	12 (2 vols./yr. 6 issues ea.)	\$175.00 (\$87.50/vol.)
Soviet Physics Journal <i>Izvestiya VUZ, fizika</i>	12	\$180.00
Soviet Radiochemistry <i>Radiokhimiya</i>	6	\$165.00
Theoretical and Mathematical Physics <i>Teoreticheskaya i matematicheskaya fizika</i>	12 (4 vols./yr. 3 issues ea.)	\$160.00

Back volumes are available. For further information, please contact the Publishers.

The Plenum/China Program.

An event of singular importance for international science and technology.

Following closely upon the appearance of the first scientific periodicals in China since the Cultural Revolution, Plenum proudly announces the publication of authoritative, cover-to-cover translations of the major, primary journals from China, under the Plenum/China Program imprint.

These authoritative journals contain papers prepared by China's leading scholars and present original research from prestigious Chinese institutes and universities.

In addition to the biomedical and geoscience journals listed for 1974, the Plenum/China Program will publish cover-to-cover translations of periodicals in physics, chemistry, computer science, automation, mathematics and the engineering disciplines. The translations will be prepared by a large team of experts selected especially for the program, and each journal will be under the direct supervision of an outstanding authority in the field.

The first issue of each of the translation journals will be published in early 1974, and, as with our Russian periodicals under the Consultants Bureau imprint, the translations of the Chinese journals will be available within six months following the appearance of the original Chinese edition.

Subscriptions are now being accepted. Examination copies will be available in early 1974.

available in 1974

Subscription Rates*

Acta Botanica Sinica (2 issues)	\$ 75
Acta Entomologica Sinica (2 issues)	\$ 55
Acta Geologica Sinica (2 issues)	\$ 75
Acta Geophysica Sinica (1 issue)	\$ 27.50
Acta Microbiologica Sinica (2 issues)	\$ 55
Acta Phytotaxonomica Sinica (4 issues)	\$125
Acta Zoologica Sinica (4 issues)	\$125
Chinese Medical Journal (12 issues)	\$195
Geochimica (4 issues)	\$110
Kexue Tongbao—Scientia (6 issues)	\$ 90
Scientia Geologica Sinica (4 issues)	\$125
Vertebrata Palasiatica (2 issues)	\$ 60

forthcoming

Acta Astronomica Sinica (2 issues)
Acta Biochimica et Biophysica Sinica (2 issues)
Acta Mathematica Sinica (4 issues)
Genetics Bulletin (4 issues)
Huaxue Tongbao—Chemical Bulletin (6 issues)

*These prices are for the 1973 Chinese volumes which will be published in translation during 1974. Prices somewhat higher outside the U.S.

plenum
PLENUM PUBLISHING CORPORATION
227 West 17 Street, New York, N.Y. 10011
In United Kingdom: 8 Scrubs Lane, Harlesden, London, NW10 6SE, England.